

## Smart Materials for Microrobots

Fernando Soto,<sup>†</sup> Emil Karshalev,<sup>†</sup> Fangyu Zhang, Berta Esteban Fernandez de Avila, Amir Nourhani, and Joseph Wang\*

 Cite This: *Chem. Rev.* 2022, 122, 5365–5403

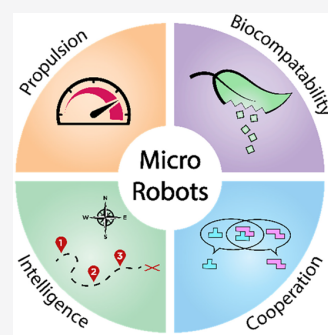
 Read Online

ACCESS |

 Metrics & More

 Article Recommendations

**ABSTRACT:** Over the past 15 years, the field of microrobotics has exploded with many research groups from around the globe contributing to numerous innovations that have led to exciting new capabilities and important applications, ranging from *in vivo* drug delivery, to intracellular biosensing, environmental remediation, and nanoscale fabrication. Smart responsive materials have had a profound impact on the field of microrobotics and have imparted small-scale robots with new functionalities and distinct capabilities. We have identified four large categories where the majority of future efforts must be allocated to push the frontiers of microrobots and where smart materials can have a major impact on such future advances. These four areas are the propulsion and biocompatibility of microrobots, the cooperation between individual units and human operators, and finally, the intelligence of microrobots. In this Review, we look critically at the latest developments in these four categories and discuss how smart materials contribute to the progress in the exciting field of microrobotics and will set the stage for the next generation of intelligent and programmable microrobots.



### CONTENTS

1. Introduction to Small Scale Robotics	5366	4.2. Robot–Robot Interactions	5379
2. Propulsion	5367	4.3. Robot–User Interactions	5381
2.1. Material Requirements	5367	4.4. Assembly	5382
2.2. Autonomous Engines	5368	4.5. Swarming	5384
2.2.1. Catalytic and Transient Materials for Chemical Engines	5368	5. Intelligence	5385
2.2.2. Biological Materials for Chemical Engines	5369	5.1. Material Requirements	5385
2.3. Responsive Engines	5370	5.2. Environmental Taxits	5385
2.3.1. Flexible and Rigid Materials for Magnetic Engines	5370	5.3. Sensing	5386
2.3.2. Material Density and Asymmetry Driven Ultrasound Engines	5370	5.4. Off-Board Intelligence	5388
2.3.3. Photothermal and Photocatalytic Materials for Light Powered Engines	5371	6. Outlook: What's Next?	5388
2.3.4. Polarizable Materials for Electrically Powered Engines	5371	6.1. Summary	5388
2.4. Hybrid Power Sources	5372	6.2. Ideal Features of the Microrobot of the Future	5389
2.5. Tunable Motion and Modulation of Speed	5372	Author Information	5390
2.5.1. Temperature-Based Modulation	5372	Corresponding Author	5390
2.5.2. Chemically Tunable Motion	5373	Authors	5390
2.5.3. External Field Motion Modulation	5373	Author Contributions	5390
3. Biocompatibility	5375	Notes	5390
3.1. Material Requirements	5375	Biographies	5390
3.2. Biocompatible Coatings	5375	Acknowledgments	5391
3.3. Biodegradable Materials	5376	References	5391
3.4. Deformability	5378		
4. Cooperation	5378		
4.1. Material Requirements	5378		

**Special Issue:** Smart Materials

**Received:** September 14, 2020

**Published:** February 1, 2021



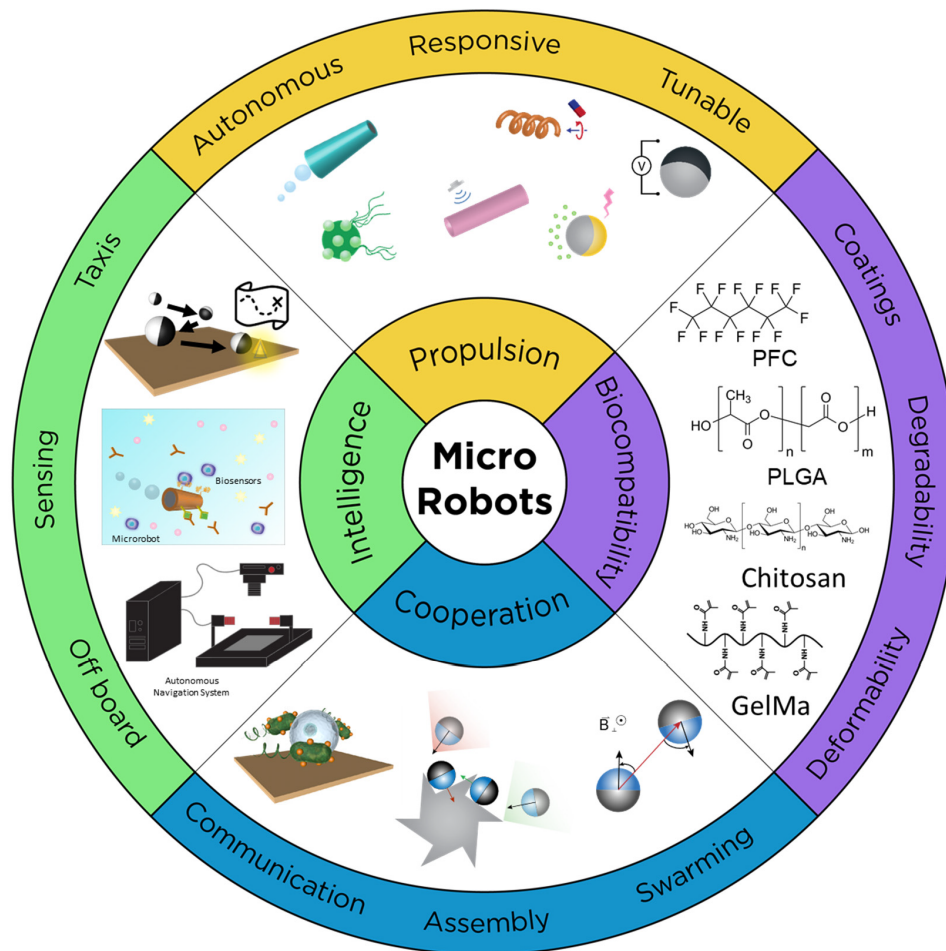


**Figure 1.** Main areas where smart materials can advance the performance of microrobotics: propulsion, biocompatibility, cooperation, and intelligent behavior.

## 1. INTRODUCTION TO SMALL SCALE ROBOTICS

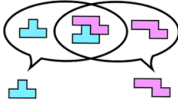
Robots have been a transformative force to society by enhancing our capabilities beyond biological limitations and by providing a better life quality for the world population.<sup>1–3</sup> For example, the Da Vinci surgical system operates inside patients with more precision than a freehand physician.<sup>4</sup> Moreover, robots are fundamental to the exploration of extreme environments such as the current NASA Rover.<sup>5</sup> While certain technological advances in materials development have resulted in lightweight yet strong macroscale structures with superior performance, the majority of improvement has been on the software side. On the hardware side, current robotic designs consist of an assembly of discrete mechanical and electronic components with individually prescribed functionalities. Such macroscale robots mainly rely on operator inputs or artificial intelligence software to adapt to their ever-changing environmental conditions. Nature, on the other hand, programs adaptability and multifunctionality directly in the constituent materials. For example, microorganisms contain the necessary tools to adapt to and function in dynamically varying environments and replicate and synthesize an assembly of molecules and cells.<sup>6–8</sup> Inspired by microorganisms, we can learn from nature how to develop cell-sized

robots furnished with their own propulsion, intelligence, programmability, and adaptability to the environment.

Microrobots are too small to host common electronic circuitry. Therefore, the traditional view of robot programmability using computational units and software at macroscale cannot be translated to microscale. We need to look at this challenge through a new lens and define a new paradigm for addressing the challenge of programmability at the microscale by directly embedding intelligence through reconfigurable geometry and advanced materials. Smart materials are essential for creating programmable actuators, valves, and active surfaces of versatile microrobots. Hence, we must focus on the biological and physicochemical aspects of such building block materials to incorporate the desired behavior and functionality in microrobots.<sup>9–11</sup>

Smart materials offer visible and tangible reactions to changes in their surroundings or to external stimuli. Such materials are also called “intelligent” or “responsive” because of their unique self-adaptability, self-sensing, or memory capabilities. Due to these remarkable properties, smart materials are gaining considerable importance in many industries and can have a profound impact on the microrobot field. Major advances in smart materials and their integration with innovative fabrication techniques have already enabled the development of small-scale

Table 1. Ideal Features for the Next-Generation Programmable Microrobots

Material Feature	Justification
<b>Propulsion</b> 	<ul style="list-style-type: none"> <li>• Change shape to alternate between different modes of propulsion</li> <li>• Deformation would allow to reach difficult areas (e.g. red blood cells)</li> <li>• Additional functionality for accomplishing tasks (e.g. picking up cargo)</li> <li>• “Built-in” activation mechanism could regulate propulsion for accelerating or braking</li> <li>• Optimal fuel consumption and increased locomotion efficiency</li> </ul>
<b>Biocompatibility</b> 	<ul style="list-style-type: none"> <li>• Purposeful and predetermined breakdown into safe components</li> <li>• Biocompatibility with biomedical applications, safe in vivo use</li> <li>• Prescribed disintegration for a purpose i.e. release of drug</li> <li>• Shielding and protective barriers (e.g. antibiofouling)</li> </ul>
<b>Cooperation</b> 	<ul style="list-style-type: none"> <li>• Rudimentary communication and signaling between individual microrobots</li> <li>• Individual microrobots come together to form a new structure or complete a task that can only be achieved when together (e.g. controlled swarming behavior)</li> <li>• Cooperation of microrobots to interact with environments and assembly parts</li> <li>• Use of microrobots to fabricate new micro/nano structures <i>in situ</i></li> </ul>
<b>Intelligence</b> 	<ul style="list-style-type: none"> <li>• Autonomous response and taxis towards environmental cues</li> <li>• Ability to control release kinetics under selective stimuli</li> <li>• Feedback behavior (e.g. self-correcting)</li> <li>• Decision making and independence</li> <li>• Transport of materials along predetermined paths towards micro-assembly lines</li> </ul>

robots of only a few micrometers with novel capabilities. A new paradigm of robot design has emerged in which we must consolidate multiple functionalities, capabilities, and design considerations within a small volume of carefully fabricated microstructure to make a programmable and smart microrobot that can explore their surroundings and respond to environmental cues. While still a far-reaching goal under the current state of material science and fabrication technology, recent advances in the field promise a plethora of diverse building materials for new generations of microrobots.<sup>12–14</sup> Such use of advanced smart responsive materials for imparting small-scale robots with new distinct functionalities will greatly facilitate the design of intelligent programmable microrobots and offer unique future opportunities. The ability of smart materials to respond to stimuli paves the way for the creation of reconfigurable flexible microrobots with attractive new capabilities and increased adaptability for complex operations. So far, the field of microrobotics has seen a variety of initial proof-of-concept applications supporting the potential use of these devices in different fields, including medicine,<sup>15–19</sup> environmental remediation,<sup>20–22</sup> and microfabrication.<sup>23–25</sup> Moving forward, beyond the developments of the past decade, we should ask ourselves a set of key questions the answers to which lay the foundation for the future directions of microrobotics:

- Can microrobots lead to significant technological innovations?
- How can we make microrobots intelligent or programmable?
- How can we make microrobots biocompatible with human health and the environment?
- How will microrobots work collectively in small or large ensembles together toward accomplishing complex tasks?
- What are the possible communication channels and designs between the microrobots and a human user, their

macroscale operators, and the microscale environment as a whole?

- How can we integrate microrobots with our current technology and society, and how can we create novel perspectives on solving problems the world is facing?

In this Review, we take a critical look at the foundation of the next generation of small-scale robots from a materials science perspective. Existing technical difficulties and challenges require a paradigm shift in the fabrication, powering, and collective interactions of microrobots. To provide guidelines for future developments, we elucidate four main areas where smart materials will advance the frontiers of microrobotics: propulsion, biocompatibility, cooperation, and intelligence (Figure 1 and Table 1). Within the context of robotics, these categories address the challenge of utilizing “smart materials” for microscale robotics. Embedding of the operating code responsible for microrobot behavior is accomplished by the judicious selection of the constituent materials and fabrication of innovative designs of reconfigurable structures with self-sustaining power sources. We “program” microrobot instructions into its structure directly by selecting the constituent materials with task-specific tailored chemical, physical, and biological properties and functions. Through the concept of “programmability of materials”, we will address such limitations in the following sections.

## 2. PROPULSION

### 2.1. Material Requirements

Locomotion of small-scale objects through fluid environments is a challenging and exciting field. While macroscopic robots exploit bulk body inertia to pass through fluids, their microscale counterparts encounter viscous surface forces that dominate the inertial bulk effects. Thus, microscopic robots require non-reciprocal motion mechanisms for overcoming the challenges of propulsion at low Reynolds numbers and the effects of Brownian

Table 2. Strengths, Challenges, and Opportunities of Current Types of Microrobot Powering Mechanisms

Energy source	Locally powered		Externally powered			
	Chemical	Biohybrids	Magnetic	Ultrasound	Light	Electrical
<b>Strengths</b>	Autonomous motion, robust, strong mixing, chemotaxis, scalable, collective behavior	Energetic autonomy, and sensing capabilities, scalable	Precise localization, fuel-free, controllable	Fuel-free, preconcentration, collective motion, robust	Controllable movement, swarming, phototaxis, collective behavior	Controllable movement, swarming, fuel-free
<b>Challenges</b>	Not controllable, requires toxic fuel or have a short life span, can change chemical environment	Operation limited to biocompatible environment, limited volume to add functionality based on synthetic particle	Not autonomous, slow speed, complex and high-cost equipment, limited by workspace size	Not autonomous, restricted by chamber geometry and material selection	Limited speed and power due to light penetration and medium characteristics	Restricted by chamber geometry, only in low carrier concentration environment
<b>Opportunities</b>	<b>Autonomy</b> Microscale mixing, environmental remediation, drug delivery			<b>Control</b> Microsurgery, pre-concentration, drug delivery		

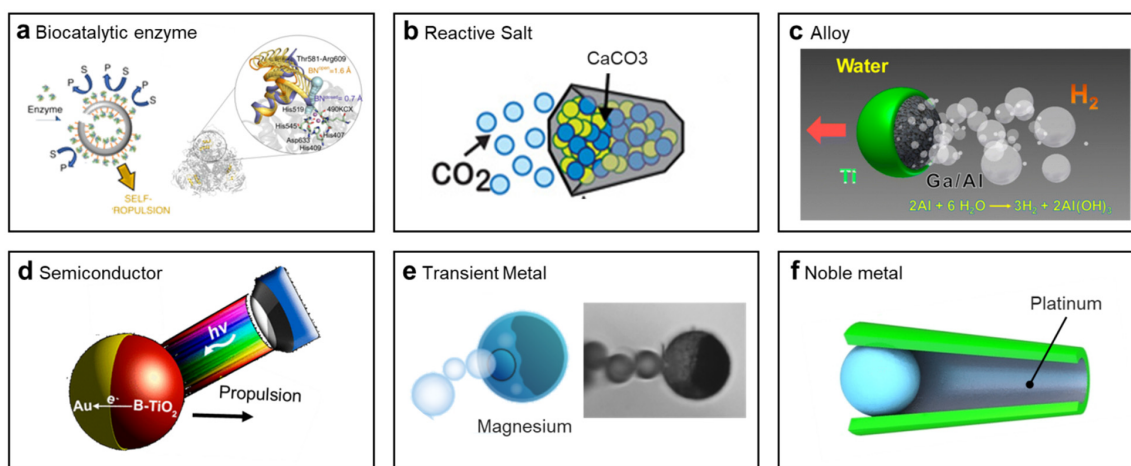


**Figure 2.** Catalytic materials for chemical propulsion. (a) Biocatalytic enzymatic-based propulsion of hollow silica microcapsules functionalized with urease. Reprinted with permission from ref 55. Copyright 2019, Nature Publishing Group. (b) Steel hull propelled by  $\text{CaCO}_3$  decomposition into  $\text{CO}_2$  gas microbubbles. Reprinted with permission from ref 43. Copyright 2016, Nature Publishing Group. (c) Water-driven hydrogen-propelled Al–Ga/Ti microengine. Reprinted with permission from ref 46. Copyright 2012, American Chemical Society. (d) Janus B-TiO<sub>2</sub>/Au engine power by photocatalysis. Reprinted with permission from ref 51. Copyright 2017, American Chemical Society. (e) Transient bubble-propelled Mg-TiO<sub>2</sub> microengine. Reprinted with permission from ref 41. Copyright 2020, American Association for the Advancement of Science. (f) Bubble propulsion of hollow tubular PPY/Pt catalytic microrockets. Reprinted with permission from ref 80. Copyright 2012, American Chemical Society.

motion. Such mechanisms require symmetry breaking in the microrobot structure or surface activity by constantly applying power source (as inertial effects are negligible), or deformation of the swimmer in nonreciprocal dynamics, similar to the cilia power stroke and recovery from microorganisms.<sup>26,27</sup> In addition, the small size limitation of microrobots does not allow for on-board power capability. Within this context, we define a “microengine” as a micro/nanostructure that harvests energy from its surrounding environment and converts it into mechanical energy, such as motion or physical actuation, while defining a “microrobot” as a microstructure that performs a predefined function while taking advantage of the above-mentioned motion.<sup>28</sup> Thus, according to our definition, a microrobot is usually composed of a microengine along with additional functional parts. The constituent materials of the microengine depend on the type of microrobot’s power sources<sup>29</sup> which can be local (chemical reaction and biohybrid designs), external (magnetic, ultrasound actuation, light, electric) or a combination of both.<sup>30</sup> Table 2 summarizes the

strengths, challenges, and opportunities for each type of microbot propulsion mechanism. In the following sections we will describe in detail different types of materials utilized as engines, their function, and how they can be exploited to tailor and tune the microbot locomotion.

## 2.2. Autonomous Engines

### 2.2.1. Catalytic and Transient Materials for Chemical Engines.

A large group of locally powered microrobots relies on catalytic engines that harvest chemical energy from their surrounding environment and convert it into motion (Figure 2). A variety of chemically active materials,<sup>31</sup> including noble metals (platinum, gold, silver),<sup>32–34</sup> transient metals (iron,<sup>35,36</sup> zinc,<sup>37–39</sup> and magnesium<sup>40–42</sup>), reactive minerals (calcium carbonate),<sup>43–45</sup> alloys,<sup>46–48</sup> semiconductors,<sup>49–51</sup> and biocatalytic enzymes (urease,<sup>52–57</sup> catalase,<sup>58–60</sup> and glucose oxidase<sup>61–63</sup>) are utilized. The integration of these catalytic materials into distinct geometries and engine designs,<sup>64,65</sup> coupled with a wide range of environmental fuels, result in diverse propulsion mechanisms. The early generation of artificial

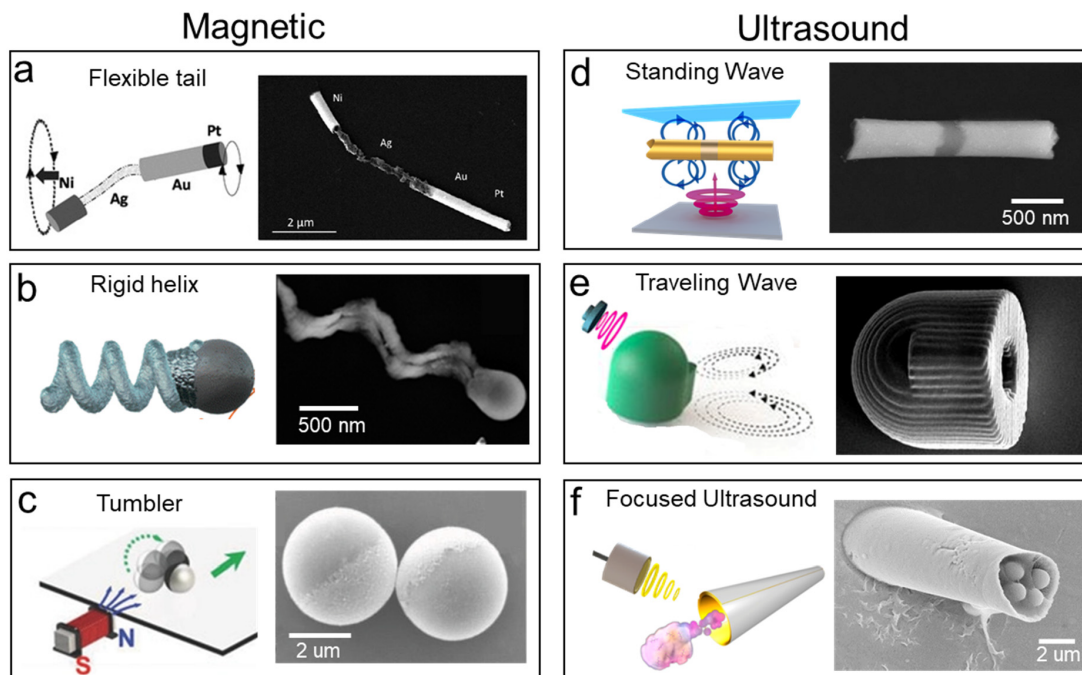


**Figure 3.** Externally powered microengines. Magnetically propelled microengines based on: (a) magnetically propelled microengine composed of Au/Ag/Ni nanowires; the silver segment was flexible under etching conditions, and the nickel segments served for magnetic actuation under a rotating magnetic field. Reprinted with permission from ref 126. Copyright 2010, American Chemical Society. (b) Rigid microhelices composed of SiO<sub>2</sub> helices coated with cobalt as magnetically responsive material. Reprinted with permission from ref 123. Copyright 2014, American Chemical Society. (c) Rotating microwalker composed by coupling two Ni/SiO<sub>2</sub> magnetic Janus microspheres. Reprinted with permission from ref 139. Copyright 2018, Wiley-VCH. Ultrasound propelled microengines based on (d) standing wave powered asymmetric Au nanowire with a concave end and a nickel segment for magnetic guidance. Reprinted with permission from ref 149. Copyright 2013, American Chemical Society. (e) Traveling wave induced oscillation of a bubble trapped in a hydrophobic 3D printed microstructure. Reprinted with permission from ref 170. Copyright 2020, United States National Academy of Sciences. (f) Focus ultrasound induced jet streaming of perfluorocarbon fuel emulsion loaded inside a graphene oxide/Au hollow microcannon. Reprinted with permission from ref 172. Copyright 2012, Wiley-VCH.

catalytic engines were bimetallic nanowires (composed primarily of gold and platinum segments) and immersed in the hydrogen peroxide fuel solution to generate a self-electrophoretic gradient over their surface that results in their locomotion.<sup>66</sup> The electrokinetic flow is generated due to the asymmetric reduction and oxidation electrochemical half-reactions occurring in each segment of the nanowires.<sup>67,68</sup> Other designs included multicomponent segments of inert and active materials.<sup>69,70</sup> A limitation of these types of engines is that environmental factors can hinder the propulsion mechanism. For example, the velocity of self-electrophoretic microengines depends on the thickness of the electric double layer around the particle and thus they operate poorly in environments with high salinity, limiting their use for practical environmental and medical applications.<sup>71</sup> Similarly, the decomposition of chemical fuels on surfaces with asymmetric composition can result in self-diffusiophoretic locomotion,<sup>72–74</sup> where molecules involved in the catalytic reaction move toward lower concentration, thus producing flow field due to the solute gradients. Again, the operation of self-diffusiophoretic micromotors depends on the thickness of the interaction layer near the particle surface.

Another locally powered mechanism of chemical locomotion consists of the continuous ejection of gas microbubbles generated in internal cavities of the microrobot engine, akin to rockets used to propel into space.<sup>75–78</sup> To achieve directional motion, the catalytic surface is enclosed by an inert material (silicon,<sup>79</sup> parylene,<sup>41</sup> polypyrrole,<sup>80</sup> graphene<sup>81</sup>), leaving an

opening for the fuel to enter and the chemical reaction to occur. Typical engine designs include a hollow tube with a catalytic interior and an inert exterior, and Janus microspheres with diverse degrees of coverage (half coating or nearly complete shell with a small opening).<sup>82,83</sup> To increase the bubble production and enhance the microengine propulsion, composite materials, surface roughness, and geometric design have been integrated into the engine.<sup>84–89</sup> A limitation of chemically powered engines is that some of the common fuels, e.g., hydrogen peroxide,<sup>90–92</sup> hydrazine,<sup>93,94</sup> sodium borohydride,<sup>95,96</sup> are toxic, while other biocompatible microengines (based on magnesium, zinc, calcium carbonate) have short lifetimes. Moreover, the byproduct of the chemical reaction might change the local pH environment or increase the concentration of charged species.

**2.2.2. Biological Materials for Chemical Engines.** Living microorganisms have been used as the engines for the propulsion of biohybrid systems. The coupling of motile microorganisms as the engine for small scale robotics with synthetic structures offers unique capabilities.<sup>97–100</sup> Microorganisms possess locomotion autonomy by harvesting energy from their environment and have built-in systems for modulating their propulsion. Developed and optimized over a long time by evolution, microorganisms add enhanced features and functionality to the microrobot. The coupling of a living organism and synthetic components can be achieved through diverse mechanisms, including covalent interactions, electro-

static interactions, and physical entrapment. In developing such microcyborgs, material characteristics can be used to target different adhesion sites. The key factors in selecting the microorganism should consider the desired task and materials for the artificial component. Most studies utilize small flagellated microorganisms ( $\sim 1 \mu\text{m}$ ) such as sperm,<sup>101–105</sup> algae,<sup>106,107</sup> or *E. coli*,<sup>108–110</sup> which are ideal for navigating through confined spaces and already capable of diverse modification mechanisms through external chemical functionalization or genetic engineering. In addition, recent studies have taken advantage of larger ciliated organisms ( $>100 \mu\text{m}$ ), such as rotifer<sup>111</sup> or vorticella.<sup>112,113</sup> Such large microorganisms rely on their cilia beating in a coordinated motion to induce motion or generate large scale fluid mixing. These larger biohybrid systems have been used for potential environmental remediation and microfluidic mixing. The widespread use of biohybrid engines will require improving control mechanisms and developing immune compatibility with other biosystems. More recently, advances in synthetic biology have provided the opportunities to program genetically engineered bacteria to produce functional components within themselves, such as magnetic particles<sup>114,115</sup> or gas-filled microstructures.<sup>116,117</sup>

### 2.3. Responsive Engines

**2.3.1. Flexible and Rigid Materials for Magnetic Engines.** Responsive or externally powered systems offer a wide range of opportunities for powering micro/nanoengines over prolonged periods.<sup>118</sup> A microrobot containing magnetic materials can respond to external magnetic fields which can guide their directionality or generate their locomotive force.<sup>119–122</sup> The first microrobots used magnetic materials in their design to reorient their axis to a magnetic field, commonly generated by a permanent magnet or Helmholtz coil, that enable them to achieve locomotion through predetermined paths. Moreover, magnetic materials have been widely used as responsive engines that convert an incident magnetic field into mechanical actuation. For example, magnetic helical microrobots need to rotate about their principal axis to move forward at low Reynolds flow and oscillating magnetic fields have been used to apply the required torque. The resulting corkscrew motion translates magnetic force to mechanical thrust and power to the engineered microstructures.<sup>123</sup> The key factor for achieving locomotion relies on the integration of magnetic components (iron, nickel, iron oxide) into the helical structure of the microrobot main body and the careful magnetization orientation. The external magnetic field can be finely tuned to adjust the oscillation frequency, resulting in speed modulation.

A class of magnetically actuated microswimmers is a set of flexible structures for which an oscillating magnetic field leads to undulation of the flexible part and the propulsion of the whole microstructure.<sup>124</sup> For example, a magnetic microengine was constructed by self-assembly of red blood cell attached to a linear chain of one micrometer-sized magnetic microbeads. These beads were coated with streptavidin and linked together by biotinylated DNA strands.<sup>125</sup> This resulting flexible structure resembles an artificial flagellum powered by inducing a beating pattern via an external oscillating magnetic field. Similarly, a flexible magnetically actuated microengine was built by integrating a rigid gold head, a flexible porous middle body (obtained by selective silver etching), and a magnetic nickel tail.<sup>126</sup> The oscillating magnetic field induces the rotation of the nickel end, which resulted in the rotation of the gold head on the adjacent section. The phase and amplitude difference between

both ends generates the bending of the middle flexible silver section, thus breaking the system symmetry and resulting in locomotion (Figure 3a). The development of flexible hinges with diverse joints has resulted in diverse types of “swimming” behavior.<sup>127,128</sup>

Rigid helical microengines containing magnetic materials can be actuated under the influence of an external oscillating magnetic field (Figure 3b), leading to numerous propulsion mechanisms, most notable corkscrew motion.<sup>123,129,130</sup> These types of rigid structures can have diverse arbitrary shapes that function as cargo compartments,<sup>131,132</sup> or as a template for cell culture.<sup>133–137</sup>

In both scenarios of rigid microhelices and flexible microstructures, each microswimmer propels by actuated rotation or oscillation rather than being dragged by the external magnetic field. These magnetic microrobots swim suspended in solution. On the other hand, tumblers or walker-based microrobots, roll onto a surface to generate locomotion. This latter propulsion mode offers unique opportunities, as it is one of the few types of microrobots that are in constant interaction with a surface. One potential application for such rollers is for scanning cancer cells in blood vessels or decontaminating pollutants from surfaces (Figure 3c).<sup>138–142</sup> The main advantage of magnetically propelled engines relies on its high degree of control and long-lasting operation, although this method has limitations based on the small domain of operation and requirement of specialized equipment.<sup>143,144</sup>

Microengines with magnetic properties can be controlled and directed by using uniform magnetic fields without necessarily inducing motion.<sup>145,146</sup> The magnetic field lines of the uniform magnetic field apply magnetic torque to the magnetic segment embedded in the microrobot, thus aligning and redirecting its locomotion.

**2.3.2. Material Density and Asymmetry Driven Ultrasound Engines.** Another important class of externally powered microengines relies on the use of ultrasound acoustic waves.<sup>147</sup> Ultrasound is an attractive power source due to its biocompatibility and tunability. Different powering mechanisms can be achieved by the generation of standing waves, traveling waves or focused ultrasound. The early generations of ultrasound-powered microrobots consisted of asymmetric metallic nanowires powered by the oscillation of the microstructure at the nodes of standing waves in fluid and the resulting acoustic streaming (Figure 3d).<sup>148,149</sup> These types of microrobots have been used in a wide range of biomedical applications including intracellular delivery,<sup>150–154</sup> preconcentration of biological targets<sup>155</sup> and transport of therapeutic payloads.<sup>149,156</sup> Theoretical and experimental studies suggest that this type of acoustic propulsion is influenced by the microstructure density asymmetry in bimetallic systems, especially for geometrically symmetric microstructures. Utilizing shape design and material asymmetry we can break the microstructure symmetry in a variety of ways and develop microrobots with distinct motion modes.<sup>157–162</sup> The operation of this propulsion mechanism is restricted to the small domain at and in the vicinity of the acoustic nodes.<sup>163</sup> Another powering mechanic for microengines is the use of traveling acoustic waves by the ultrasound-induced beating of flexible bodies, similar to a fish tail or bacterial flagella<sup>164–167</sup> and the oscillation of bubbles trapped in microstructures (Figure 3e).<sup>168–171</sup> Finally, high intensity focused ultrasound has been used to induce rapid vaporization of chemical propellants (for example, perfluorocarbon emulsions) inside a combustion chamber ( $<5 \mu\text{m}$ ) resulting in rapid

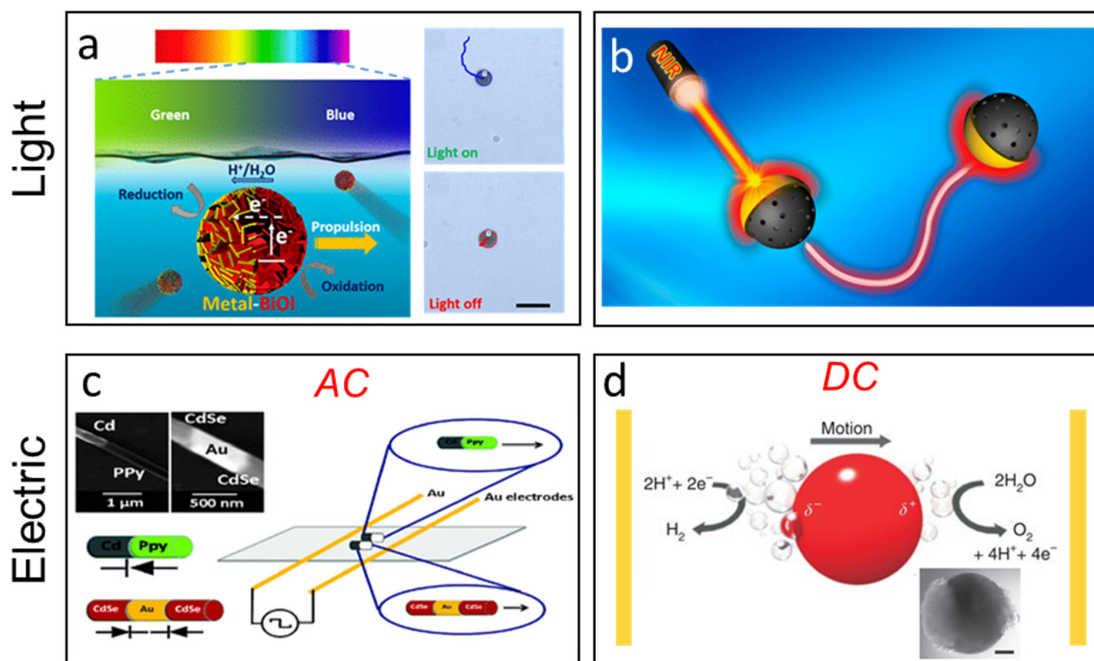


**Figure 4.** Light propulsion based on (a) photochemical motion of a bismuth oxyiodide (BiOI)-metal Janus microrobots under visible light. Reprinted with permission from ref 186. Copyright 2017, American Chemical Society. (b) Photothermal actuation of mesoporous silica nanoparticles coated with a gold cap under near-infrared actuation. Reprinted with permission from ref 203. Copyright 2016, American Chemical Society. Electric propulsion based on (c) propulsion of semiconductor diode multicomponent nanowires (Cd/PPy and CdSe/Au/CdSe) under application of an external AC electric field. Reprinted with permission from ref 209. Copyright 2010, Royal Society of Chemistry. (d) Use of DC electric field to generate bipolar chemistry over the surface of a steel sphere. Reprinted with permission from ref 219. Copyright 2011, Nature Publishing Group.

firing of the microrobot in a bullet-like fashion, reaching the mm/s speed range (Figure 3f).<sup>172–174</sup>

These types of engines have the potential to operate inside the body due to the ability of traveling waves and focused ultrasound to penetrate into a variety of tissues.<sup>175,176</sup> The main material consideration here is the use of materials with high-density contrast relative to the surrounding fluid. For example, gas microbubbles embedded inside engineered microstructures have a density contrast with their medium, thus the application of an acoustic field results in strong propulsion.<sup>177,178</sup> Similarly, a high relative density compared to fluid is required to actuate and propel solid micro engines using a standing wave, as experimental results indicate that polymeric micro engines (with similar density with water) have negligible propulsion when compared to metallic micro engines.<sup>179,180</sup>

**2.3.3. Photothermal and Photocatalytic Materials for Light Powered Engines.** Light has also been used to power microengines.<sup>181–184</sup> Similar to solar cells, for microrobots a diversity of materials can be viable candidates to harvest the energy of different portions of the electromagnetic spectrum and turn it into mechanical work.<sup>185</sup> One class of these materials use light to enhance or catalyze chemical reactions required for self-propulsion (Figure 4a). Thus, light can be used to induce self-electrophoretic,<sup>186–190</sup> self-diffusiophoretic,<sup>191–193</sup> and bubble propulsion.<sup>194,195</sup> The photoactive materials enhance photochemical reactions such as the electrolysis of water or breakdown of fuels like hydrogen peroxide. Titanium dioxide, silicon dioxide, bismuth oxyiodide, and oxometallates<sup>196</sup> are the most commonly used materials for light-induced degradation or breakdown of water. For example, exposure to ultraviolet light provides the energy necessary to excite electrons from the

valence band to the conduction band and thus induce electrophotochemical reactions depending on the microengines' material.

Another class of candidate material to exploit light for propulsion turns light energy to heat. The corresponding microengines are designed to induce asymmetric preferential absorption of near-infrared light.<sup>197</sup> This leads to the formation of a thermal gradient over the surface of the microengine and thus a gradient in the properties of the solution encompassing the particle. Thus, the particle can self-propel due to thermophoresis (Figure 4b).<sup>198–204</sup> More recently, interfacial tension gradient-based light-driven trans/cis isomerization of photochromic materials and the use of light-induced deformation of liquid crystal elastomers have also been proposed as light-driven propulsion mechanism for small-scale robots.<sup>205,206</sup> Light powered microengines have a high degree of tunability and the potential to use different portions of the electromagnetic spectrum (such as ultraviolet, visible light, and infrared) for self-propulsion in large scale operation outside the laboratory.<sup>207</sup> Nevertheless, the current generation of light propelled microengines faces diverse challenges as they are limited by light penetration in biological samples and environments with high ionic strength.

**2.3.4. Polarizable Materials for Electrically Powered Engines.** The use of external electric fields has also led to a wide range of propulsion and actuation mechanisms.<sup>121</sup> This type of propulsion was achieved by combining materials with distinct electric susceptibility. For example, metallic materials are more strongly polarizable than dielectric materials. The combination of direct currents (DC) and alternating currents (AC) can generate electrokinetic flow fields that guide the motion of small-

scale diodes (Figure 4c).<sup>208,209</sup> Induced-charge-electrophoresis is achieved by using AC fields to polarize a section of the microrobotic engine<sup>210–214</sup> leading to electroosmotic flows (generated by the accumulation of counter charges in the electric double layer around the surface of the particle) or by applying an electric field between two conducting plates generating an induced dipole on the surface of the microengine. The use of DC fields has been used to generate spatially separated redox reactions (bipolar reaction) that leads to motion by the asymmetric conversion of fuels over the engine of the microrobot (Figure 4d).<sup>215–219</sup> The applications of electrically driven microrobots will be described in detail in Section 4, Cooperation. The use of novel electroactive materials could improve energy consumption and precision control. We note that although both light and electrical engines involve chemical reactions, they require an external energy source to obtain the catalytic activity required for locomotion; thus, they are included in the section of responsive and not autonomous engines.

#### 2.4. Hybrid Power Sources

Use of a local power source is beneficial for performing tasks such as autonomous cargo carrying and enhanced mixing, where the direction of motion is determined by the microrobot and its local environment. On the other hand, external actuation can provide tunable and on-demand actuation for longer time periods. Similar to recent trends in hybrid car engines, microrobots with dual or multiple engines, capable of converting both local or external power sources into locomotion, have been developed to address the limitations of the individual power sources.<sup>220–224</sup> These include the combination of chemical and magnetic engines containing a flexible magnetized tail with a catalytic head. The two engines can work simultaneously in parallel or in a sequential manner. For example, at first the microengine moves through the solution using solely chemical locomotion, but when the fuel is depleted an external field is applied to power its motion by oscillating the flexible tail.<sup>225</sup> Chemical/acoustic hybrid engines based on asymmetric bimetallic nanowires have also been developed. Similarly, an ultrasound field can be used to modulate the chemical propulsion and act as the sole source of powering when the fuel is depleted.<sup>226,227</sup> A similar design approach has been used for chemical/light hybrid engines.<sup>228</sup> Finally, magnetoacoustic engines have been developed using a microstructure composed of helical structure coupled with a concave gold segment.<sup>229</sup> Such a combination resulted in finely tunable locomotion and swarming behavior. The use of dual power sources could offer new possibilities and modes of motion (such as acceleration or brake) that would not be possible by using a single engine type. Other future combinations of different engine combinations should offer new possibilities for microscale motion and interaction in new environments.

#### 2.5. Tunable Motion and Modulation of Speed

One approach to build smart microrobots is the use of responsive materials that adapt their physicochemical properties as a result of changes to their environment. This alteration can be locally initiated or externally triggered.<sup>230–232</sup> Each powering source has unique advantages and challenges for fine-tuning microrobot locomotion. Locally powered chemical microrobots present an inherent actuation challenge. Unlike a macroscale robot that carries its fuel supply and uses it on demand for an internal combustion or jet propulsion rocket engine, chemically powered microrobots are submerged and swim in their fuel, and thus, there is always access of the fuel to the catalytic engine

portion. Therefore, controlling the amount of local fuel consumption in microrobots and modulating their speed is a challenge. To address this matter, different strategies have been proposed for modulating the propulsion of chemically powered microrobots by an integrated programmed behavior triggered by distinct environmental cues. We note that engines which use external power sources can be modulated easily by changing the applied field; hence, we focus solely on chemical engines.

**2.5.1. Temperature-Based Modulation.** Temperature can be used to modulate the performance of microengines such as fuel consumption rate in chemically powered microrobots.<sup>233</sup> For example, the movement of catalytic metallic nanowire can be controlled and regulated on-demand by applying an external on/off temperature switch and correspondingly changing the catalytic rate of decomposition. A direct speed–temperature dependence was observed. The microrobot's speed is modulated by the temperature variation (Figure 5a) resulting in an alteration of the thermal activation of the fuel redox processes and the viscosity of the medium surrounding the microrobot. The thermal modulation of the movement holds great promise for providing an on-demand (spatial and temporal) activation of nanoscale transport systems. The increase in temperature is also shown to change the mode of

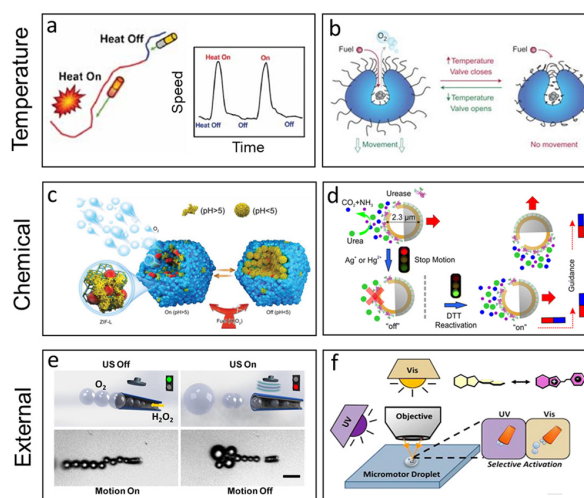


**Figure 5.** Tunable motion of microengines. (a) Temperature induced acceleration of gold platinum nanowires under spikes in temperature. Reprinted with permission from ref 233. Copyright 2009, Wiley-VCH. (b) Schematic representation of the reversible control over the speed of PNIPAM-modified microengines by changing the temperature. Reprinted with permission from ref 235. Copyright 2017, Nature Publishing Group. (c) Schematic representation of the microrobots with pH-responsive on/off motion of responsive ZIF-L particles. Reprinted with permission from ref 240. Copyright 2019, Wiley-VCH. (d) Schematic of the speed modulation by reversible catalyst inhibition of urease enzyme in the presence of heavy metals in solution. Reprinted with permission from ref 241. Copyright 2016, American Chemical Society. (e) Use of acoustic fields to modulate bubble propulsion by inducing bubble coalescence and aggregation under secondary Bjerknes force. Reprinted with permission from ref 247. Copyright 2014, American Chemical Society. (f) Reversible light-based speed modulation based on the tuning of photochromic molecular motor's properties to hinder the bubble propulsion mechanism of a micro-rocket. Reprinted with permission from ref 253. Copyright 2016, American Chemical Society.

motion from linear to circular trajectories and increase the speed of chemically powered microengines.<sup>234</sup>

Temperature-responsive polymers have been also used to regulate the response of microrobots. Chemically driven microrobots with temperature-responsive valves composed of poly(*N*-isopropylacrylamide) (PNIPAM) have the ability to reversibly actuate the valve and modulate the amount of fuel reaching the microengine catalyst (Figure 5b).<sup>235</sup> The use of PNIPAM on Janus Au–Pt microrobots has been reported to modulate the direction of motion by temperature fluctuations. At room temperature, PNIPAM brushes on the Au side were hydrophilic and swelled, allowing a self-electrophoretic motion typical of Au–Pt bimetallic microrobots. However, above 32 °C, the polymer collapsed, making the gold surface hydrophobic and endowing the microrobot with an insulator–metal structure. Under this condition, the motion is slowed, and the mechanism of motion changes to self-diffusiophoresis akin to a Pt–SiO<sub>2</sub> microrobot. The use of thermoresponsive material allows a reversible switching between hydrophobic and hydrophilic or conductive and nonconductive states; we can change the material properties of a microrobot on-demand and hence alter its locomotion.<sup>236</sup> The properties of PNIPAM have also been explored for making reversible shape-shifting microrobots made of polymeric layers with a thin film of platinum as catalyst. The flexibility and swelling capabilities of the polymer at room temperature allow folding upon cooling and unfolding upon warming of the polymeric layers. The Pt layer used for self-propulsion is thus also folded and unfolded. Such temperature-based actuation can modulate the curvature of the tubular-shaped microrobot and affect the formation of bubbles and the propulsion.<sup>237</sup> Finally, a motile microrobot used wireless power to enable locomotion via inductive coupling, resulting in the tunable local heating of the catalyst engine and enabling controlled speed.<sup>238</sup>

**2.5.2. Chemically Tunable Motion.** Programmable catalytic surfaces can also be used for tuning the motion of chemical microrobots. The propulsion of artificial biocatalytic microswimmers, which rely on enzymes to convert energy into motion, can be controlled by chemically inhibiting and reactivating the enzymatic activity. For instance, the motion of enzyme-powered biocompatible polymeric (PEDOT)/Au-catalase tubular microrobot was controlled by toxin-induced inhibition of the enzyme catalase.<sup>239</sup> Reversible pH-responsive on/off motility of microrobots was demonstrated using succinylated  $\beta$ -lactoglobulin and catalase in porous framework particles composed of zeolitic imidazolate framework-L (ZIF-L). The permeability of  $\beta$ -lactoglobulin at pH 7 allowed fuel permeability and microrobot propulsion. However, at pH 5, the access to fuel into the microrobots was impeded (Figure 5c).<sup>240</sup> Silica particles coated with urease for propulsion experience modulation of their velocity by chemically inhibiting (using Ag<sup>+</sup> or Hg<sup>2+</sup> ions) and reactivating (using dithiothreitol) the enzymatic activity of urease (Figure 5d).<sup>241</sup>

A similar principle has been applied using other synthetic catalysts. For example, the speed of self-propelled microrobots based on metal–organic frameworks (MOF) was reduced by addition of suitable chelators as chemical “brakes”, which sequester the catalytic metal ion of the MOF engine and suppress its catalytic activity.<sup>242,243</sup> Moreover, programmable speed modulation has been achieved by using built-in delay-activation materials, such as polymeric enteric coatings or metal alloys. Enteric materials delay the propulsion activation based on their coating thickness or ionic environment.<sup>244</sup> On the other

hand, an inner Pt–Cu alloy in the catalytic area of the microrobot allowed delayed microrobot activation via timed dealloying.<sup>48</sup> The preferential gradual corrosion of Cu initiated the propulsion through delayed exposure of the catalytic Pt surface. The microrobot activation time can thus be tailored by controlling the composition of the Cu–Pt alloy layer and the surrounding media, including the fuel and salt concentrations, and local pH.<sup>48</sup> The addition of microstructures has also been used to guide the fluid flow around the microrobot structure, thus modulating the microengine speed.<sup>245,246</sup>

The tunable capabilities demonstrated in previous studies pave the way for the inclusion of new programmable materials and new designs toward “built-in” activation mechanism that could regulate propulsion via accelerating or braking, optimizing the fuel consumption, and increasing the locomotion efficacy.

**2.5.3. External Field Motion Modulation.** Chemical propulsion can also be externally modulated by sound, electric field, or light stimuli. The use of external forces provides a distinct signal that does not induce propulsion by itself because a chemical engine is not affected by the low intensity of the field or does not contain a responsive material; instead, the external field works by increasing the reaction rate or inducing a physical force over the microswimmer. For example, ultrasound was used to stop and decelerate bubble-propelled PEDOT/Ni/Pt microrobots. Precise, reversible, and rapid speed increase/decrease at low/high ultrasound powers was thus obtained within seconds (Figure 5e).<sup>247</sup> Ultrasound was also used to produce stop/go motion of bubble-propelled microrobots via the mutual force experienced between bubbles oscillating nearby each other. Such force is generated by the interaction of the individual bubbles with an acoustic node through the primary and secondary radiation forces, which are responsible for generating the oscillation of the bubbles.<sup>248,249</sup> Such external manipulation with sound waves allows control of the motion and directionality.<sup>248</sup> Blue light was used to modulate the speed of supramolecular nanorobotic valves by regulating the access of the peroxide fuel into the engine of the nanorobot through the light-induced formation of inclusion complexes.<sup>250</sup>

The propulsion of microrobots has also been tuned through illumination with a white-light source which suppresses the microbubble generation in conical Ti/Cr/Pt catalytic microstructures.<sup>251</sup> Both peroxide fuel and surfactant were degraded at wavelengths between 450 and 700 nm light, being more rapid at lower wavelengths, thus impeding the motion. The propulsion of ZnO–Pt microrockets has been enhanced with light-induction.<sup>252</sup> Upon irradiation with ultraviolet (UV) light, the photocatalytic properties of ZnO and Pt were enriched, allowing increments of the microrobot speed. The light increases the number of photoexcited electrons and holes in ZnO for gas formation toward faster propulsion. Photochromic molecular microrobots have been used to change the medium properties toward modulating the speed of bubble-propelled microengines (Figure 5f).<sup>253</sup> Furthermore, AC voltage has been used for 2D control of the motion of PS/Pt/Au spherical microrobots loaded between ITO electrodes.<sup>254</sup> The direction of the microrobots could be regulated for one or multiple microrobots by controlling the electroosmotic and dielectrophoretic forces in the fluid flow. The use of AC and DC fields and a more complex 3D microelectrode setup were used for guiding and modulating the propulsion of catalytic Au–Pt nanowires.<sup>255</sup>

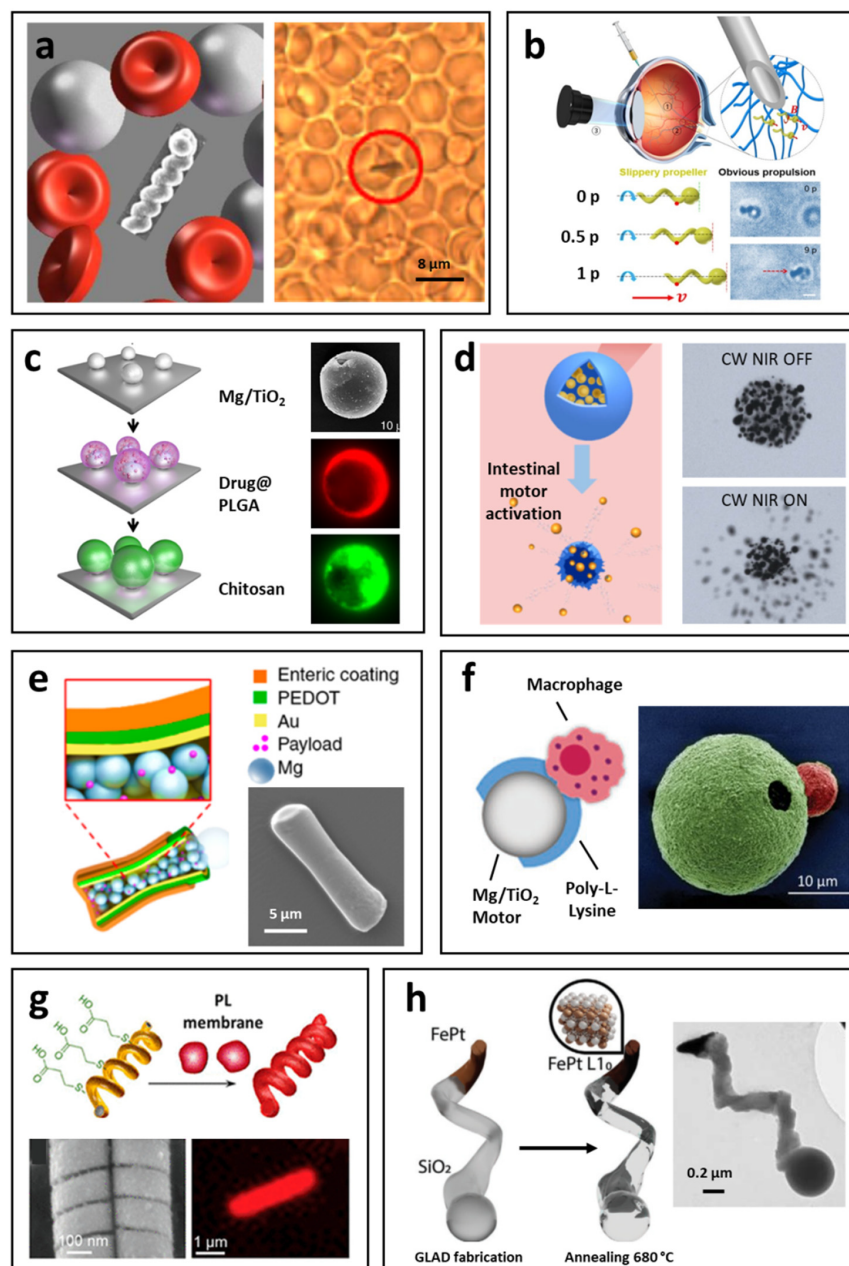


**Figure 6.** Prescribing biocompatibility. (a) Magnetic nanohelices with ferrite coatings offer controlled motion in blood. Reprinted with permission from ref 261. Copyright 2014, American Chemical Society. (b) Perfluorocarbon-coated magnetic micropropellers toward operation in the eye. Reprinted with permission from ref 262. Copyright 2018, American Association for the Advancement of Science. (c) Mg-based Janus microrobots toward *in vivo* therapy of bacterial infection. Reprinted with permission from ref 268. Copyright 2017, Nature Publishing Group. (d) A microcapsule enveloping Mg-based microrobots releases the loaded microrobots in the intestinal tract upon NIR irradiation for subsequent *in vivo* visualization by PACT. Reprinted with permission from ref 269. Copyright 2016, American Association for the Advancement of Science. (e) Enteric coated Mg-based tubular microrobots for precise positioning in the GI tract. Reprinted with permission from ref 244. Copyright 2016, American Chemical Society. (f) Macrophage-Mg hybrid microrobots with rapid propulsion in water-based environments and biological functions provided by the live MΦ cell: schematic and colored SEM image showing the attachment of the Mg-microrobot and the macrophage (in green and pink, respectively). Reprinted with permission from ref 272. Copyright 2019, Wiley-VCH. (g) Magnetic helical nanorobots cloaked with the plasma membrane of human platelets, display magnetic propulsion in whole blood while possessing inherent biological functions of platelets. Reprinted with permission from ref 277. Copyright 2018, Wiley-VCH. (h) Biocompatible ferromagnetic FePt nanorobots. Reprinted with permission from ref 280. Copyright 2020, Wiley-VCH.

### 3. BIOCOMPATIBILITY

#### 3.1. Material Requirements

Biocompatibility is critical for designing microrobots for biomedical applications, as the material selection would require proper attention regarding the safety, toxicology, and material biocompatibility to minimize or eliminate harmful side effects.<sup>256</sup> Along this direction, research efforts have recently aimed at integrating a diversity of materials for biocompatibility, degradation, deformability, and reconfigurability at the individual microrobot level and self-assembly at the collective level. An attractive approach to avoid accumulation in organs and blood vessels, achieve a zero-waste profile, and eliminate the need for retrieval, would be to design time-dependent decomposable structures and soft microrobots.<sup>257,258</sup> Moreover, the material selection for engines and coatings needs to consider the heterogeneous biological environments (gastric acid, blood vessels, mucus) and how those environments could produce biofouling or induce immune response in the body.<sup>259</sup> Thus, before considering the real implementation of microrobots in human subjects, it is crucial to carefully study and address the biocompatibility of such microrobotic systems, their potential biodegradability in the body, and understand their interaction with biological elements. In the following sections, we will focus on describing the efforts made by the microrobotic community toward this end.

#### 3.2. Biocompatible Coatings

As introduced above, the fabrication of microrobots with biocompatible materials is essential before considering their practical *in vivo* application. In this context, during the past decade we have observed a series of proof-of-concept demonstrations aiming at addressing such biocompatibility issues. Despite significant progress in microscale fabrication and actuation, adapting these robotic systems into more complex biological environments still suffers practical limitations, such as the lifetime of the microrobots in corrosive environments, viscosity of biofluids, and microrobot fouling inside complex biological environments.<sup>260</sup> New strategies have focused on creating protective coatings such as fluorinated, enzymatic, or ferrite coatings<sup>261–263</sup> (Figure 6a) based on diverse materials that provide stable actuation in a variety of complex biofluids. These protective coatings have facilitated the movement of microstructures in complex viscoelastic fluids, such as whole blood or the vitreous of the eye (Figure 6b). The use of advanced responsive materials for site-specific active delivery is expected to result in effective active delivery systems to further advance the fields of biomedicine and micromotors. Porous microrobots used a coating of gated phenylboronic acid valves for smart insulin delivery.<sup>264</sup> The pH-responsive nanovalves released insulin from a porous silica segment based on the change of pH induced by decomposition of glucose by glucose oxidase enzyme into gluconic acid, causing the protonation of the phenylboronic acid valve and release of the loaded insulin. Protective coatings based on biodegradable copolymers such as poly(lactic-co-glycolic acid) (PLGA) and methacrylic acid copolymers or biopolymers such as chitosan have also demonstrated good biocompatibility in connection to different cargo delivery strategies at the gastrointestinal tract (GI) level.<sup>265,266</sup> For example, a methacrylic acid polymer coating was used as a pH-responsive layer to autonomously release an encapsulated payload upon gastric acid neutralization by the consumption of the engine Mg core of the microrobot.<sup>267</sup>

The first demonstration of *in vivo* therapy was reported using Mg-based microrobots coated with an antibiotic-loaded PLGA layer and an outer chitosan coating which ensured microrobot adhesion to the stomach wall through electrostatic interactions (Figure 6c). The PLGA-chitosan-based microrobots offered prolonged microrobot retention in the stomach wall, leading to a more efficient therapeutic treatment.<sup>268</sup> Considerable efforts have been devoted to controlling the activation of microrobots and the delivery of the corresponding payloads in desired destinations of the GI tract by protecting the microrobots with enteric coatings that respond to different pH conditions. Toward this end, the encapsulation of Mg-based microrobots in enteric microcapsules was used to ensure the microrobot activation in the intestinal tract under pH-triggered release (Figure 6d).<sup>269</sup> The intestinal fluid-activated microrobots were visualized in real time *in vivo* by photoacoustic computed tomography (PACT), demonstrating migration from the enteric capsule, efficient propulsion in the targeted area, and enhanced tissue retention. The protection of individual microrobots with enteric coatings was reported using tubular microrobots loaded with Mg microparticles (Figure 6e).<sup>244</sup> In this study, Mg-based microrobots were protected with enteric coatings of different thickness, demonstrating controllable position and activation in desired sections of the GI tract. An *in vivo* toxicity study in mice demonstrated the biocompatible and safe character of such enteric-coated microrobots. Another type of microrobot material, which has been widely used for cargo delivery applications due to its biocompatibility and high surface area, is mesoporous silica. For example, antibiotic-loaded mesoporous silica microtube structures were integrated with *Magneto-spirillum gryphiswalense* (MSR-1) magnetotactic bacteria, resulting in a biohybrid microswimmer with antibiofilm capabilities.<sup>270</sup> Similarly, urease-powered mesoporous silica-based microrobots gated with pH-responsive supramolecular nanovalves have displayed effective cargo delivery intracellularly without compromising the cell viability.<sup>271</sup>

Another approach for establishing biocompatibility is to develop biohybrid microstructures, including cell-based microrobots consisting of synthetic structures attached to living cells<sup>272–275</sup> (Figure 6f) or synthetic microrobots coated with natural cell membranes (Figure 6g).<sup>276–278</sup> Combining microrobots with natural cell components improves the overall biocompatibility of the microrobotic system, thus reducing immune response. More importantly, combining the efficient movement of synthetic microrobots with the natural biological properties and functions of cellular components has resulted in cell mimicking microrobots with inherent biological functionality, including toxin- and pathogen-removing capabilities, which hold great promise toward therapeutic applications. The use of cells (including cellular components or whole cells) and natural proteins with the dynamic movement of microrobots has led to novel and specific isolation of pathogenic cells and related toxins. For example, magnetically propelled microrobots were coated with the membrane of natural platelets (PL), demonstrating strong and selective binding to Shiga toxin and *Staphylococcus aureus* (Figure 6g).<sup>277</sup> Acoustically propelled microrobots have also been coated with biological cell membranes, consisting of dual red blood cell@PL, thus offering the biological capabilities of both cellular components.<sup>279</sup> Recently, a new design of magnetic nanopropeller consisting of the codeposition of iron and platinum were tested toward intracellular plasmid delivery, demonstrating noncytotoxicity and excellent biocompatibility (Figure 6h).<sup>280</sup> In addition, the

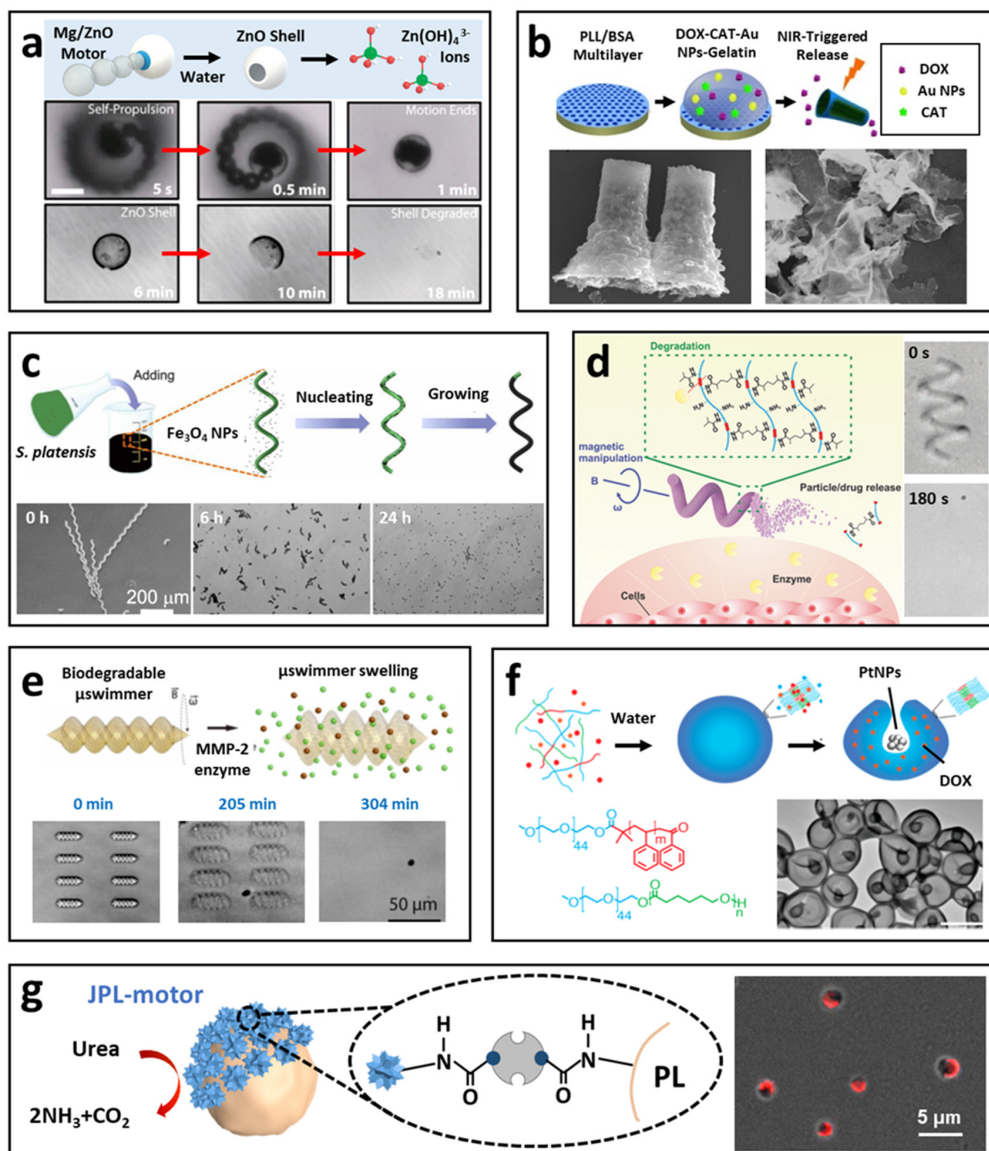


**Figure 7.** Prescribing biodegradability. (a) Biodegradable transient Mg/ZnO Janus microrobots. Reprinted with permission from ref 284. Copyright 2016, American Chemical Society. (b) Biodegradable protein-based microrockets. Reprinted with permission from ref 289. Copyright 2015, American Chemical Society. (c) *S. platensis*/Fe<sub>3</sub>O<sub>4</sub> NP-based magnetic microrobots. Reprinted with permission from ref 293. Copyright 2017, American Association for the Advancement of Science. (d) Biodegradable helical microrobots with collagenase induced degradation. Reprinted with permission from ref 295. Copyright 2018, Wiley-VCH. (e) Magnetically powered hydrogel microswimmer with matrix metalloproteinase-2 (MMP-2)-based enzymatic degradation. Reprinted with permission from ref 296. Copyright 2018, American Chemical Society. (f) Degradable drug-loaded hybrid microrobots. Reprinted with permission from ref 299. Copyright 2017, American Chemical Society. (g) Urease-powered Janus platelet cell microrobot. Reprinted with permission from ref 300. Copyright 2017, American Association for the Advancement of Science.

interaction dynamics between the structural design parameters of microswimmers and the immune system was studied recently, exploring the interaction between magnetically propelled helical microswimmers and mouse macrophages and splenocytes. Overall, the above studies suggested that structural design optimizations of the microrobot directly affect their locomotion performance in biological fluids and have profound implications in conferring microrobots of immunogenicity.<sup>281</sup>

### 3.3. Biodegradable Materials

Biocompatibility is an essential but not exhaustive requirement when searching for the practical microrobots for medical applications. The behavior of the constituent biocompatible materials should assist the functionality of the microrobot. New smart materials are highly desired to offer triggered autonomous actuation and degradability, thus avoiding potential toxicity issues when applied to *in vivo* systems. Having biodegradable materials that autonomously decompose into harmless ionic species or smaller polymer fragments is highly desirable for *in*

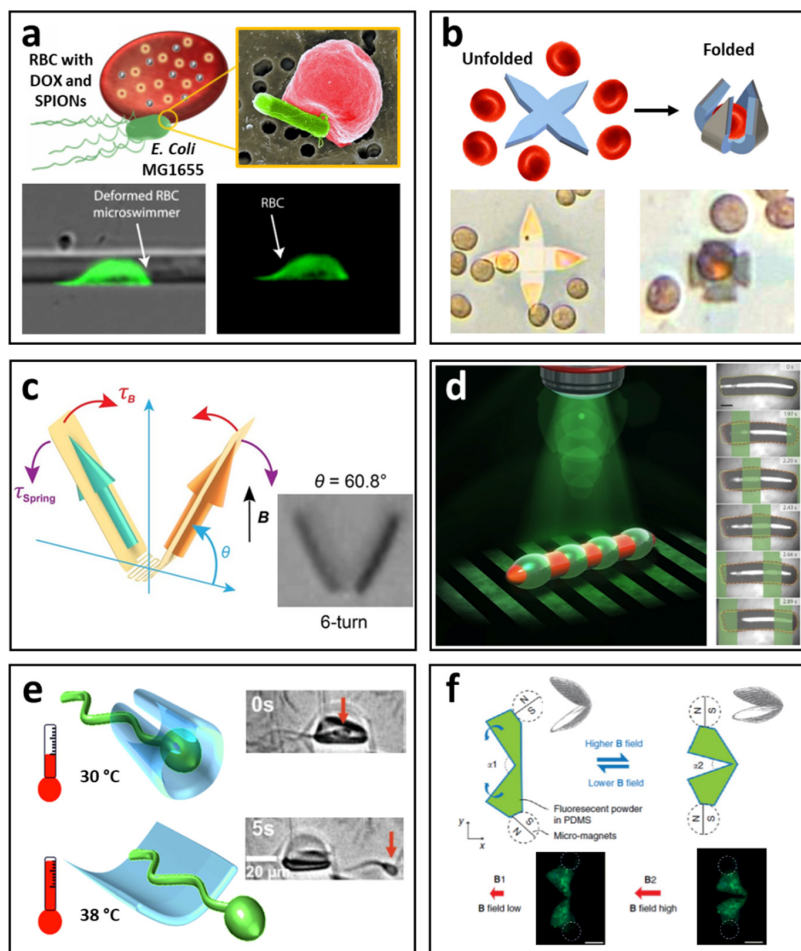


**Figure 8.** Prescribing deformability. (a) Soft RBC-based bacterial microswimmers. Reprinted with permission from ref 305. Copyright 2018, American Association for the Advancement of Science. (b) Self-folding grippers for single cell capturing. Reprinted with permission from ref 308. Copyright 2014, American Chemical Society. (c) Shape-morphing microrobots based on spatially resolved magnetic properties. Reprinted with permission from ref 310. Copyright 2019, Nature Publishing Group. (d) Photoresponsive soft microrobot consisting of photoactive liquid-crystal elastomers showing the deformation of an anchored microrobot under a periodic light pattern. Reprinted with permission from ref 206. Copyright 2016, Nature Publishing Group. (e) Thermoresponsive polymeric microtubes for remote-controlled release of single sperm cells. Reprinted with permission from ref 314. Copyright 2016, Wiley-VCH. (f) Scallop-like microswimmer displaying opening and closing shape change when actuated by an external magnetic field. Reprinted with permission from ref 315. Copyright 2014, Nature Publishing Group.

*in vivo* applications.<sup>44,282,283</sup> For example, fully autonomous chemically propelled degradable microrobots, which are powered by the consumption of a transient metal propellant with water/acid reactions, have exhibited efficient motion and degradation in biological environments. Different transient metal propellants can be used such as magnesium (Figure 7a),<sup>40,284,285</sup> zinc,<sup>37,286</sup> or iron.<sup>35,36</sup> In these cases, the biofluid fully degrades the corresponding propellant leaving a minimal inert residue. Such biodegradable metal-based microrobots represent a good alternative to the use of peroxide-dependent microrobots and pave the way for operation in diverse biological environments. Different designs of self-destroyed Janus microrobots, including Mg/ZnO microrobots, have reported the ability to propel in different biofluids and autonomously disappear without leaving any residues (Figure 7a). The materials of such transient microrobots can dissolve at a predictable rate into nontoxic products<sup>284</sup> and be programmed

to present different behaviors based on the use of hydrophilic and hydrophobic coatings.<sup>41</sup>

Layer-by-layer fabrication with functional proteins presents another attractive approach for preparing self-propelled microrobots with degradable properties.<sup>287,288</sup> These biological materials not only enhance the biocompatibility of the microstructure, but can be utilized as a biodegradable support structure into which catalytic compounds can be loaded to initiate and sustain the propulsion reaction (Figure 7b).<sup>289–292</sup> Microrobots actuated from externally controlled fields are designed with this consideration in mind. Using biological templates such as *Spirulina* microalgae (Figure 7c)<sup>293,294</sup> or 3D microfabricated biodegradable microswimmers (Figure 7d)<sup>295</sup> offers triggering degradation by external stimuli<sup>296</sup> or a built-in response to pathological markers (Figure 7e).<sup>297,298</sup> Despite the major advantages of the previously discussed transient materials and biodegradable microrobots, the size of the majority of such microrobots still constitutes a limitation for their implementa-

tion in biomedical applications that requires systemic administration. In this direction, stomatocyte-based nanoscale microrobots with biodegradable behavior, made of soft self-assembled block copolymers (poly(ethylene glycol)-*b*-polystyrene (PEG-*b*-PS) and poly(ethylene glycol)-*b*-poly( $\epsilon$ -caprolactone) (PEG-*b*-PCL), were reported (Figure 7f).<sup>299</sup> PCL is a polymer of slow biodegradability, high biocompatibility, and good drug permeability, which has allowed its combination with microrobots for sustained delivery applications. During the degradation of PCL, large pores were formed onto the stomatocyte microrobots, thus leading to sustained DOX cargo release. Still, the requirement of hydrogen peroxide fuel in the previously discussed microrobot design compromised the biocompatibility of the system toward practical applications. A recent study has demonstrated a totally biocompatible and biodegradable cell-based microrobot based on the asymmetric modification of natural platelet cells with the enzyme urease (Figure 7g).<sup>300</sup> Such enzyme-modified cell microrobots, based on fully biocompatible and biodegradable materials, are capable of movement in the presence of the bioavailable fuel, urea, and can be loaded with therapeutic and imaging payloads for *in vivo* applications without carrying any toxicity risks.

### 3.4. Deformability

Most early generation microrobot structures relied on rigid materials, including hard metallic or oxide structures with simple geometries such as spheres, rods and helices. To develop microrobots capable of navigating through narrow channels while avoiding blockage or damage, soft, deformable, or reconfigurable materials will be needed.<sup>301</sup> This requirement necessitates the use of materials with Young's modulus close to that of cellular materials, which is orders of magnitude lower than metals or oxides. Additionally, for practical use, deformability must be controllable and reversible. Here, materials, such as hydrogels, which are soft and easily functionalized, come to mind. Another subset of materials are rubbery elastomers that possess high creep resistance and large stretchability.<sup>296,297</sup> Deformable microrobots would allow shape morphing tailored for specific tasks as well as safer interaction with the surrounding objects and surfaces in dynamic environments. Therefore, motile bacteria and human cells have served as viable candidates owing to their deformability, dynamic reshaping under stress, and autonomy.<sup>304</sup> For instance, microorganisms loaded with therapeutic cargo can withstand active deformation while passing through confined channels and preserve their integrity and motility (Figure 8a).<sup>305</sup> Microorganisms pose remarkable plasticity and adaptability to varying physical and chemical environmental conditions. Additionally, other motile cells, such as sperm, can act as attractive deformable mobile platforms.<sup>101,104</sup>

In terms of deformability and control in artificial systems, millimeter-scale robot designs are more advanced than microrobots.<sup>306</sup> However, recent developments have enabled the translation of these design principles toward miniaturization, into structures of a few micrometers in size. Microrobots composed of deformable materials offer broad versatility in terms of functionality, softness and recoverable strain.<sup>307</sup> For example, this is done by careful and precise control over magnetization and the use of hinges<sup>298–310</sup> (Figure 8b and 8c) to implement programming responsiveness to the external field and provide deformability for adaptive locomotion.<sup>145,311–313</sup> Light, as an external stimulus or external energy source, can also be exploited to induce programmable responsiveness and

deformation for gripper actuation (Figure 8d).<sup>206,313</sup> Deformable biohybrid microrobots based on the use of thermoresponsive PNIPAM microtubes have been presented for the capture, transport and release of sperm cells (Figure 8e).<sup>314</sup> Scallop-shape microrobots consisting on single-hinge microswimmers which are propelled by periodic body-shape changes have also been reported (Figure 8f).<sup>315</sup> Prescribing biocompatibility, biodegradability, and deformability in microrobot designs is among the fundamental characteristics essential for ensuring that these motile microstructures are safe to use in medical applications.

## 4. COOPERATION

### 4.1. Material Requirements

Despite the many attractive capabilities of small scale microrobots, a single microrobot will hardly be able to make an impact on a macroscale system. Thus, we need to ensure that many of these microrobots can be used simultaneously to accomplish tasks.<sup>316–318</sup> In macroscopic robotics, communication and cooperation between individual robots and swarming has been a topic of interest and a source of numerous research opportunities. In such systems, collective dynamics are enabled through coding and computer language embedded into the processing units of the robot.<sup>319,320</sup> Translating the same technology to microscale robots is not a viable path, at least at the current state of art, because it is not possible to embed complicated electronics into a microstructure. We need to think about a new paradigm of programmability, communication, and processing units to develop microrobots with desired collective behavior. The main key to navigating this paradigm is building microstructures with smart and responsive materials and designing communication strategies through physical or chemical signaling.<sup>321–323</sup> For example, microrobots can feel their surroundings or the presence of their neighbors through physiochemical interactions. Highly sensitive catalysts can serve as candidates for such purpose as they can quickly and efficiently convert fuel or target substances to products that augment their chemical surroundings.<sup>324,325</sup> Materials that can be easily polarized or whose charge can be neutralized or enhanced can be used to exploit electrostatic interactions. Additionally, van der Waals and short-range hydrophobic interactions between larger biomolecules or other organic materials can form the basis for communication between neighboring microrobots.<sup>326</sup> Moreover, external fields can induce interactions, depending on the field characteristics such as its nature, strength, and possible frequency. For example, magnetic fields can be used to tune the interaction of microrobots that contain of ferro- or paramagnetic materials. Magnetic materials offer many capabilities, such as attractive and repulsive interactions, which can be modulated with high precision by application of a multicoil apparatus. For electrical field stimulation, semiconducting and metallic particles can be controlled by two or four electrode setups and thus share the behavior control and precision with magnetic fields. Light-sensitive materials, such as structure changing photochromic spiropyrans or azobenzenes, can be used to initiate conformal changes. Finally, selecting materials with different densities and arranging them in various configurations can yield structures that are sensitive to acoustic forces and promote swarming or active behavior. To conclude, selecting the right materials is a critical step to endow microrobots with abilities to communicate between themselves and form desired swarm dynamics.<sup>327</sup>

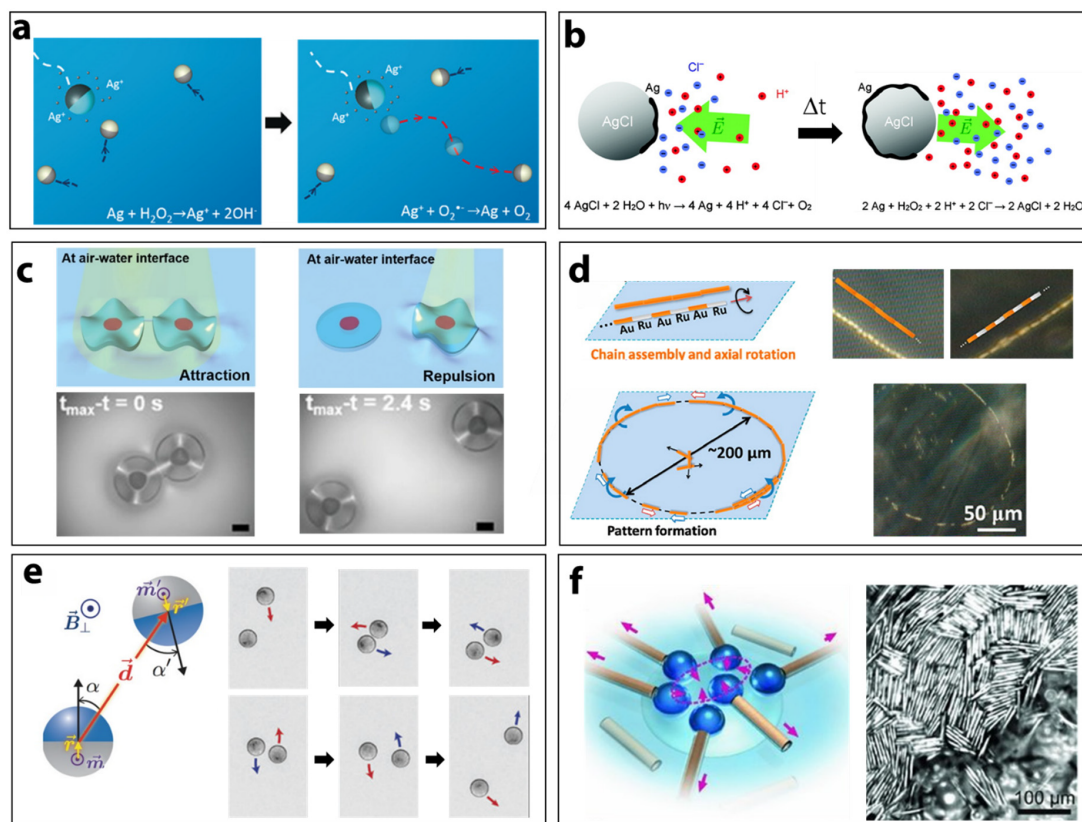


**Figure 9.** Interactions between individual microrobots. (a) Chemical communication between an activator microrobot (teal) releasing  $\text{Ag}^+$  and the activated  $\text{SiO}_2/\text{Pt}$  microrobot (gray) which accelerates due to formation of  $\text{Ag}/\text{Pt}$  on the surface. Reprinted with permission from ref 335. Copyright 2018, Wiley-VCH. (b) Change in surface coverage from  $\text{AgCl}$  to  $\text{Ag}$  and back to  $\text{AgCl}$  due to UV-based decomposition in water and  $\text{H}_2\text{O}_2$ . Reprinted with permission from ref 336. Copyright 2010, American Chemical Society. (c) Capillary force induced attraction (left) and repulsion (right) of hydrogel disks at the air–water interface due to light-based wrinkling. Reprinted with permission from ref 338. Copyright 2019, Wiley-VCH. (d) Interactions between spinning  $\text{Au}/\text{Ru}$  rods in a standing wave acoustic field to produce head-to-tail alignment in chain and ring formations. Reprinted with permission from ref 148. Copyright 2012, American Chemical Society. (e) Contactless interaction between  $\text{SiO}_2/\text{Ni}/\text{Pt}$  Janus microrobots, demonstrating long-range chemical propulsion followed by magnetic interaction and mutual orbiting at close range and finally separation due to dipole–dipole repulsion. Reprinted with permission from ref 339. Copyright 2017, Wiley-VCH. (f) Meniscus-climbing interactions between  $\text{Ti}/\text{Cr}/\text{Pt}$  tubular microrobots which generate large-scale assembly. Reprinted with permission from ref 340. Copyright 2010, Wiley-VCH.

#### 4.2. Robot–Robot Interactions

An important feature to develop in the field of microrobotics is establishing communication and signaling between individual micromachines. The ability to communicate is fundamental to design complex emergent behavior, collective dynamics, and smart swarming. Similar to powering and programmability, a change from macroscale to microscale requires a new paradigm for communication. While macroscopic robots can communicate through wires or wireless networks using electronic senders and receivers, microrobots are too small to host such elements. We need to exploit physical, chemical, and hydrodynamic interactions as means to relay information to a microrobot about its surrounding environment. For example, chemically self-propelled microrobots can communicate with each other using particle–particle interactions that can be attractive or repulsive. One such type of communication is based on the release of chemical compounds from a microswimmer, which could result in acceleration or braking of surrounding microswimmers.<sup>328–334</sup>

The redox nature of silver was employed to accelerate a microrobot due to close range chemical interactions between

particles (Figure 9a);<sup>335</sup> activator microrobots release  $\text{Ag}^+$  ions due to  $\text{H}_2\text{O}_2$  oxidation. When  $\text{SiO}_2/\text{Pt}$  microrobots pass by,  $\text{Ag}$  is reduced on the  $\text{Pt}$  surface, generating a highly catalytic alloy which accelerates its speed due to communication with the activator microrobot. Moreover, light illumination may induce further decomposition reactions which affect the flow of ionic species and thus the diffusiophoretic dynamics in solution.  $\text{AgCl}$  crystals which release a multitude of ions under UV illumination produce a net electric field around the particle and propel it by phoretic forces have also been reported (Figure 9b).<sup>336</sup>  $\text{Ag}$  is reduced on the surface, passivating the  $\text{AgCl}$  surface until small amounts of  $\text{H}_2\text{O}_2$  are added, which regenerate the  $\text{AgCl}$  coating, causing an oscillation in the particle population and dynamics.

Light irradiation can be used to cause attractions between the active and passive particles, leading to the formation of dimers<sup>337</sup> or resulting in wrinkle structures which induce interactions between the microstructures (Figure 9c).<sup>338</sup>  $\text{Au}$  nanoparticles have thus been embedded in thermoresponsive gel disks that wrinkle upon illuminating to white light. The associated capillary force causes wrinkled disks to attract each other if both are illuminated or repel if only one is wrinkled. The

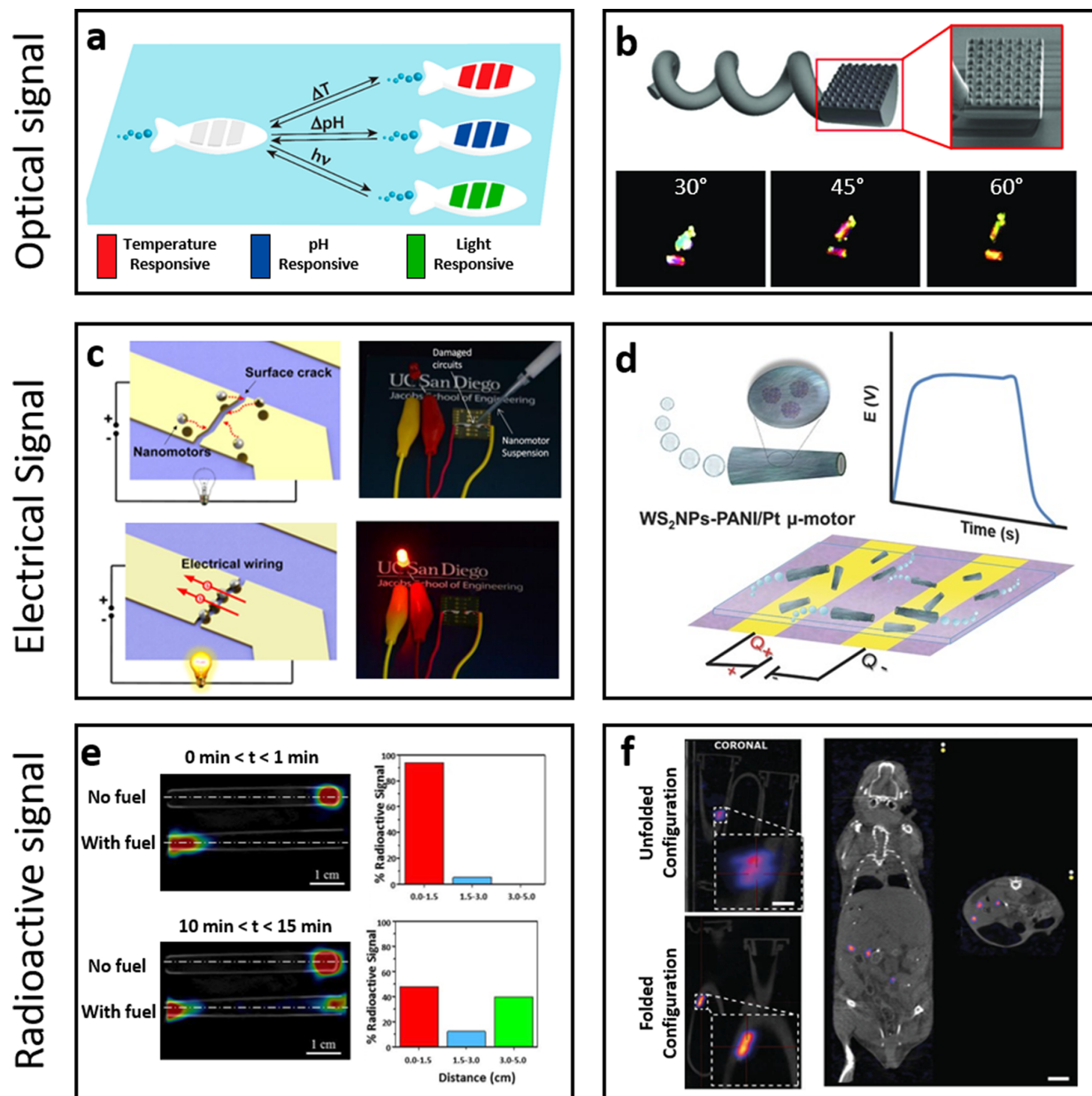


**Figure 10.** Material configurations which transform microrobots into information probes. (a) Small-scale swimmer relays information about the environment through multistimuli responsive color changes. Reprinted with permission from ref 341. Copyright 2018, American Chemical Society. (b) 3D printed helical microrobot with columnar pattern on the head which produces structural coloration with angle-dependent behavior. Reprinted with permission from ref 342. Copyright 2020, Wiley-VCH. (c) Au/Pt alkanethiol-modified microrobots seek and collect at cracks and restore the conductivity of an electrical circuit. Reprinted with permission from ref 343. Copyright 2015, American Chemical Society. (d)  $WS_2$  NP@PANI/Pt microrobots acting as micro-supercapacitors by attaching to an existing electronic circuit and augmenting its capacitive behavior. Reprinted with permission from ref 344. Copyright 2016, Wiley-VCH. (e) Pt/PEDOT/Au tubular microrobots, loaded with radioactive NaI, and used as contrast agents in PET-CT imaging, demonstrating that the microrobots' position can be tracked with time. Reprinted with permission from ref 348. Copyright 2018, American Chemical Society. (f) SPECT images of PEGDA/NIPAM-AAm-PEGDA-MNP microrobots with embedded  $^{99m}Tc$  nanocolloid demonstrating stronger signal in the folded configuration both *in vitro* and *ex vivo* in a mouse model. Reprinted with permission from ref 350. Copyright 2019, Wiley-VCH.

ability to tune interparticle interactions by illumination serves as signals by which the particles communicate to form different collective dynamics.

Other physical properties can be used for particle communication. Acoustic standing waves is used to force Au/

Ru nanorods into a variety of configurations, such as chains or rings (Figure 9d).<sup>148</sup> While the nanorods constantly spin around their long axis doublets with head-to-tail attachments are dominant and head-to-head configurations are rarely observed. Such rudimentary form of communication and pairing between

individual microrobots enables the formation of larger structures. Other physical properties can be used for contactless particle–particle interactions that lead to long-range attraction, short-range repulsion, and mutual alignment between adjacent swimmers. SiO<sub>2</sub>/Ni/Pt microrobots based on magnetic dipole–dipole interaction demonstrate such behavior (Figure 9e).<sup>339</sup> The microrobots are able to feel each other and even lock into spinning doublets and triplets before disassembling. This behavior was used to push cargo or form larger assemblies. An external object can also induce interactions between microrobots, leading to the formation of larger structured aggregates. For instance, meniscus-climbing interactions between Ti/Cr/Pt microtubes and their bubble tails due to the H<sub>2</sub>O<sub>2</sub> decomposition reaction were used to form large assemblies (Figure 9f).<sup>340</sup> By varying the surface tension via surfactant concentration and bubble production via number of microtubes in solution the assembly dynamics can be controlled. The integration of short-range (e.g., magnetic, hydrodynamic, and van der Waals forces) and long-range (e.g., electromagnetic fields) interactions could enable microscale robots to communicate and interact with each other to form more complex structures or perform tasks at the macroscale, as will be described in the following sections.

### 4.3. Robot–User Interactions

Microscale robots can communicate with each other and interact based on short-range and long-range interactions to form more complex structures or perform tasks. However, as human operators, we desire to understand and translate microscopic interactions that the microrobots experience into easy to interpret signals at the macroscale. To fully take advantage of small-scale robotics we need interfaces that communicate information to macroscale counterparts, such as a human users or computers. In this regard, researchers have used diverse responsive materials that serve as probes to signal information to the macroworld. The ability of microrobots to transmit optical signals through the use of smart materials could improve the visualization and identification of motile small-scale robots. One such example is the use of a microfish robot capable of color changing in response to a variety of environmental stimuli and thus communicating its state to an external observer (Figure 10a).<sup>341</sup> This communication approach focuses on the use of microrobot swimmers which probe and report their environment information through reversible color change of multifunctional strips embedded on the robot surface. Combinations of different responsive materials were used to provide multiplexing signals, including the use of thermochromic or halochromic dyes to indicate change of temperature or pH, respectively. Moreover, other reported designs included the addition of a strontium aluminate phosphorescent pigment strip to provide phosphorescence in dark environments, allowing location of the swimmer at night or in a dark environment. Such capabilities aim to simulate aquatic species that use bioluminescence for signaling, camouflage, or communication.

Optical signals based on structural coloration have been explored by taking inspiration from the nanostructures in butterflies and beetles to obtain their vivid color patterns (Figure 10b).<sup>342</sup> Helical microrobot are fabricated by printing out of photoresist with a head section which features nanosized patterns of pillars. Then, thin layers of Ni and Ge are used for magnetic navigation and structural coloration. Depending on the angle of the head to the viewer a different color can be observed, and a suitable tracking algorithm can be devised

describing not only the microrobot's position but orientation in three-dimensional space.

While microrobots are unable to use electronic components due to their size, they can serve as parts of electrical circuits and augment macroscopic systems. For example, the use of self-propelled microrobots to autonomously seek and localize at cracks in broken electrodes and restore their electrical conductivity has been explored in recent years (Figure 10c).<sup>343</sup> The Au/Pt microrobots move toward and accumulate inside the electrode crack. To prevent dissipation of the accumulated microrobots away from the crack the Au surfaces of the Janus structures were functionalized with hydrophobic monolayers to stick to the underlying glass surface. In another case, the use of WS<sub>2</sub> nanoparticles@PANI/Pt microrockets that act as a supercapacitor was explored (Figure 10d).<sup>344</sup> The microrobots swim toward an electric circuit and augment its behavior once they attach to it. Performing electrical characterization of the augmented circuit reveals a much larger capacitive behavior compared to a bare electrode demonstrating the ability to enhance electrical components with actively propelled microrobots. Liquid metal microrobots composed of Galinstan (GaInSn alloy) were also used as welding filler in electrodes made from a Ag nanowire network.<sup>345</sup> The alloy microrobots actively move along the Ag wires and accumulate at the contact junctions, fusing with the network at room temperature by reacting with acid vapor. This addition results in lowering the contact resistance and demonstrates the ability of the microrobots to form strong electrical connections and enhance conductivity of the circuit.

As mentioned in the biocompatibility section, microrobots offer considerable potential for *in vivo* applications of drug delivery, isolation of toxic materials and interactions with live cells. However, in majority of cases these microrobots are released into the body and any subsequent communication with them is lost until they are recovered through secondary processes. Recently, a strong effort has been aimed to directly visualize their location and utilize them as motile imaging probes.<sup>346,347</sup> For example, Pt/PEDOT/Au microtubes were incubated with radioactive NaI and used as the imaging agent for positron emission tomography with computerized tomography (PET-CT) (Figure 10e).<sup>348</sup> The microrobots reported excellent contrast and were easy to detect in phantom samples. Additionally, their motion and location can be accurately tracked over time compared to a static sample. This imaging platform was used to monitor the collective behavior of urease powered microrobots inside living animals.<sup>349</sup> A soft hydrogel matrix microrobot capable of magnetically actuated motion and temperature-responsive morphological change as an imaging agent has been realized recently (Figure 10f).<sup>350</sup> The hydrogel body was prepared via lithographic approaches and filled with magnetic nanoparticles and <sup>99m</sup>Tc[Tc] colloids. The colloids are stable and highly contrasting in single-photon emission computed tomography (SPECT) imaging and provide visualization from multiple angles *in vitro* and *in vivo* in a mouse model. Once positioned by magnetic actuation the microrobots are actuated via irradiation with near-infrared light to unfold them and anchor them in the desired location. Thus, the incorporation of stimuli-responsive, electrically active, and radioactive materials can greatly enhance the communication capabilities of microrobots as active information probes.

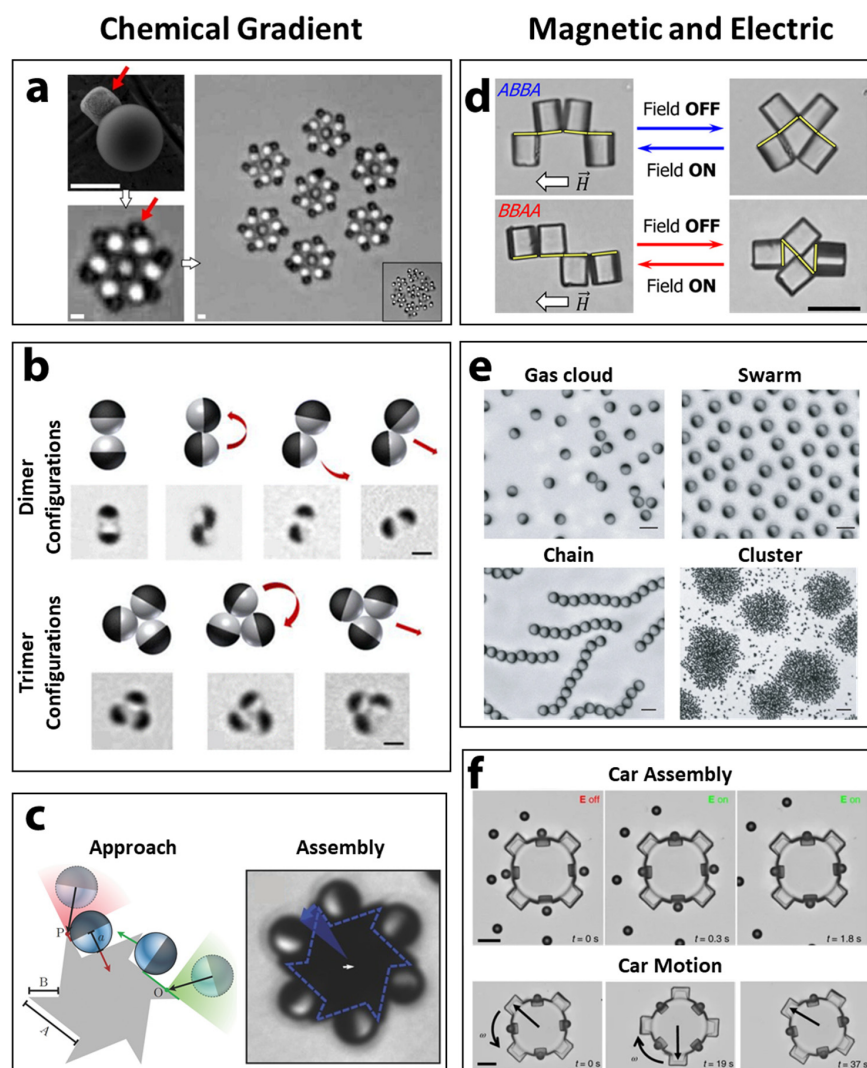


**Figure 11.** Assembly of microrobots. (a) Microrobots composed of a polymer bead and a hematite cube assemble into self-spinning rotors due to the decomposition of  $\text{H}_2\text{O}_2$  under UV light. Reprinted with permission from ref 354. Copyright 2018, Nature Publishing Group. (b) Different configurational assembly of  $\text{SiO}_2/\text{Pt}$  Janus microrobots due to alkanethiol functionalization and subsequent hydrophobic interactions. Reprinted with permission from ref 357. Copyright 2013, American Chemical Society. (c)  $\text{SiO}_2/\text{Pt}$  microrobots propel, approach, attach, and rotate a microgear in the presence of  $\text{H}_2\text{O}_2$ . Reprinted with permission from ref 358. Copyright 2016, Wiley-VCH. (d) Different configurations of magnetic-based assembly of functional cubes leading to clam-like opening and closing (top) or wrapping and unwrapping (bottom). Reprinted with permission from ref 359. Copyright 2017, American Association for the Advancement of Science. (e) Different assembly configurations of  $\text{SiO}_2/\text{Ti}/\text{SiO}_2$  particles with varying frequency of the electric field forming from top left to bottom right: gaseous clouds, swarms, chains, and clusters. Reprinted with permission from ref 210. Copyright 2016, Nature Publishing Group. (f) Assembly of the wheels (superparamagnetic polystyrene particles) onto the chassis via a DEP force (top) and the subsequent motion of the whole “car” by rotational magnetic fields (bottom). Reprinted with permission from ref 360. Copyright 2019, Nature Publishing Group.

#### 4.4. Assembly

Interactions between individual microrobots are important for studying emergent behavior. However, controlling these interactions leads to sophisticated and programmable behavior which takes advantage of a multitude of microrobots assembled into various structures.<sup>313,351</sup>

Plasmonic materials can be used to induce interactions between microstructures. For instance, magnetic coils decorated with silver nanoparticles served as optical tweezers under optical illumination.<sup>352,353</sup> Another case of microrobotic assembly are hematite cube/polymer bead composites. Under UV light

illumination the hematite cube decomposes the  $\text{H}_2\text{O}_2$  fuel, causing a phoretic force to attract and assemble the microrobots in a symmetric pattern (Figure 11a).<sup>354</sup> A gear assembly made of a group of seven microrobot–microrobots then proceeds to rotate. Even superassemblies occur when multiple gears assemble and complement or interfere with each other. Spiropyran coated  $\text{SiO}_2$ –Pt microrobots presented dynamic assembly based on surface electrostatic attractions induced by UV light irradiation.<sup>355</sup> Similarly, *E. coli* and microbeads, functionalized with proteins PhyB and PIF6, demonstrated reversible assembly. Such processes relied on the binding

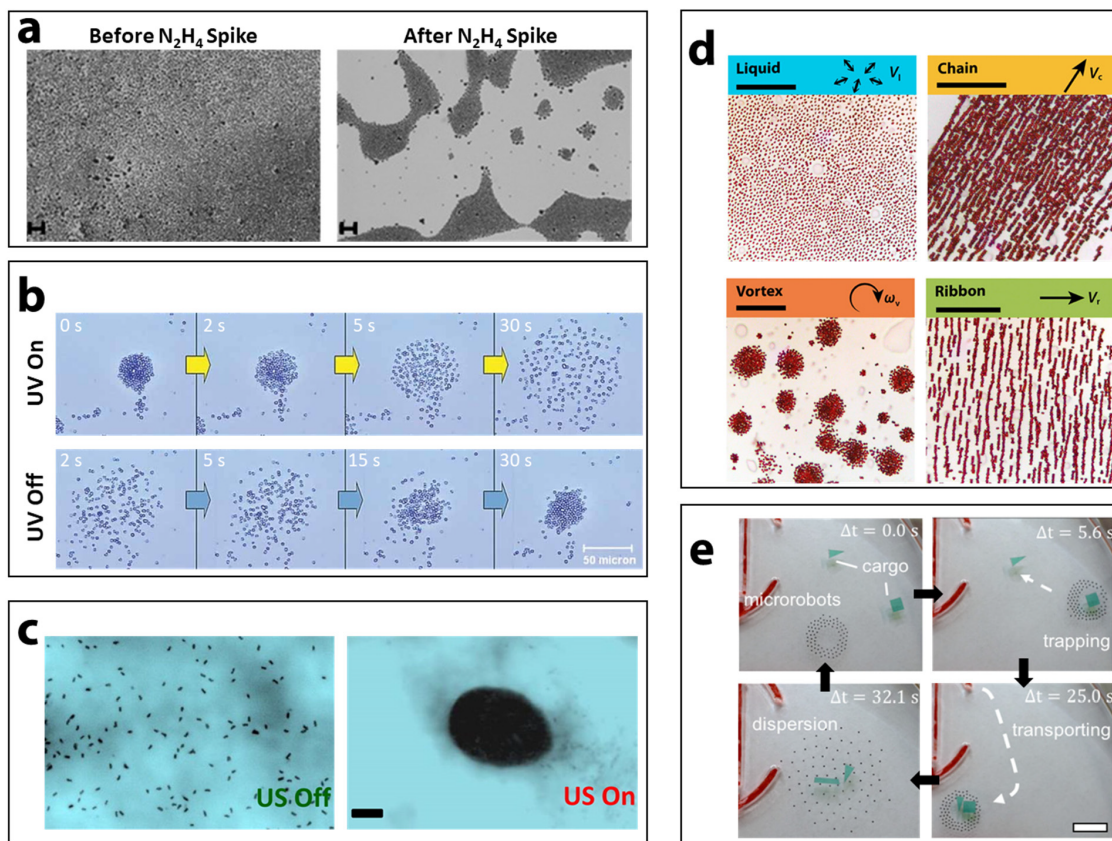


**Figure 12.** Swarming behavior of microrobots. (a) Reversible swarm formation of Au microparticles in a solution of  $\text{N}_2\text{H}_4$  and  $\text{H}_2\text{O}_2$ . Reprinted with permission from ref 378. Copyright 2011, American Chemical Society. (b) Reversible clustering of  $\text{SiO}_2/\text{TiO}_2$  Janus microrobots and subsequent dispersal upon application of UV light in deionized water. Reprinted with permission from ref 379. Copyright 2010, Wiley-VCH. (c) Reversible localization of chemically propelled Au/Pt rods to the low pressure nodes due to acoustic radiative forces. Reprinted with permission from ref 380. Copyright 2015, American Chemical Society. (d) Transformation of hematite peanut-shaped particles into oscillating (liquidlike), rolling (chainlike), spinning (vortexlike), and tumbling (ribbonlike) states by applying different magnetic fields. Reprinted with permission from ref 391. Copyright 2019, American Association for the Advancement of Science. (e) Direct control of a swarm of magnetically controlled NdFeB/resin disks, including formation of the swarm, trapping, and transportation of the object and dispersion of the swarm. Reprinted with permission from ref 385. Copyright 2020, SAGE Publishing.

between these proteins under red light and their dissociation from each other under far-red light.<sup>356</sup> Assemblies of Janus particles are common due to direct molecular interactions as well.  $\text{SiO}_2/\text{Pt}$  microrobots functionalized with an alkanosilane compound exhibit assembly behavior (Figure 11b).<sup>357</sup> The long oily chains on the  $\text{SiO}_2$  side interact via hydrophobic interactions to join otherwise actively propelling Janus particles. A multitude of possible configurations emerge from dimers that attached head-to-head or side-to-side, as well as trimers and even heptamers. These interactions were much more permanent compared to the UV light induced interactions of Figure 11a.

Self-propelled microrobots can assemble equally well with inert components.  $\text{SiO}_2/\text{Pt}$  Janus microrobot and a lithographically prepared gear wheel demonstrate this concept clearly (Figure 11c).<sup>358</sup> The freely moving microrobots approach the edges of the gear and slide into position to begin spinning the wheel. Depending on the dimension of the gear and the microrobots, the chance of misalignment with respect to the edge varies which ultimately leads to a change in the speed of rotation. Thus, microrobots can assemble to perform mechanical work utilizing a chemical fuel ( $\text{H}_2\text{O}_2$ ) reminiscent of macroscale engines.

Interaction of external fields, such as magnetic fields, with responsive materials can also generate assembled structures. One such instance is photoresist cubes covered by a cobalt magnetic layers (Figure 11d).<sup>359</sup> After magnetization, the cubes assemble side-to-side (AA) or edge-to-edge (AB). Further, these structures can assemble again forming ABBA or BBAA configurations which can be actuated in a variety of ways under a magnetic field forming an open, closed, or wrapping conformation. Assembly of polarizable  $\text{SiO}_2/\text{Ti}/\text{SiO}_2$  Janus microrobots was accomplished by varying the frequency and amplitude of the applied vertical electric field (Figure 11e).<sup>210</sup> The established potential difference coupled with the imbalance of polarizability on the two halves of the Janus structure causes an induced-charge electrophoresis (ICEP) force which together with dipole–dipole interactions of individual microrobot leads to their assembly. Depending on the switching speed of the AC field, the assemblies can take the form of a gaseous cloud, swarms, chains, or clusters. Going one step further by combining both magnetic and electrical fields, microrobots can assemble onto a microcar and power it (Figure 11f).<sup>360</sup> The car is constructed by movement of the superparamagnetic polystyrene wheels into the appropriate locations via a dielectrophoretic

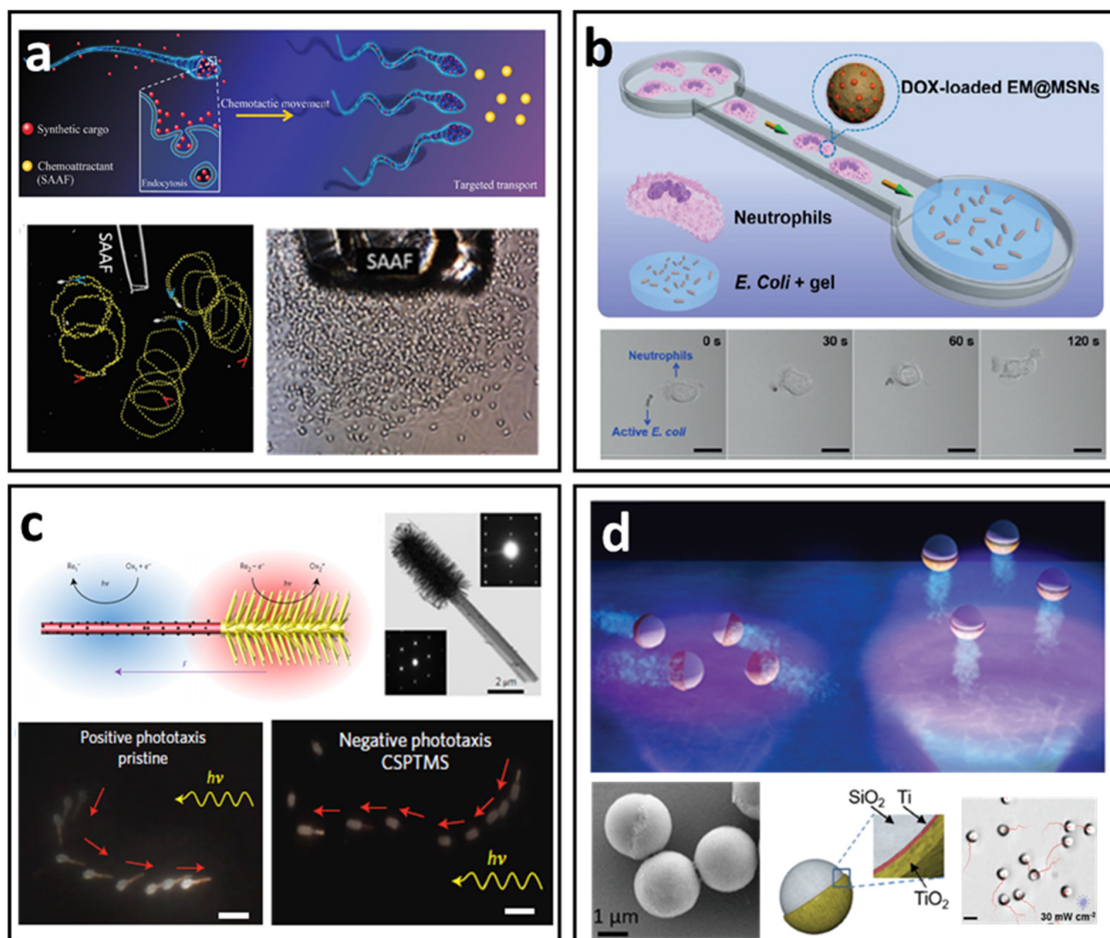


**Figure 13.** Environmental taxis. (a) Cargo-loaded spermatozoa exhibit taxis due to a chemical attractant released by the egg. Reprinted with permission from ref 391. Copyright 2018, Wiley-VCH. (b) Neutrophil engineered by drug-loaded bacterial membrane coated SiO<sub>2</sub> nanoparticle for targeted drug delivery. Reprinted with permission from ref 392. Copyright 2019, Wiley-VCH. (c) Janus TiO<sub>2</sub>/Si nanotrees move toward and away from UV illumination. Reprinted with permission from ref 50. Copyright 2016, Nature Publishing Group. (d) TiO<sub>2</sub> coated SiO<sub>2</sub> Janus microrobot with controllable photogravitactic behavior by tuning the UV light intensity. Reprinted with permission from ref 397. Copyright 2018, Wiley-VCH.

force (DEP). This force is based on the material properties of the wheels, the 3D printed chassis, and the design of the wheel openings. Next, using rotating magnetic fields to which the wheels are highly responsive the whole car can be navigated and operated by a human user. While magnetic fields and close range chemical interactions are the most common assembly mechanisms, acoustic fields can also generate the assembly of microscopic structures.<sup>361,362</sup> At the same time, active–passive interactions have also found uses in cargo delivery,<sup>363–365</sup> highlighting the large material and stimuli library we possess to produce sophisticated assembly behavior at the microscale.

#### 4.5. Swarming

Still, many real applications would require hundreds if not thousands of these tiny microrobots to complete a task with macroscopic results. The stochastic dynamics at the microscale can have significant influence on the active propulsion dynamics and affect the microrobot dispersal.<sup>366,367</sup> For example, the coupling of Brownian noise and active rotation results in emergent phenomena such as chiral<sup>368</sup> and spiral<sup>369</sup> diffusion of rotary microrobots. Moreover, for targeted motion in traveling a distance from point A to point B, a fraction of microswimmers

fail to accomplish the task and leave the population during the trip because of the effect of Brownian motion and random noises in the system. Thus, cooperation between a large number of active structures is crucial, especially if we can tune their interactions such that they can stay together for a desirable amount of time. One approach for assembling and managing populations of microrobot relies on using chemical interactions and signaling. For example, the chemical gradients resulting from self-propulsion chemical reactions may cause collective attractive motion and formation of large swarms.<sup>191,326,370–377</sup> For instance, one of the simplest methods to assemble a swarm of microparticles is based on the formation of byproducts from chemical reaction. This approach was demonstrated using Au microparticles in a solution of hydrazine (N<sub>2</sub>H<sub>4</sub>) and H<sub>2</sub>O<sub>2</sub> (Figure 12a).<sup>378</sup> Here, the gold surface acts as a catalyst, enabling a cascade of redox reactions resulting in fast local formation of H<sup>+</sup> ions. This in turn establishes strong electric and electroosmotic forces which bring the particles together until the N<sub>2</sub>H<sub>4</sub> supply is depleted.

As we have seen so far, chemical reactions can be further modulated by a variety of physical methods. Ultraviolet light as a

knob to control the aggregation of functional microparticles was also explored (Figure 12b).<sup>379</sup> In pure water Janus microrobots comprised of TiO<sub>2</sub> and SiO<sub>2</sub> tend to aggregate with each other due to attractive surface interactions. However, when irradiated with UV light the clusters disperse within 30 s due to the disbalance in chemo- and osmophoretic forces associated with the formation of radicals and hydrogen molecules from the TiO<sub>2</sub> surface. A useful method to localize and aggregate a large number of self-propelling microrobots has been realized. (Figure 12c).<sup>380</sup> While utilizing commonly used Au/Pt self-propelling rods, the authors took advantage of the density mismatch of the two constituent materials. In a closed chamber a standing wave can be established by an acoustic field resulting in low-pressure nodes where the microrobots are localized. The advantage here is that by changing the parameters of the ultrasound field, the aspects of the chamber such as size and height, and the density of the microrobots, the swarm's size and position can be varied, not to mention that swarms can be instantaneously dissolved. The flexibility in manipulating the swarm can lead to designing programmable behavior. In terms of complexity of swarm behavior, however, magnetic interactions show the most potential, demonstrating not only aggregation but also a multifaceted programmable behavior (Figure 12d).<sup>381</sup> With a combination of oscillating and rotating magnetic fields a variety of behaviors can be extracted from the peanut-shaped hematite colloids. Starting from a liquid-like state, swarms can be formed in the form of chains, vortices, and ribbons due to rolling, spinning, and tumbling associated movement, producing exciting new capabilities from otherwise inert particles.<sup>382–384</sup> The concept was taken one step further by producing Nd<sub>2</sub>Fe<sub>12</sub>B/resin disks which float on the surface of water and are controlled by an array of external magnets underneath (Figure 12e).<sup>385</sup> With control over the coupling of the driving external magnets and the magnetization of the disks, complex behavior is attained in the form of swarms, caging and transporting cargo and finally of dispersing the cluster. Thus, by controlling the fundamental forces and interactions at the microscale, such as chemical reactions, electrostatic balance and long-range field effects, swarm-like cooperation can be established between individual microrobots enabling them to perform tasks that a single one cannot achieve.

## 5. INTELLIGENCE

### 5.1. Material Requirements

On the question of how we make microrobots intelligent, we need first to define intelligence within the context of microscale microrobots. Self-locomotion, by itself, is not a sign of intelligence, but rather an intelligent microrobot should be capable to perform a specific task it has been programmed to or take cues from the environment influencing it in the way it accomplishes this task. The unique challenges of establishing artificially intelligent microrobot would require developments beyond simply motile active matter. Based on the context of this Review, we consider that a microrobot is intelligent if it can make decisions based on processing information available in its surrounding environment. For example, locally powered microrobots can follow chemical gradients resulting in a motile platform that “chooses where to go” based on fuel availability. In another case, a micromotor can have selective surfaces that can distinguish between the substances in a heterogeneous solution and bind selectively to a specific target, thus serving as sensors on the move. Finally, the intelligence of the microrobot can rely on

its ability to follow instructions from an algorithm or external force, similarly to how macroscale robots in assembly lines follow a set of preprogrammed instructions.

### 5.2. Environmental Taxis

Nature provides straightforward approaches to guidance and intelligence in the microworld.<sup>386</sup> For example, microorganisms have complex communication mechanisms based on chemical clues, and such chemotactic behavior significantly affects many biofunctions, such as immune response, tissue repair, and fertilization.<sup>387–389</sup> Chemotactic microorganisms have been combined with synthetic components toward creating biohybrid microrobots capable of responding to chemical cues from the environment. For example, *S. marcescens*-based biohybrid microrobots coated with fluorescent polyester beads reported navigating toward L-serine gradient.<sup>390</sup> Sperm functionalized with doxorubicin and quantum dots moved toward specific chemical attractant and release payloads in various biological media (Figure 13a).<sup>391</sup> Another approach used neutrophils with drug-loaded mesoporous silica nanoparticles camouflaged by bacteria membrane toward self-guided targeted drug delivery (Figure 13b).<sup>392</sup> Asymmetric enzyme-coated polymersomes have shown chemotactic capabilities. The microrobot used glucose oxidase and catalase biocatalytic enzymes to direct the microstructure up a glucose gradient.<sup>321</sup> Besides the motion toward higher chemical concentrations (positive chemotaxis), negative chemotaxis is observed by tuning the enzyme and substrates. By adding the phosphate ion (Pi), the ATPase-bound liposome exhibited negative chemotactic behavior, whereas the microrobot displayed positive chemotaxis in the absence of Pi.<sup>393</sup>

Phototaxis describes the phenomenon that microorganisms swim toward (positive phototaxis) or away from (negative phototaxis) the light. This behavior is seen in some motile microorganisms such as green algae. The behavior of the photoactive microrobots can be similarly affected by the incident optical field, and these phenomena can be used for a wide range of applications including navigation to a specific place or sensing the environment. Phototactic microrobots are made of photocatalytic materials which can generate electron and hole pairs under light, and actuate the propulsion. Isotropic semiconductor microrobots composed solely of TiO<sub>2</sub> demonstrate the ability to swim and tunable locomotion based on the light source location due to the induced asymmetrical surface chemical reactions.<sup>394</sup>

Janus TiO<sub>2</sub>/Si nanotree structures perform phototactic behavior and light-induced propulsion by self-electrophoresis under UV illumination. The nanotree robot exhibited positive phototaxis by positive charge modification of the TiO<sub>2</sub> ends. On the contrary, the microrobot moved away from the light and exhibited negative phototaxis under negative charge modification (Figure 13c).<sup>50</sup> An extension of this work demonstrated the ability to encode a distinct spectral response by loading the microrobot surface with different dyes, enabling to individually control each structure from within a large group.<sup>395</sup> Carbon-nitride decorated microrobots show both positive and chemotaxis using water as the fuel under irradiation of white light.<sup>396</sup> TiO<sub>2</sub> /SiO<sub>2</sub> microrobots can swim against gravity under photochemical stimulation. The application of large light intensity at the surface resulted in the microrobot lift-off away from the light source (Figure 13d).<sup>397</sup> A microrobot consisting of a multilayer onion inspired structure, was developed as a motile microtrap for attraction, trapping, and destruction of

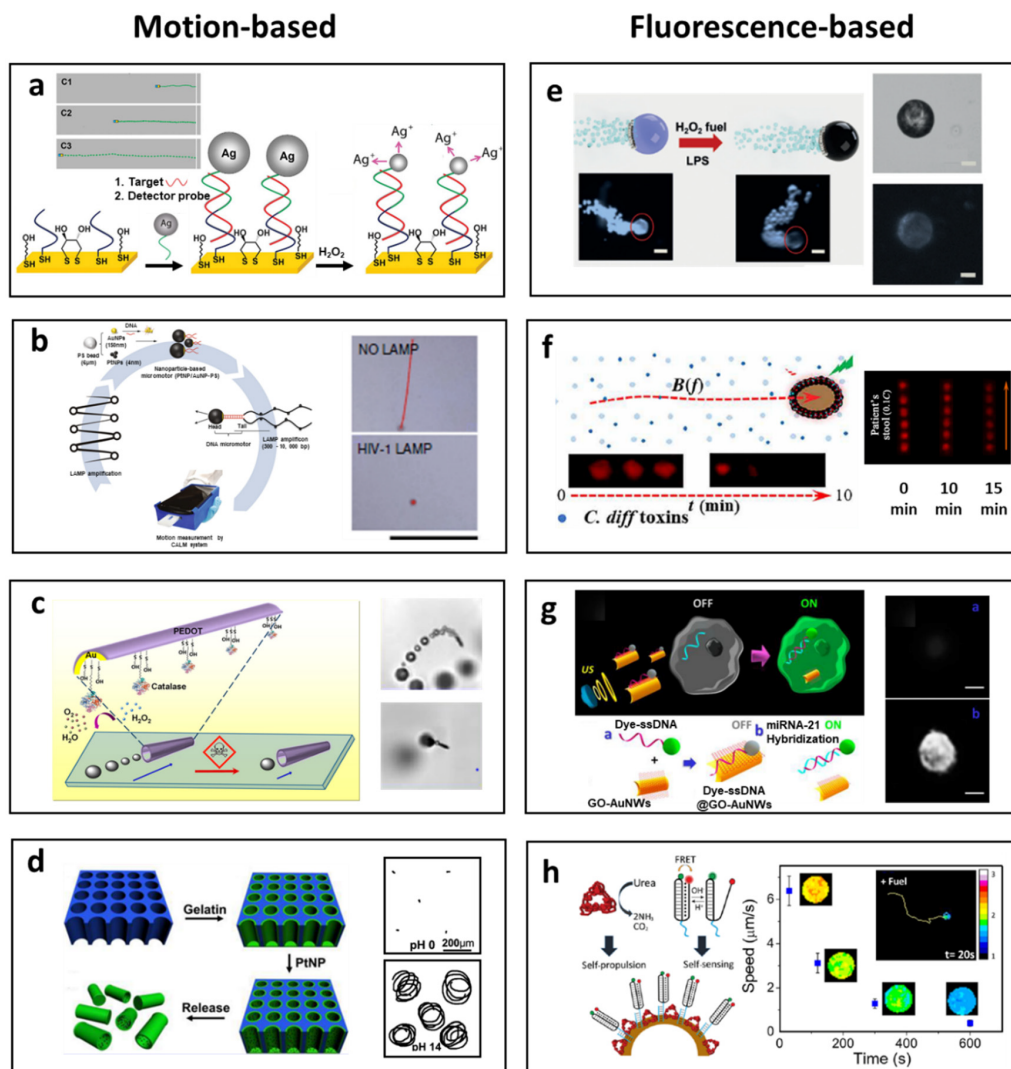


**Figure 14.** Motion- and fluorescence-based sensing. (a) Speed-enhanced Ag nanoparticle decorated Au–Pt microrobots for DNA detection. Reprinted with permission from ref 399. Copyright 2010, Nature Publishing Group. (b) Cellphone diagnosis of HIV by motion decrease of DNA modified catalytic microrobot. Reprinted with permission from ref 408. Copyright 2020, Nature Publishing Group. (c) Speed inhibition of catalase-powered tubular microrobot due to heavy metal ion induced toxic effect on the catalytic activity of enzyme. Reprinted with permission from ref 239. Copyright 2013, American Chemical Society. (d) Responsive motion behavior of Pt nanoparticle encapsulated gelatin microrobot at different pH. Reprinted with permission from ref 412. Copyright 2016, American Chemical Society. (e) Fluorescent probe functionalized Janus Pt microrobot with fluorescence quenching effect after exposure to endotoxin. Reprinted with permission from ref 415. Copyright 2017, Wiley-VCH. (f) Magnetic nanoparticle modified spore for toxin detection in patients' stool. Reprinted with permission from ref 419. Copyright 2019, American Association for the Advancement of Science. (g) Intracellular delivered dye-labeled DNA/graphene oxide anchored Au nanowires for sensing the miRNA expression. Reprinted with permission from ref 424. Copyright 2015, American Chemical Society. (h) pH-responsive DNA nanoswitch functionalized urease-powered microrobot for pH sensing based on monitoring FRET efficiency. Reprinted with permission from ref 426. Copyright 2019, American Chemical Society.

biological threats by controlled chemoattractant and therapeutic agent release. The micromotor onion structure contained a magnesium engine core and inner chemoattractant and therapeutic layers. The depletion of the magnesium engine resulted in the sequential dissolution of the inner layer releasing serine chemoattractant that attracted nearby motile microorganisms and capture them within the trap structures followed by the internal release of silver ions for killing the pathogen accumulated within the microtrap cavity.<sup>398</sup> Such integration of smart materials to perform autonomous task illustrate the

concept of directly embedding intelligence through material selection.

### 5.3. Sensing

Beyond the taxis properties, furnishing microrobots with sensing capabilities is crucial to construct a microsystem that interact intelligently with its environment. Surface functionalization endows microrobots with the ability to sense their surroundings and fulfill many tasks including toxin detection and removal, biological target isolation, and intracellular delivery. Several examples based on different sensing mechanisms are discussed

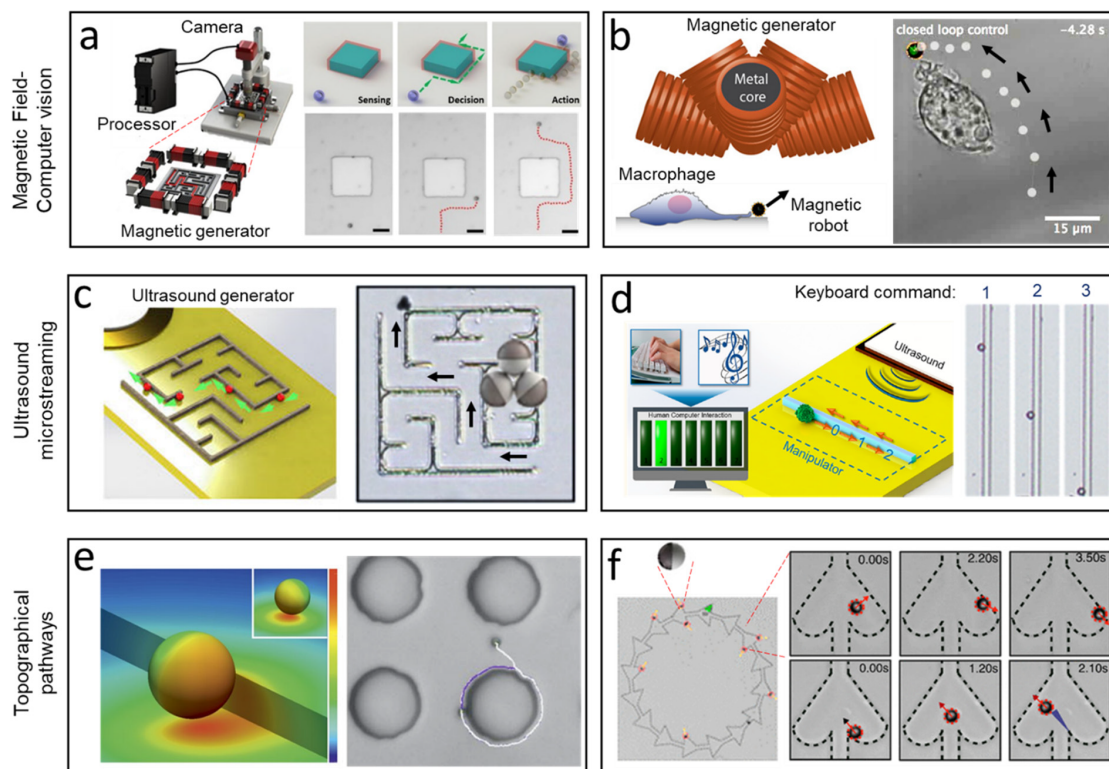


**Figure 15.** Off-board intelligence of microrobots. (a) Magnetically driven path planning navigation of microrobot in a maze structure. Reprinted with permission from ref 434. Copyright 2017, American Chemical Society. (b) Magnetic microrobot controlled by an external magnetic field toward simulating a bacteria and measure macrophage physical forces. Reprinted with permission from ref 439. Copyright 2017, American Association for the Advancement of Science. (c) Topographical manipulation of microrobots through a maze using acoustic microstreaming generated at the edges of the microstructure. Reprinted with permission from ref 446. Copyright 2017, American Chemical Society. (d) Interface acoustic microstreaming manipulation with keyboard and piano keys. Reprinted with permission from ref 444. Copyright 2019, American Chemical Society. (e) Use of topographical features for guiding microrobot directionality. Reprinted with permission from ref 455. Copyright 2016, Nature Publishing Group. (f) Induced directional flow of microrobots through alignment with micropatterned ratchets. Reprinted with permission from ref 457. Copyright 2018, American Chemical Society.

in Figure 14. The change of microrobots speeds upon their interaction with analytes has been used as a sensing platform. A motion-driven DNA biosensor microrobot was reported where the binding of DNA strands decorated with silver nanoparticles resulted in a speed change of Au–Pt catalytic microrobots (Figure 14a).<sup>399</sup> Such DNA detection was further developed with different types of motion, such as Mg-based,<sup>400</sup> catalase-based,<sup>401</sup> and tubular microrobot.<sup>402</sup> A variety of biorecognition tags has also been modified onto the surface of microrobots to fulfill specific capture and isolation of biomolecules,<sup>403–405</sup> cancer cells,<sup>406</sup> and bacteria.<sup>407</sup> Recently, the motion-based cellphone diagnostics demonstrated great specificity and high sensitivity toward efficient detection of HIV-1 and Zika virus. Such assay has the potential to broaden the smart microrobot application into rapid, low-cost, and early diagnosis of various diseases (Figure 14b).<sup>408,409</sup> Besides their use in biomedical applications, self-powered microrobots capable of motion changes are of interest for monitoring water quality to detect heavy metal ions and nerve agent vapors. The speed decrease of catalase-powered microrobot is due to the toxin-induced losses in the catalytic activity of the enzyme (Figure 14c).<sup>239,410,411</sup> Speed-dependent motion behavior has been reported for pH sensing, for instance, by incorporating Pt onto pH-sensitive materials. The speed change phenomenon is ascribed to the pH-

dependent catalytic activity and effect of pH responsive gelatin material leading to an indirect pH sensor (Figure 14d).<sup>412</sup>

A second type of microrobot sensing utilizes changes in fluorescent signals (i.e., on/off or off/on) for detection of chemical compounds and biological markers.<sup>413,414</sup> One example is the use of catalytic Janus microrobot for endotoxin detection. In this design, highly fluorescent phenylboronic acid (PABA) modified graphene quantum dots (GQDs) were encapsulated into a Pt-propelled microrobot. Fluorescence quenching was observed when PABA tagged GQDs specifically reacted with endotoxins (Figure 14e).<sup>415</sup> Similarly, many other toxins, heavy metals and nerve agents can be detected in such platform.<sup>182,416–418</sup> Furthermore, microrobots have been used for the remote detection of toxins secreted by *Clostridium difficile* in patients' stool. The fabricated magnetic spore microrobot encapsulating fluorescent probes performed real-time measurements upon mixing of the microrobot with bacteria, causing the on-site fluorescence quenching (Figure 14f).<sup>419</sup>

Another key application of fluorescence-based sensing was displayed in intracellular delivery.<sup>420–423</sup> For example, fluorescence quenched Au nanowires have been used as an intracellular sensor due to their ability to internalized cells. After internalization, dye-labeled single-strand DNA can be

displaced from the graphene oxide surface of the microrobot upon interaction with the target miRNA, leading to fluorescence recovery (Figure 14g).<sup>424</sup> Additionally, a DNA nanoswitch functionalized urease-powered microrobot was synthesized to sense the local pH change by comparing fluorescence resonance energy transfer (FRET) efficiency at different pH (Figure 14h).<sup>425,426</sup> Surface-enhanced Raman spectroscopy<sup>427,428</sup> has also been used in combination with microrobots as sensing tools. Moreover, microrobots have been used to measure the physical properties of the swimming medium. For instance, the change in locomotion can be used to measure the viscosity of the swimming medium,<sup>429,430</sup> various biofluids,<sup>431</sup> and even inside living cells.<sup>304</sup>

Overall, surface modification of microrobots provides new opportunities to enhance the useful functions such as sensing and detecting changes in the surrounding medium.

#### 5.4. Off-Board Intelligence

As discussed before, when comparing the use of autonomous vs responsive materials for microrobot engines, a similar dynamic arises for intelligence. There is a physical limitation on the degree of intelligence that can be embedded directly into the microrobot material. Therefore, there is a need to study responsive materials that can receive and execute wireless commands. The top priority requires a well-developed feedback behavior, thus allowing for self-correcting behavior in real-time. The use of externally-based intelligence is particularly promising in guiding microrobots along predetermined paths. The ability to automate the locomotion and decision making of microrobots could have far-reaching applications in medicine and nanomanufacturing. The interfacing of magnetic controllers and computer vision algorithms would be a key feature toward providing real-time microforce feedback on groups of microrobots, allowing the processing and complexity to be absorbed by a piece of external equipment, while the microrobot smart materials can receive and interpret the external signals into a practical task.

To achieve such, closed-loop microrobots should be able to communicate their spatiotemporal position. When we consider the great impact that satellite localization has brought to our everyday life, an analogous technology is required at small scales too.<sup>432,433</sup> A thorough example of the off-board intelligence was further demonstrated through autonomous and collision-free navigation using a combination of vision, artificial intelligence-based motion planning, and a magnetic field generator. This model demonstrated the ability to navigate autonomously through complex mazes and avoid colliding moving objects (Figure 15a).<sup>434</sup> More recently, the use of vision-guided microrobots has been reported toward targeted intracellular delivery. Magnetic navigation was combined with a path planning algorithm to selectively target cells and intracellular navigation, which could be further expanded toward intracellular mechanical probing.<sup>435–438</sup> In another case, a magnetic microrobot was used to simulate the interaction between a macrophage and a trapped bacteria, allowing the scientists to observe in detail how the macrophage responds to particular motions and force pulses from bacteria. This would not be possible to study using a bacteria model itself, due to their stochastic locomotion (Figure 15b).<sup>439</sup> Therefore, microrobots have much potential to study physics at the subcellular level.

Another off-board intelligence example consists of the use of electrical and light fields to control of the locomotion and

actuation of microrobots.<sup>440–442</sup> By the judicious selection of the semiconductor materials, microrobot behavior can be finely tuned to actively propel or induce interactions between multiple microrobots.<sup>443</sup> Moreover, ultrasound has been used to generate microassembly lines, where localized acoustically generated microstreaming forces generated around the edges of engineered topological microstructures. This results in the capability to trap and guide microrobots along a predetermined trajectory based on the topographic microstructure features (Figure 15c).<sup>444–446</sup> These forces allowed manipulating single and groups of microrobots synchronously along a determined trajectory based on applied acoustic field and the local topographic features.<sup>444–446</sup> This ultrasound-based automated guidance protocol has recently been interfaced with keyboards and pianos keys toward making the control of microrobots more user-friendly (Figure 15d).<sup>444</sup>

Finally, we should consider topological patterns in the substrate as another option to provide intelligence to untethered motile microrobots. By designing a specific track or topological environment, the microrobot's behavior can be guided and programmed without changing the engine. For example, the use of boundaries is reported to guide the motion of self-propelled microorganisms.<sup>447–451</sup> This design principle served as an inspiration to guide the locomotion of synthetic microrobots, by using topographical features (Figure 15e)<sup>452–455</sup> or background potential such as acoustic tweezers<sup>456</sup> to dock and guide motile microrobots along its edge. This guiding mechanism has been expanded to induced directionality of multiple microrobots trapped inside a microfluidic chip through alignment with micropatterned ratchets (Figure 15f).<sup>457</sup>

## 6. OUTLOOK: WHAT'S NEXT?

### 6.1. Summary

In summary, we have critically discussed the material foundation of small-scale robots from a materials science perspective. We have identified four main areas where the use of smart materials can advance the operation of microrobots: propulsion, biocompatibility, cooperation, and intelligence. We discussed the role of such materials in these areas and how the judicious choice of the constituent materials can greatly enhance these microrobotic functions. For example, autonomous and responsive materials have been used as the engines of microrobots, enabling a high degree of tunability and control. The biocompatibility of microrobots has been achieved by using smart coatings, flexible designs, and degradable materials, ensuring their safety in the short and long term. Overall, the examples presented in this Review illustrate how the use of smart responsive materials imparts targeted distinct functionalities that lead to intelligent programmable microrobots with distinct capabilities, capable of addressing future challenges and meeting emerging opportunities of small-scale robots. Further material selection should consider predetermined breakdown of the material into safe components to ensure biocompatibility with biomedical applications. Moreover, the materials could have prescribed disintegration for the desired application, such as releasing drugs or shielding as protective barriers against antibiofouling. We have also described how microrobots can communicate between themselves and with an external user, ultimately working together in large numbers to accomplish a common objective, and that microrobots can show intelligence, namely that they are able to make decisions based on processing information available in their surrounding environment.

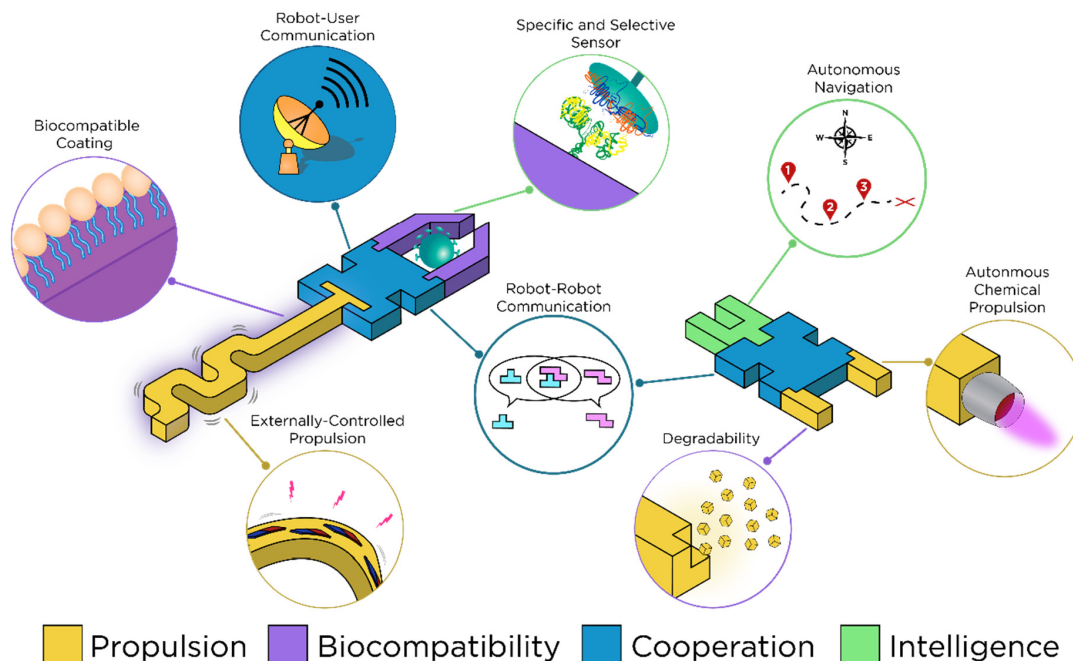


**Figure 16.** Visualization of ideal features of next-generation programmable nano/microrobots.

## 6.2. Ideal Features of the Microrobot of the Future

During the past decade, microrobotic research has been based on the principle of simplicity in design, powering, and fabrication of autonomous robotic systems. This choice in the design was required, as typical macroscale robotic strategies present a particular challenge to adapt to small scales. Therefore, it is necessary to define at this stage the expectations from the next generation of microrobots and create a roadmap that guides future research for realizing this vision.<sup>458–460</sup>

First, research should transition away from the current standards of microrobots based on simple geometries (spheres, wires, and hollow tubes) and rigid homogeneous materials into modular designs embedded with hybrid and soft material compositions. The microrobots will not only be built from building blocks present in the environment or transported by them, but they will also be able to do this collectively by communicating and even joining together to form complex assemblies. It is easy to see the appeal and capabilities of such structures in examples such as the nanorobots featured in the movie *Big Hero 6*<sup>461</sup> or Michael Crichton's novel *Prey*.<sup>462</sup> Not only can we create more novel and diverse geometries due to the latest advances in additive manufacturing techniques,<sup>463</sup> but we can also exploit the smooth gradient transition in materials,<sup>464</sup> analogous to what is seen in the animal kingdom.

Such tools create a problem of having infinite possibilities of design and complexity which requires a deterministic structure where the whole unit is needed to be designed before fabrication, resulting in rigid and slow prototyping developments while still requiring specialized machinery and code instructions. For example, different parts of the microrobot should be responsible for different parts of its behavior (Figure 16). The engine is responsible for motion, while a sensing center is responsible for probing its environment. Coupled to this center is the decision making “brain”. Thus, the development of organs or in robotic terms “modules” will become paramount.

So, at the end of this Review, as we look forward to the future, we introduce the most vital modules which must be developed for the next generation of intelligent microrobots.

First, a portion of any such microrobot must have a propulsion capability. As was mentioned earlier, this could be based on a reaction between a fuel and catalyst or direct decomposition, or instead converting electromagnetic energy into mechanical energy. As stated before, chemically powered microengines commonly use fuel in the environment and catalyze its decomposition to propel themselves, but recent efforts have shown the ability to design microrobots which carry their own fuel might show the way forward.<sup>465</sup> Once this portion of the structure is achieved, we have to ensure that the microrobot can probe its environment. One way to do this is by utilizing the large surface to volume ratio of our structures. Having a large surface allows functionalization with a wide variety of chemical moieties that can bind to markers or sense foreign agents in the surrounding solution to affect the propulsion. Moreover, the ability to selectively control and give instructions to individual microrobots could enhance the microrobot utility by combining myriads of diverse populations of microrobots that respond to specific stimuli.<sup>466,467</sup>

Additionally, sensing can happen by a mechanical signal due to a gripper or soft and deformable extensions. Loading and unloading cargo is of great importance for any task driven microrobot.<sup>468</sup> Being able to communicate to a microscopic robot which cargo to pick up, navigate and drop it off at a targeted location with high temporal accuracy is crucial for the future. Now that our ideal microrobot can move and sense its environment, it is important to make sure it can communicate and cooperate with its fellow active partners. Again, whether through chemical cues or electromagnetic/sound wave interactions, microscopic robots can “talk” to each other in a variety of ways to form simple swarms or change their behavior to perform specific tasks that a single microrobot cannot do. Integrating smart materials gradients in the microrobot

composition and design could introduce time delay and dynamic behavior that induce oscillating behaviors.<sup>469</sup> Finally, we envision these structures will get closer and closer to their living analogues. Thus, we see that putting on-board synthesis micro factories as an absolute necessity. Then, our micro/nanorobots could process fuels or reagents into useful molecules and more building blocks, whether making *in situ* adhesive, such as mollusks or DNA kill sequences, to just name a few. With such complex synthesis and assembly capabilities microrobots might become closer to animal counterparts with different parent and child types of microrobots or even one generation releasing another or even making replicas of itself.<sup>470</sup>

While microrobots are too small to host on-board electronic components, a recent study published just before the submission of this Review illustrated electronically integrated microrobots based on the combination of electronic components made of silicon photovoltaics with four moving legs relying on voltage-controlled electrochemical actuators.<sup>423</sup> By taking a substantial step toward silicon-based functional robotic systems and incorporating computational power into microscopic robots, this approach would allow the mass production of a million robots per four-inch wafer and will open the door to exciting new opportunities.

Throughout this Review, we have provided insights into the diverse applications of microrobotics, ranging from therapeutic delivery, sensing, microfabrication, and environmental remediation. However, before actual marketplace translation can take place, we need to assess and address the most pertinent challenges:

- (i) The mass fabrication of microrobots with a high degree of design flexibility and reproducibility will be paramount as currently most microrobotic research is focused on creating batches using laboratory protocols. Standardization on the reporting of microrobotic fabrication and testing is also of considerable importance, as the different propulsion mechanisms, sizes, and material properties make it hard to compare the potential of each microrobot design. Relevant standardization parameters should also include degradation time/recovery methods, storage lifetime, and locomotion lifetime, among others.<sup>471</sup>
- (ii) Identification of commercially viable proof of concept applications to demonstrate the value proposition of microrobots.<sup>472</sup> Most of the current research in microrobotics is focused on biomedical applications; thus, initial research should focus on offering microrobots as complementary tools to targeted drug delivery or surgical applications. For instance, microrobots could be integrated with catheters to reach smaller vessels that are currently not accessible by traditional medical tools. The use of microrobots inside human patients still has a long road ahead, as regulating bodies require thorough testing that requires long approval times and a major financial investment. Thus, the use of microrobots in *in vitro* sensing assays and biochips or their use in microfabrication could offer a faster route for reaching the marketplace due to less stringent regulatory processes.
- (iii) Integration with macroscale systems. At this point, microrobotic research has begun to take advantage of the opportunities of artificial intelligence and machine learning. Future microrobotic research should focus on creating a simple user interface to guide, locate, and obtain information from microrobots.<sup>473</sup> It is also important to

develop novel ways to analyze the microrobots without requiring a sophisticated microscope or even a human user.

We should also consider that the next decade is essential for the future of microrobotics. Currently, most efforts are focused on very narrow research. It is clear that realizing the vision of intelligent microrobots and expanding their scope require the close collaboration of researchers in diverse fields ranging from materials science, robotics, chemistry, and artificial intelligence. Commercialization will help to drive the research. Thus, researchers should consider problem selection, aim at tackling unmet needs, and think outside the box. It is impossible to imagine how microscopic robots will look in the next few years, but just like the development of microprocessors, miniaturization of everyday tools could have a profound impact on future technological revolutions.

## AUTHOR INFORMATION

### Corresponding Author

**Joseph Wang** – Department of Nanoengineering, Chemical Engineering Program and Contextual Robotics Institute, University of California San Diego, La Jolla, California 92093, United States; [orcid.org/0000-0002-4921-9674](https://orcid.org/0000-0002-4921-9674); Email: [josephwang@eng.ucsd.edu](mailto:josephwang@eng.ucsd.edu)

### Authors

**Fernando Soto** – Department of Nanoengineering, Chemical Engineering Program and Contextual Robotics Institute, University of California San Diego, La Jolla, California 92093, United States; [orcid.org/0000-0001-8494-9325](https://orcid.org/0000-0001-8494-9325)

**Emil Karshalev** – Department of Nanoengineering, Chemical Engineering Program and Contextual Robotics Institute, University of California San Diego, La Jolla, California 92093, United States

**Fangyu Zhang** – Department of Nanoengineering, Chemical Engineering Program and Contextual Robotics Institute, University of California San Diego, La Jolla, California 92093, United States

**Berta Esteban Fernandez de Avila** – Department of Nanoengineering, Chemical Engineering Program and Contextual Robotics Institute, University of California San Diego, La Jolla, California 92093, United States

**Amir Nourhani** – Department of Mechanical Engineering, Department of Mathematics, Biology, Biomimicry Research and Innovation Center, University of Akron, Akron, Ohio 44325, United States; [orcid.org/0000-0002-7951-9483](https://orcid.org/0000-0002-7951-9483)

Complete contact information is available at:

<https://pubs.acs.org/10.1021/acs.chemrev.0c00999>

### Author Contributions

<sup>†</sup>F.S. and E.K. contributed equally.

### Notes

The authors declare no competing financial interest.

### Biographies

**Fernando Soto** received his B.Sc. in nanotechnology engineering at Instituto Tecnológico de Tijuana, México and his M.S. and Ph.D. in Nanoengineering from the University of California San Diego (UCSD) under the supervision of Prof. Joseph Wang. His doctoral research was focused on developing micro/nanorobots and medical devices with a particular interest in harvesting acoustic energy to power micro/nano machines. He is currently a postdoctoral researcher at the radiology

department at Stanford University working under Prof. Utkan Demirci, where he aims to interface biology and nanotechnology towards developing scalable and affordable scientific tools. His research interest includes robotics, bioengineering, and creativity driven innovation.

**Emil Karshalev** received his Ph.D. in Materials Science at the University of California San Diego under the supervision of Prof. Joseph Wang in 2020. His research included the fabrication, control, and application of novel small-scale microrobots for the controlled delivery of drugs and imaging agents *in vivo*. He is an awardee of the Charles Lee Powell Foundation Scholarship and is also an Advancing Science in America (ARCS) Scholar. He received his B.S. and M.S. from University of California Irvine (UCI) with a focus on protein and polymer thin films for camouflage and thermal regulation.

**Fangyu Zhang** is currently a Ph.D. candidate in nanoengineering under Prof. Joseph Wang's supervision at UCSD. He is working on the design of various microrobot systems for biomedical applications, specializing in using hybrid modes of propulsion, biological substrates, and targeted drug delivery to solve the most challenging problems of today, including the COVID-19 pandemic. Prior to joining UCSD, he received his B.S. in material science in 2013 from Shanghai Jiao Tong University under the supervision of Prof. Tao Deng as well as an M.S. in biological engineering in 2016 from Cornell University under the supervision of Prof. Minglin Ma and Prof. Dan Luo.

**Berta Esteban-Fernández de Ávila** holds an M.S. in Chemistry (Science and Chemical Technology; 2011) and a European Ph.D. in Analytical Chemistry (2014) from the Complutense University of Madrid (Spain). Her doctoral research was focused on the development of different formats of electrochemical affinity biosensors for the early detection of diverse biomarkers. Since then, she has been a Postdoctoral Scholar in Nanoengineering at the UCSD, where her research activities involve the preparation of advanced nanomotors and nanosensors with applications in the fields of biomedicine and biosecurity. Since August 2020, she has been working as a Senior Scientist at Dexcom on the design and development of novel sensing systems for disease management.

**Amir Nourhani** is a theorist and an Assistant Professor in the Departments of Mechanical Engineering, Biology, and Mathematics, and a core faculty member of the Biomimicry Research and Innovation Center at the University of Akron. He holds a Ph.D. in Chemical Engineering (2012) and another Ph.D. in Physics (2014) from the Pennsylvania State University. He obtained his two B.Sc. degrees in Polymer Engineering and Physics from Amirkabir University of Technology and his M.Sc. degree in theoretical physics from the Sharif University of Technology. Before joining the University of Akron, he had postgraduate experience at the Pennsylvania State University, University of California Berkeley, Northern Arizona University, and the UCSD. His interdisciplinary research spans a wide range of topics, including active soft matter, microrobotics, nonequilibrium statistical physics, and fluid dynamics. He has developed kinematic matrix theory for self-propellers and self-consistent nonlocal feedback theory for electrocatalytic nanomotors.

**Joseph Wang** is Distinguished Professor, SAIC Endowed Chair, and former Chair of the Department of Nanoengineering at UCSD. He is also the Director of the UCSD Center of Wearable Sensors and Co-Director of the UCSD Center of Mobile Health Systems and Applications (CMSA). He served as the director of Center for Bioelectronics and Biosensors of Arizona State University (ASU) before joining UCSD. Prof. Wang has published more than 1150 papers, 11 books, and holds 35 patents. He received two American Chemical Society National Awards, one in 1999 (Instrumentation) and the other in 2006 (Electrochemistry), the ECS Sensor Achievement

Award (2018), the Spiers Memorial Award (RSC), the Heyrovsky Memorial Medal (Czech Republic), the Breyer Medal (Australia), and six Honorary Professorships from Spain, Argentina, Czech Republic, Romania, China, and Slovenia. Prof. Wang is an RSC and AIMBE Fellow and a Thomson Reuters Highly Cited Researcher (2015–2020). He was the Founding Editor of *Electroanalysis* (Wiley). His scientific interests are concentrated in the areas of bioelectronics, microrobots and nanomachines, wearable devices, biosensors, bionanotechnology, flexible materials, and electroanalytical chemistry.

## ACKNOWLEDGMENTS

J.W. acknowledges NSF Grant 1937653. F.S. was supported by a UC MEXUS-CONACYT Doctoral Fellowship. A.N. acknowledges funding from the University of Akron.

## REFERENCES

- (1) Cianchetti, M.; Laschi, C.; Menciassi, A.; Dario, P. Biomedical Applications of Soft Robotics. *Nat. Rev. Mater.* **2018**, *3*, 143–153.
- (2) Rich, S. I.; Wood, R. J.; Majidi, C. Untethered Soft Robotics. *Nat. Electron.* **2018**, *1*, 102–112.
- (3) Yang, G. Z.; Bellingham, J.; Dupont, P. E.; Fischer, P.; Floridi, L.; Full, R.; Jacobstein, N.; Kumar, V.; McNutt, M.; Merrifield, R.; Nelson, B. J.; Scarsellati, B.; Taddeo, M.; Taylor, R.; Veloso, M.; Wang, Z. L.; Wood, R. The Grand Challenges of Science Robotics. *Sci. Robot.* **2018**, *3*, No. eaar7650.
- (4) Ngu, J.; Tsang, C.; Koh, D. The Da Vinci Xi: A Review of Its Capabilities, Versatility, and Potential Role in Robotic Colorectal Surgery. *Robot. Surg. Res. Rev.* **2017**, *4*, 77–85.
- (5) Chien, S.; Wagstaff, K. L. Robotic Space Exploration Agents. *Sci. Robot.* **2017**, *2*, 4831.
- (6) Xia, F.; Jiang, L. Bio-Inspired, Smart, Multiscale Interfacial Materials. *Adv. Mater.* **2008**, *20*, 2842–2858.
- (7) Fu, F.; Shang, L.; Chen, Z.; Yu, Y.; Zhao, Y. Bioinspired Living Structural Color Hydrogels. *Sci. Robot.* **2018**, *3*, No. eaar8580.
- (8) Wegst, U. G. K.; Bai, H.; Saiz, E.; Tomsia, A. P.; Ritchie, R. O. Bioinspired Structural Materials. *Nat. Mater.* **2015**, *14*, 23–36.
- (9) Wang, W.; Duan, W.; Ahmed, S.; Mallouk, T. E.; Sen, A. Small Power: Autonomous Nano- and Micromotors Propelled by Self-Generated Gradients. *Nano Today* **2013**, *8*, 531–554.
- (10) Wang, J. Can Man-Made Nanomachines Compete with Nature Biomotors? *ACS Nano* **2009**, *3*, 4–9.
- (11) Sanchez, S.; Soler, L.; Katuri, J. Chemically Powered Micro- and Nanomotors. *Angew. Chem., Int. Ed.* **2015**, *54*, 1414–1444.
- (12) Wang, H.; Pumera, M. Fabrication of Micro/Nanoscale Motors. *Chem. Rev.* **2015**, *115*, 8704–8735.
- (13) Wang, H.; Pumera, M. Emerging Materials for the Fabrication of Micro/Nanomotors. *Nanoscale* **2017**, *6*, 2109–2116.
- (14) Dong, Y.; Wang, L.; Wang, J.; Wang, S.; Wang, Y.; Jin, D.; Chen, P.; Du, W.; Zhang, L.; Liu, B.-F. Graphene-Based Helical Micromotors Constructed by “Microscale Liquid Rope-Coil Effect” with Microfluidics. *ACS Nano* **2020**, *14*, 16600.
- (15) Sitti, M. Miniature Soft Robots - Road to the Clinic. *Nat. Rev. Mater.* **2018**, *3*, 74–75.
- (16) Li, J.; Esteban-Fernandez de Avila, B.; Gao, W.; Zhang, L.; Wang, J. Micro/Nanorobots for Biomedicine: Delivery, Surgery, Sensing, and Detoxification. *Sci. Robot.* **2017**, *2*, No. eaam6431.
- (17) Ceylan, H.; Yasa, I. C.; Kilic, U.; Hu, W.; Sitti, M. Translational Prospects of Untethered Medical Microrobots. *Prog. Biomed. Eng.* **2019**, *1*, 012002.
- (18) Abdelmohsen, L. K. E. A.; Peng, F.; Tu, Y.; Wilson, D. A. Micro- and Nano-Motors for Biomedical Applications. *J. Mater. Chem. B* **2014**, *2*, 2395–2408.
- (19) Cappelleri, D.; Bi, C.; Noguera, M. Tumbling Microrobots for Future Medicine. *Am. Sci.* **2018**, *106*, 210.
- (20) Gao, W.; Wang, J. The Environmental Impact of Micro/Nanomachines: A Review. *ACS Nano* **2014**, *8*, 3170–3180.

- (21) Soler, L.; Sánchez, S. Catalytic Nanomotors for Environmental Monitoring and Water Remediation. *Nanoscale* **2014**, *6*, 7175–7182.
- (22) Orozco, J.; Mercante, L. A.; Pol, R.; Merkoci, A. Graphene-Based Janus Micromotors for the Dynamic Removal of Pollutants. *J. Mater. Chem. A* **2016**, *4*, 3371–3378.
- (23) Chang, X.; Chen, C.; Li, J.; Lu, X.; Liang, Y.; Zhou, D.; Wang, H.; Zhang, G.; Li, T.; Wang, J.; Li, L. Motile Micropump Based on Synthetic Micromotors for Dynamic Micropatterning. *ACS Appl. Mater. Interfaces* **2019**, *11*, 28507–28514.
- (24) Li, J.; Gao, W.; Dong, R.; Pei, A.; Sattayasamitsathit, S.; Wang, J. Nanomotor Lithography. *Nat. Commun.* **2014**, *5*, 1–7.
- (25) Cappelleri, D.; Efthymiou, D.; Goswami, A.; Vitoroulis, N.; Zavlanos, M. Towards Mobile Microrobot Swarms for Additive Micromanufacturing. *Int. J. Adv. Robot. Syst.* **2014**, *11*, 150.
- (26) Sanhai, W. R.; Sakamoto, J. H.; Canady, R.; Ferrari, M. Seven Challenges for Nanomedicine. *Nat. Nanotechnol.* **2008**, *3*, 242–244.
- (27) Purcell, E. M. Life at Low Reynolds Number. *Am. J. Phys.* **1977**, *45*, 3–11.
- (28) Wang, J. *Nanomachines: Fundamentals and Applications*; Wiley-VCH, 2013.
- (29) Ning, H.; Zhang, Y.; Zhu, H.; Ingham, A.; Huang, G.; Mei, Y.; Solovev, A. Geometry Design, Principles and Assembly of Micromotors. *Micromachines* **2018**, *9*, 75.
- (30) Chen, C.; Soto, F.; Karshalev, E.; Li, J.; Wang, J. Hybrid Nanovehicles: One Machine, Two Engines. *Adv. Funct. Mater.* **2019**, *29*, 1806290.
- (31) Liu, W.; Chen, X.; Lu, X.; Wang, J.; Zhang, Y.; Gu, Z. From Passive Inorganic Oxides to Active Matters of Micro/Nanomotors. *Adv. Funct. Mater.* **2020**, *30*, 2003195.
- (32) Soler, L.; Magdanz, V.; Fomin, V. M.; Sanchez, S.; Schmidt, O. G. Self-Propelled Micromotors for Cleaning Polluted Water. *ACS Nano* **2013**, *7*, 9611–9620.
- (33) Li, J.; Rozen, I.; Wang, J. Rocket Science at the Nanoscale. *ACS Nano* **2016**, *10*, 5619–5634.
- (34) Teo, W. Z.; Wang, H.; Pumera, M. Beyond Platinum: Silver-Catalyst Based Bubble-Propelled Tubular Micromotors. *Chem. Commun.* **2016**, *52*, 4333–4336.
- (35) Alcántara, C. C. J.; Kim, S.; Lee, S.; Jang, B.; Thakolkaran, P.; Kim, J.; Choi, H.; Nelson, B. J.; Pané, S. 3D Fabrication of Fully Iron Magnetic Microrobots. *Small* **2019**, *15*, 1805006.
- (36) Karshalev, E.; Chen, C.; Marolt, G.; Martín, A.; Campos, I.; Castillo, R.; Wu, T.; Wang, J. Utilizing Iron's Attractive Chemical and Magnetic Properties in Microrocket Design, Extended Motion, and Unique Performance. *Small* **2017**, *13*, 1700035.
- (37) Sattayasamitsathit, S.; Kou, H.; Gao, W.; Thavarajah, W.; Kaufmann, K.; Zhang, L.; Wang, J. Fully Loaded Micromotors for Combinatorial Delivery and Autonomous Release of Cargoes. *Small* **2014**, *10*, 2830–2833.
- (38) Gao, W.; Uygun, A.; Wang, J. Hydrogen-Bubble-Propelled Zinc-Based Microrockets in Strongly Acidic Media. *J. Am. Chem. Soc.* **2012**, *134*, 897–900.
- (39) Zhou, M.; Hou, T.; Li, J.; Yu, S.; Xu, Z.; Yin, M.; Wang, J.; Wang, X. Self-Propelled and Targeted Drug Delivery of Poly(Aspartic Acid)/Iron-Zinc Microrocket in the Stomach. *ACS Nano* **2019**, *13*, 1324–1332.
- (40) Mou, F.; Chen, C.; Zhong, Q.; Yin, Y.; Ma, H.; Guan, J. Autonomous Motion and Temperature-Controlled Drug Delivery of Mg/Pt-Poly(*n*-Isopropylacrylamide) Janus Micromotors Driven by Simulated Body Fluid and Blood Plasma. *ACS Appl. Mater. Interfaces* **2014**, *6*, 9897–9903.
- (41) Nourhani, A.; Karshalev, E.; Soto, F.; Wang, J. Multigear Bubble Propulsion of Transient Micromotors. *Research* **2020**, 2020, 7823615.
- (42) Gao, W.; Feng, X.; Pei, A.; Gu, Y.; Li, J.; Wang, J. Seawater-Driven Magnesium Based Janus Micromotors for Environmental Remediation. *Nanoscale* **2013**, *5*, 4696–4700.
- (43) Guix, M.; Meyer, A. K.; Koch, B.; Schmidt, O. G. Carbonate-Based Janus Micromotors Moving in Ultra-Light Acidic Environment Generated by HeLa Cells in Situ. *Sci. Rep.* **2016**, *6*, 1–7.
- (44) Baylis, J. R.; Yeon, J. H.; Thomson, M. H.; Kazerooni, A.; Wang, X.; St. John, A. E.; Lim, E. B.; Chien, D.; Lee, A.; Zhang, J. Q.; Piret, J. M.; Machan, L. S.; Burke, T. F.; White, N. J.; Kastrup, C. J. Self-Propelled Particles That Transport Cargo through Flowing Blood and Halt Hemorrhage. *Sci. Adv.* **2015**, *1*, No. e1500379.
- (45) Baylis, J. R.; St. John, A. E.; Wang, X.; Lim, E. B.; Statz, M. L.; Chien, D.; Simonson, E.; Stern, S. A.; Liggins, R. T.; White, N. J.; Kastrup, C. J. Self-Propelled Dressings Containing Thrombin and Tranexamic Acid Improve Short-Term Survival in a Swine Model of Lethal Junctional Hemorrhage. *Shock* **2016**, *46*, 123–128.
- (46) Gao, W.; Pei, A.; Wang, J. Water-Driven Micromotors. *ACS Nano* **2012**, *6*, 8432–8438.
- (47) Liu, R.; Sen, A. Autonomous Nanomotor Based on Copper-Platinum Segmented Nanobattery. *J. Am. Chem. Soc.* **2011**, *133*, 20064–20067.
- (48) Jodra, A.; Soto, F.; Lopez-Ramirez, M. A.; Escarpa, A.; Wang, J. Delayed Ignition and Propulsion of Catalytic Microrockets Based on Fuel-Induced Chemical Dealloying of the Inner Alloy Layer. *Chem. Commun.* **2016**, *52*, 11838–11841.
- (49) Li, J.; Singh, V. V.; Sattayasamitsathit, S.; Orozco, J.; Kaufmann, K.; Dong, R.; Gao, W.; Jurado-Sanchez, B.; Fedorak, Y.; Wang, J. Water-Driven Micromotors for Rapid Photocatalytic Degradation of Biological and Chemical Warfare Agents. *ACS Nano* **2014**, *8*, 11118–11125.
- (50) Dai, B.; Wang, J.; Xiong, Z.; Zhan, X.; Dai, W.; Li, C. C.; Feng, S. P.; Tang, J. Programmable Artificial Phototactic Microswimmer. *Nat. Nanotechnol.* **2016**, *11*, 1087–1092.
- (51) Jang, B.; Hong, A.; Kang, H. E.; Alcántara, C.; Charreyron, S.; Mushtaq, F.; Pellicer, E.; Büchel, R.; Sort, J.; Lee, S. S.; Nelson, B. J.; Pané, S. Multiwavelength Light-Responsive Au/B-TiO<sub>2</sub> Janus Micromotors. *ACS Nano* **2017**, *11*, 6146–6154.
- (52) Patiño, T.; Feiner-Gracia, N.; Arqué, X.; Miguel-López, A.; Jannasch, A.; Stumpp, T.; Schäffer, E.; Albertazzi, L.; Sánchez, S. Influence of Enzyme Quantity and Distribution on the Self-Propulsion of Non-Janus Urease-Powered Micromotors. *J. Am. Chem. Soc.* **2018**, *140*, 7896–7903.
- (53) Ma, X.; Jannasch, A.; Albrecht, U. R.; Hahn, K.; Miguel-López, A.; Schäffer, E.; Sánchez, S. Enzyme-Powered Hollow Mesoporous Janus Nanomotors. *Nano Lett.* **2015**, *15*, 7043–7050.
- (54) Hortelao, A. C.; Carrascosa, R.; Murillo-Cremaes, N.; Patino, T.; Sánchez, S. Targeting 3D Bladder Cancer Spheroids with Urease-Powered Nanomotors. *ACS Nano* **2019**, *13*, 429–439.
- (55) Arqué, X.; Romero-Rivera, A.; Feixas, F.; Patiño, T.; Osuna, S.; Sánchez, S. Intrinsic Enzymatic Properties Modulate the Self-Propulsion of Micromotors. *Nat. Commun.* **2019**, *10*, 1–12.
- (56) Hermanová, S.; Pumera, M. Biocatalytic Micro- and Nanomotors. *Chem. - Eur. J.* **2020**, *26*, 11085–11092.
- (57) Arqué, X.; Andrés, X.; Mestre, R.; Ciraulo, B.; Ortega Arroyo, J.; Quidant, R.; Patiño, T.; Sánchez, S. Ionic Species Affect the Self-Propulsion of Urease-Powered Micromotors. *Research* **2020**, 2020, 2424972.
- (58) Schattling, P. S.; Ramos-Docampo, M. A.; Salgueiriño, V.; Städler, B. Double-Fueled Janus Swimmers with Magnetotactic Behavior. *ACS Nano* **2017**, *11*, 3973–3983.
- (59) Sengupta, S.; Patra, D.; Ortiz-Rivera, I.; Agrawal, A.; Shklyav, S.; Dey, K. K.; Córdova-Figueroa, U.; Mallouk, T. E.; Sen, A. Self-Powered Enzyme Micropumps. *Nat. Chem.* **2014**, *6*, 415–422.
- (60) Ma, X.; Sanchez, S. A Bio-Catalytically Driven Janus Mesoporous Silica Cluster Motor with Magnetic Guidance. *Chem. Commun.* **2015**, *51*, 5467–5470.
- (61) Pantarotto, D.; Browne, W. R.; Feringa, B. L. Autonomous Propulsion of Carbon Nanotubes Powered by a Multienzyme Ensemble. *Chem. Commun.* **2008**, *13*, 1533–1535.
- (62) Schattling, P.; Thingholm, B.; Städler, B. Enhanced Diffusion of Glucose-Fueled Janus Particles. *Chem. Mater.* **2015**, *27*, 7412–7418.
- (63) Bunea, A. I.; Pavel, I. A.; David, S.; Gáspár, S. Sensing Based on the Motion of Enzyme-Modified Nanorods. *Biosens. Bioelectron.* **2015**, *67*, 42–48.

- (64) Johnson, J. N.; Nourhani, A.; Peralta, R.; McDonald, C.; Thiesing, B.; Mann, C. J.; Lammert, P. E.; Gibbs, J. G. Dynamic Stabilization of Janus Sphere Trans -Dimers. *Phys. Rev. E: Stat. Phys., Plasmas, Fluids, Relat. Interdiscip. Top.* **2017**, *95*, 042609.
- (65) Nourhani, A.; Byun, Y. M.; Lammert, P. E.; Borhan, A.; Crespi, V. H. Nanomotor Mechanisms and Motive Force Distributions from Nanorotor Trajectories. *Phys. Rev. E* **2013**, *88*, 062317.
- (66) Paxton, W. F.; Kistler, K. C.; Olmeda, C. C.; Sen, A.; St. Angelo, S. K.; Cao, Y.; Mallouk, T. E.; Lammert, P. E.; Crespi, V. H. Catalytic Nanomotors: Autonomous Movement of Striped Nanorods. *J. Am. Chem. Soc.* **2004**, *126*, 13424–13431.
- (67) Nourhani, A.; Lammert, P. E.; Crespi, V. H.; Borhan, A. A General Flux-Based Analysis for Spherical Electrocatalytic Nanomotors. *Phys. Fluids* **2015**, *27*, 1–15.
- (68) Nourhani, A.; Crespi, V. H.; Lammert, P. E.; Borhan, A. Self-Electrophoresis of Spheroidal Electrocatalytic Swimmers. *Phys. Fluids* **2015**, *27*, 092002.
- (69) Gibbs, J. G.; Zhao, Y.-P. Design and Characterization of Rotational Multicomponent Catalytic Nanomotors. *Small* **2009**, *5*, 2304–2308.
- (70) Gibbs, J. G.; Zhao, Y.-P. Design and Characterization of Rotational Multicomponent Catalytic Nanomotors. *Small* **2009**, *5*, 2304–2308.
- (71) Zhao, G.; Viehriig, M.; Pumera, M. Challenges of the Movement of Catalytic Micromotors in Blood. *Lab Chip* **2013**, *13*, 1930–1936.
- (72) Zhou, C.; Zhang, H. P.; Tang, J.; Wang, W. Photochemically Powered AgCl Janus Micromotors as a Model System to Understand Ionic Self-Diffusiophoresis. *Langmuir* **2018**, *34*, 3289–3295.
- (73) Golestanian, R.; Liverpool, T. B.; Ajdari, A. Propulsion of a Molecular Machine by Asymmetric Distribution of Reaction Products. *Phys. Rev. Lett.* **2005**, *94*, 220801.
- (74) Mozaffari, A.; Sharifi-Mood, N.; Koplík, J.; Maldarelli, C. Self-Diffusiophoretic Colloidal Propulsion near a Solid Boundary. *Phys. Fluids* **2016**, *28*, 053107.
- (75) Gao, W.; Sattayasamitsathit, S.; Orozco, J.; Wang, J. Highly Efficient Catalytic Microengines: Template Electrosynthesis of Polyaniline/Platinum Microtubes. *J. Am. Chem. Soc.* **2011**, *133*, 11862–11864.
- (76) Solovev, A. A.; Mei, Y.; Bemúdez Ureña, E.; Huang, G.; Schmidt, O. G. Catalytic Microtubular Jet Engines Self-Propelled by Accumulated Gas Bubbles. *Small* **2009**, *5*, 1688–1692.
- (77) Gibbs, J. G.; Zhao, Y. P. Autonomously Motile Catalytic Nanomotors by Bubble Propulsion. *Appl. Phys. Lett.* **2009**, *94*, 163104.
- (78) Kumar, B. V. V. S. P.; Patil, A. J.; Mann, S. Enzyme-Powered Motility in Buoyant Organoclay/DNA Protocells. *Nat. Chem.* **2018**, *10*, 1154–1163.
- (79) Vilela, D.; Hortelao, A. C.; Balderas-Xicohténcatl, R.; Hirscher, M.; Hahn, K.; Ma, X.; Sánchez, S. Facile Fabrication of Mesoporous Silica Micro-Jets with Multi-Functionalities. *Nanoscale* **2017**, *9*, 13990–13997.
- (80) Gao, W.; Sattayasamitsathit, S.; Uygün, A.; Pei, A.; Ponedal, A.; Wang, J. Polymer-Based Tubular Microbots: Role of Composition and Preparation. *Nanoscale* **2012**, *4*, 2447.
- (81) Martín, A.; Jurado-Sánchez, B.; Escarpa, A.; Wang, J. Template Electrosynthesis of High-Performance Graphene Microengines. *Small* **2015**, *11*, 3568–3574.
- (82) Jurado-Sánchez, B.; Pacheco, M.; Maria-Hormigos, R.; Escarpa, A. Perspectives on Janus Micromotors: Materials and Applications. *Appl. Mater. Today* **2017**, *9*, 407–408.
- (83) Pourrahimi, A. M.; Pumera, M. Multifunctional and Self-Propelled Spherical Janus Nano/Micromotors: Recent Advances. *Nanoscale* **2018**, *10*, 16398–16415.
- (84) Ma, X.; Hortelao, A. C.; Miguel-López, A.; Sánchez, S. Bubble-Free Propulsion of Ultrasmall Tubular Nanojets Powered by Biocatalytic Reactions. *J. Am. Chem. Soc.* **2016**, *138*, 13782–13785.
- (85) Li, J.; Liu, Z.; Huang, G.; An, Z.; Chen, G.; Zhang, J.; Li, M.; Liu, R.; Mei, Y. Hierarchical Nanoporous Microtubes for High-Speed Catalytic Microengines. *NPG Asia Mater.* **2014**, *6*, No. e94.
- (86) Choudhury, U.; Soler, L.; Gibbs, J. G.; Sanchez, S.; Fischer, P. Surface Roughness-Induced Speed Increase for Active Janus Micromotors. *Chem. Commun.* **2015**, *51*, 8660–8663.
- (87) Wang, H.; Potroz, M. G.; Jackman, J. A.; Khezri, B.; Marić, T.; Cho, N.-J.; Pumera, M. Bioinspired Spiky Micromotors Based on Sporopollenin Exine Capsules. *Adv. Funct. Mater.* **2017**, *27*, 1702338.
- (88) Zhang, X.; Zhang, B.; Wu, G.; Chen, Y.; Xu, B.; Dong, A.; Mei, Y. Epitaxial-Assembled Monolayer Superlattices for Efficient Micromotor Propulsion. *J. Phys. D: Appl. Phys.* **2020**, *53*, 274004.
- (89) Chen, Y.; Xu, B.; Mei, Y. Design and Fabrication of Tubular Micro/Nanomotors via 3D Laser Lithography. *Chem. - Asian J.* **2019**, *14*, 2472–2478.
- (90) Ye, H.; Kang, J.; Ma, G.; Sun, H.; Wang, S. High-Speed Graphene@Ag-MnO<sub>2</sub> Micromotors at Low Peroxide Levels. *J. Colloid Interface Sci.* **2018**, *528*, 271–280.
- (91) Safdar, M.; Wani, O. M.; Jänis, J. Manganese Oxide-Based Chemically Powered Micromotors. *ACS Appl. Mater. Interfaces* **2015**, *7*, 25580–25585.
- (92) Liu, W.; Ge, H.; Gu, Z.; Lu, X.; Li, J.; Wang, J. Electrochemical Deposition Tailors the Catalytic Performance of MnO<sub>2</sub>-Based Micromotors. *Small* **2018**, *14*, 1802771.
- (93) Xiao, Q.; Li, J.; Han, J.; Xu, K. X.; Huang, Z. X.; Hu, J.; Sun, J. J. The Role of Hydrazine in Mixed Fuels (H<sub>2</sub>O<sub>2</sub>/N<sub>2</sub>H<sub>4</sub>) for Au-Fe/Ni Nanomotors. *RSC Adv.* **2015**, *5*, 71139–71143.
- (94) Gao, W.; Pei, A.; Dong, R.; Wang, J. Catalytic Iridium-Based Janus Micromotors Powered by Ultralow Levels of Chemical Fuels. *J. Am. Chem. Soc.* **2014**, *136*, 2276–2279.
- (95) Srivastava, S. K.; Guix, M.; Schmidt, O. G. Wastewater Mediated Activation of Micromotors for Efficient Water Cleaning. *Nano Lett.* **2016**, *16*, 817–821.
- (96) Singh, V. V.; Soto, F.; Kaufmann, K.; Wang, J. Micromotor-Based Energy Generation. *Angew. Chem., Int. Ed.* **2015**, *54*, 6896–6899.
- (97) Wang, H.; Pumera, M. Micro/Nanomachines and Living Biosystems: From Simple Interactions to Microcyborgs. *Adv. Funct. Mater.* **2018**, *28*, 1705421.
- (98) Bente, K.; Codutti, A.; Bachmann, F.; Faivre, D. Biohybrid and Bioinspired Magnetic Microswimmers. *Small* **2018**, *14*, 1704374.
- (99) Palagi, S.; Fischer, P. Bioinspired Microrobots. *Nat. Rev. Mater.* **2018**, *3*, 113–124.
- (100) Soto, F.; Chrostowski, R. Frontiers of Medical Micro/Nanorobotics: In Vivo Applications and Commercialization Perspectives toward Clinical Uses. *Front. Bioeng. Biotechnol.* **2018**, *6*, 170.
- (101) Xu, H.; Medina-Sánchez, M.; Maitz, M. F.; Werner, C.; Schmidt, O. G. Sperm Micromotors for Cargo Delivery through Flowing Blood. *ACS Nano* **2020**, *14*, 2982–2993.
- (102) Xu, H.; Medina-Sánchez, M.; Schmidt, O. G. Magnetic Micromotors for Multiple Motile Sperm Cells Capture, Transport, and Enzymatic Release. *Angew. Chem.* **2020**, *132*, 15139–15147.
- (103) Magdanz, V.; Gebauer, J.; Sharan, P.; Eltoukhy, S.; Voigt, D.; Simmchen, J. Sperm-Particle Interactions and Their Prospects for Charge Mapping. *Adv. Biosyst.* **2019**, *3*, 1900061.
- (104) Striggow, F.; Medina-Sánchez, M.; Auernhammer, G. K.; Magdanz, V.; Friedrich, B. M.; Schmidt, O. G. Sperm-Driven Micromotors Moving in Oviduct Fluid and Viscoelastic Media. *Small* **2020**, *16*, 2000213.
- (105) Magdanz, V.; Khalil, I. S. M.; Simmchen, J.; Furtado, G. P.; Mohanty, S.; Gebauer, J.; Xu, H.; Klingner, A.; Aziz, A.; Medina-Sánchez, M.; Schmidt, O. G.; Misra, S. IRONSperm: Sperm-Templated Soft Magnetic Microrobots. *Sci. Adv.* **2020**, *6*, No. eaba5855.
- (106) Yasa, O.; Erkoc, P.; Alapan, Y.; Sitti, M. Microalga-Powered Microswimmers toward Active Cargo Delivery. *Adv. Mater.* **2018**, *30*, 1804130.
- (107) Akolpoglu, M. B.; Dogan, N. O.; Bozuyuk, U.; Ceylan, H.; Kizilel, S.; Sitti, M. High-Yield Production of Biohybrid Microalgae for On-Demand Cargo Delivery. *Adv. Sci.* **2020**, *7*, 2001256.
- (108) Akin, D.; Sturgis, J.; Ragheb, K.; Sherman, D.; Burkholder, K.; Robinson, J. P.; Bhunia, A. K.; Mohammed, S.; Bashir, R. Bacteria-Mediated Delivery of Nanoparticles and Cargo into Cells. *Nat. Nanotechnol.* **2007**, *2*, 441–449.

- (109) Mostaghaci, B.; Yasa, O.; Zhuang, J.; Sitti, M. Bioadhesive Bacterial Microswimmers for Targeted Drug Delivery in the Urinary and Gastrointestinal Tracts. *Adv. Sci.* **2017**, *4*, 1700058.
- (110) Park, S. J.; Park, S. H.; Cho, S.; Kim, D. M.; Lee, Y.; Ko, S. Y.; Hong, Y.; Choy, H. E.; Min, J. J.; Park, J. O.; Park, S. New Paradigm for Tumor Theranostic Methodology Using Bacteria-Based Microrobot. *Sci. Rep.* **2013**, *3*, 1–8.
- (111) Soto, F.; Lopez-Ramirez, M. A.; Jeerapan, I.; Esteban-Fernandez de Avila, B.; Mishra, R. K.; Lu, X.; Chai, I.; Chen, C.; Kupor, D.; Nourhani, A.; Wang, J. Rotibot: Use of Rotifers as Self-Propelling Biohybrid Microcleaners. *Adv. Funct. Mater.* **2019**, *29*, 1900658.
- (112) Nagai, M.; Hirano, T.; Shibata, T. Phototactic Algae-Driven Unidirectional Transport of Submillimeter-Sized Cargo in a Microchannel. *Micromachines* **2019**, *10*, 130.
- (113) Ryu, S.; Pepper, R. E.; Nagai, M.; France, D. C. Vorticella: A Protozoan for Bio-Inspired Engineering. *Micromachines* **2017**, *8*, 4.
- (114) Ramesh, P.; Hwang, S.-J.; Davis, H. C.; Lee-Gosselin, A.; Bharadwaj, V.; English, M. A.; Sheng, J.; Iyer, V.; Shapiro, M. G. Ultrparamagnetic Cells Formed through Intracellular Oxidation and Chelation of Paramagnetic Iron. *Angew. Chem., Int. Ed.* **2018**, *57*, 12385–12389.
- (115) Aubry, M.; Wang, W.-A.; Guyodo, Y.; Delacou, E.; Guigner, J.-M.; Espeli, O.; Lebreton, A.; Guyot, F.; Gueroui, Z. Coli for Magnetic Control and the Spatial Localization of Functions. *ACS Synth. Biol.* **2020**, *9*, 3030.
- (116) Shapiro, M. G.; Goodwill, P. W.; Neogy, A.; Yin, M.; Foster, F. S.; Schaffer, D. V.; Conolly, S. M. Biogenic Gas Nanostructures as Ultrasonic Molecular Reporters. *Nat. Nanotechnol.* **2014**, *9*, 311–316.
- (117) Bar-Zion, A.; Nourmahnad, A.; Mittelstein, D. R.; Yoo, S.; Malounda, D.; Abedi, M.; Lee-Gosselin, A.; Maresca, D.; Shapiro, M. G. Acoustically Detonated Biomolecules for Genetically Encodable Inertial Cavitation. *bioRxiv* **2019**, 620567.
- (118) Yang, Z.; Zhang, L. Magnetic Actuation Systems for Miniature Robots: A Review. *Adv. Intell. Syst.* **2020**, *2*, 2000082.
- (119) Zhang, Z.; Wang, X.; Liu, J.; Dai, C.; Sun, Y. Robotic Micromanipulation: Fundamentals and Applications. *Annu. Rev. Control. Robot. Auton. Syst.* **2019**, *2*, 181–203.
- (120) Chen, X.-Z.; Jang, B.; Ahmed, D.; Hu, C.; De Marco, C.; Hoop, M.; Mushtaq, F.; Nelson, B. J.; Pané, S. Small-Scale Machines Driven by External Power Sources. *Adv. Mater.* **2018**, *30*, 1705061.
- (121) Han, K.; Shields, C. W.; Velez, O. D. Engineering of Self-Propelling Microbots and Microdevices Powered by Magnetic and Electric Fields. *Adv. Funct. Mater.* **2018**, *28*.
- (122) Xu, T.; Gao, W.; Xu, L. P.; Zhang, X.; Wang, S. Fuel-Free Synthetic Micro-/Nanomachines. *Adv. Mater.* **2017**, *29*, 1603250.
- (123) Schamel, D.; Mark, A. G.; Gibbs, J. G.; Miksch, C.; Morozov, K. I.; Leshansky, A. M.; Fischer, P. Nanopropellers and Their Actuation in Complex Viscoelastic Media. *ACS Nano* **2014**, *8*, 8794–8801.
- (124) Li, T.; Li, J.; Zhang, H.; Chang, X.; Song, W.; Hu, Y.; Shao, G.; Sandraz, E.; Zhang, G.; Li, L.; Wang, J. Magnetically Propelled Fish-Like Nanoswimmers. *Small* **2016**, *12*, 6098–6105.
- (125) Dreyfus, R.; Baudry, J.; Roper, M. L.; Fermigier, M.; Stone, H. A.; Bibette, J. Microscopic Artificial Swimmers. *Nature* **2005**, *437*, 862–865.
- (126) Gao, W.; Sattayasamitsathit, S.; Manesh, K. M.; Weihs, D.; Wang, J. Magnetically Powered Flexible Metal Nanowire Motors. *J. Am. Chem. Soc.* **2010**, *132*, 14403–14405.
- (127) Jang, B.; Gutman, E.; Stucki, N.; Seitz, B. F.; Wendel-García, P. D.; Newton, T.; Pokki, J.; Ergeneman, O.; Pané, S.; Or, Y.; Nelson, B. J. Undulatory Locomotion of Magnetic Multilink Nanoswimmers. *Nano Lett.* **2015**, *15*, 4829–4833.
- (128) Li, T.; Li, J.; Morozov, K. I.; Wu, Z.; Xu, T.; Rozen, I.; Leshansky, A. M.; Li, L.; Wang, J. Highly Efficient Freestyle Magnetic Nanoswimmer. *Nano Lett.* **2017**, *17*, 5092–5098.
- (129) Ghosh, A.; Fischer, P. Controlled Propulsion of Artificial Magnetic Nanostructured Propellers. *Nano Lett.* **2009**, *9*, 2243–2245.
- (130) Yan, X.; Zhou, Q.; Yu, J.; Xu, T.; Deng, Y.; Tang, T.; Feng, Q.; Bian, L.; Zhang, Y.; Ferreira, A.; Zhang, L. Magnetite Nanostructured Porous Hollow Helical Microswimmers for Targeted Delivery. *Adv. Funct. Mater.* **2015**, *25*, 5333–5342.
- (131) Huang, T.-Y.; Sakar, M. S.; Mao, A.; Petruska, A. J.; Qiu, F.; Chen, X.-B.; Kennedy, S.; Mooney, D.; Nelson, B. J. 3D Printed Microtransporters: Compound Micromachines for Spatiotemporally Controlled Delivery of Therapeutic Agents. *Adv. Mater.* **2015**, *27*, 27.
- (132) Tottori, S.; Zhang, L.; Qiu, F.; Krawczyk, K. K.; Franco-Obregón, A.; Nelson, B. J. Magnetic Helical Micromachines: Fabrication, Controlled Swimming, and Cargo Transport. *Adv. Mater.* **2012**, *24*, 811–816.
- (133) Jeon, S.; Kim, S.; Ha, S.; Lee, S.; Kim, E.; Kim, S. Y.; Park, S. H.; Jeon, J. H.; Kim, S. W.; Moon, C.; Nelson, B. J.; Kim, J.-y.; Yu, S.-W.; Choi, H. Magnetically Actuated Microrobots as a Platform for Stem Cell Transplantation. *Sci. Robot.* **2019**, *4*, No. eaav4317.
- (134) Go, G.; Jeong, S. G.; Yoo, A.; Han, J.; Kang, B.; Kim, S.; Nguyen, K. T.; Jin, Z.; Kim, C. S.; Seo, Y. R.; Kang, J. Y.; Na, J. Y.; Song, E. K.; Jeong, Y.; Seon, J. K.; Park, J. O.; Choi, E. Human Adipose-Derived Mesenchymal Stem Cell-Based Medical Microrobot System for Knee Cartilage Regeneration in Vivo. *Sci. Robot.* **2020**, *5*, No. eaay6626.
- (135) Li, J.; Li, X.; Luo, T.; Wang, R.; Liu, C.; Chen, S.; Li, D.; Yue, J.; Cheng, S. H.; Sun, D. Development of a Magnetic Microbot for Carrying and Delivering Targeted Cells. *Sci. Robot.* **2018**, *3*, No. eaat8829.
- (136) Kim, S.; Qiu, F.; Kim, S.; Ghanbari, A.; Moon, C.; Zhang, L.; Nelson, B. J.; Choi, H. Fabrication and Characterization of Magnetic Microrobots for Three-Dimensional Cell Culture and Targeted Transportation. *Adv. Mater.* **2013**, *25*, 5863–5868.
- (137) Wang, J.; Ahmed, R.; Zeng, Y.; Fu, K.; Soto, F.; Sinclair, B.; Soh, H. T.; Demirci, U. Engineering the Interaction Dynamics between Nano-Topographical Immunocyte-Templated Micromotors across Scales from Ions to Cells. *Small* **2020**, *16*, 20055185.
- (138) Bi, C.; Guix, M.; Johnson, B. V.; Jing, W.; Cappelleri, D. J. Design of Microscale Magnetic Tumbling Robots for Locomotion in Multiple Environments and Complex Terrains. *Micromachines* **2018**, *9*, 68.
- (139) Li, T.; Zhang, A.; Shao, G.; Wei, M.; Guo, B.; Zhang, G.; Li, L.; Wang, W. Janus Microdimer Surface Walkers Propelled by Oscillating Magnetic Fields. *Adv. Funct. Mater.* **2018**, *28*, 1706066.
- (140) Alapan, Y.; Bozuyuk, U.; Erkoc, P.; Karacakol, A. C.; Sitti, M. Multifunctional Surface Microrollers for Targeted Cargo Delivery in Physiological Blood Flow. *Sci. Robot.* **2020**, *5* (42), No. eaba5726.
- (141) Tasci, T. O.; Herson, P. S.; Neeves, K. B.; Marr, D. W. M. Surface-Enabled Propulsion and Control of Colloidal Microwheels. *Nat. Commun.* **2016**, *7*, 1–6.
- (142) Schwarz, L.; Karnaushenko, D. D.; Hebenstreit, F.; Naumann, R.; Schmidt, O. G.; Medina-Sánchez, M. A Rotating Spiral Micromotor for Noninvasive Zygote Transfer. *Adv. Sci.* **2020**, *7*, 2000843.
- (143) Fischer, P.; Ghosh, A. Magnetically Actuated Propulsion at Low Reynolds Numbers: Towards Nanoscale Control. *Nanoscale* **2011**, *3*, 557–563.
- (144) Mandal, P.; Patil, G.; Kakoty, H.; Ghosh, A. Magnetic Active Matter Based on Helical Propulsion. *Acc. Chem. Res.* **2018**, *51*, 2689–2698.
- (145) Xu, T.; Zhang, J.; Salehizadeh, M.; Onaizah, O.; Diller, E. Millimeter-Scale Flexible Robots with Programmable Three-Dimensional Magnetization and Motions. *Sci. Robot.* **2019**, *4*, No. eaav4494.
- (146) Salehizadeh, M.; Diller, E. Two-Agent Formation Control of Magnetic Microrobots in Two Dimensions. *J. Micro-Bio Robot.* **2017**, *12*, 9–19.
- (147) Rao, K. J.; Li, F.; Meng, L.; Zheng, H.; Cai, F.; Wang, W. A Force to Be Reckoned With: A Review of Synthetic Microswimmers Powered by Ultrasound. *Small* **2015**, *11*, 2836–2846.
- (148) Wang, W.; Castro, L. A.; Hoyos, M.; Mallouk, T. E. Autonomous Motion of Metallic Microrods Propelled by Ultrasound. *ACS Nano* **2012**, *6*, 6122–6132.
- (149) Garcia-Gradilla, V.; Orozco, J.; Sattayasamitsathit, S.; Soto, F.; Kuralay, F.; Pourazary, A.; Katzenberg, A.; Gao, W.; Shen, Y.; Wang, J. Functionalized Ultrasound-Propelled Magnetically Guided Nano-

- motors: Toward Practical Biomedical Applications. *ACS Nano* **2013**, *7*, 9232–9240.
- (150) Wang, W.; Li, S.; Mair, L.; Ahmed, S.; Huang, T. J.; Mallouk, T. E. Acoustic Propulsion of Nanorod Motors inside Living Cells. *Angew. Chem., Int. Ed.* **2014**, *53*, 3201.
- (151) Wang, W.; Wu, Z.; He, Q. Swimming Nanorobots for Opening a Cell Membrane Mechanically. *View* **2020**, *1*, 20200005.
- (152) Venugopalan, P. L.; Esteban-Fernández de Ávila, B.; Pal, M.; Ghosh, A.; Wang, J. Fantastic Voyage of Nanomotors into the Cell. *ACS Nano* **2020**, *14*, 9423–9439.
- (153) Esteban-Fernandez de Avila, B.; Ramirez-Herrera, D. E.; Campuzano, S.; Angsantikul, P.; Zhang, L.; Wang, J. Nanomotor-Enabled pH-Responsive Intracellular Delivery of Caspase-3: Towards Rapid Cell Apoptosis. *ACS Nano* **2017**, *11*, 5367–5374.
- (154) Qualliotine, J. R.; Bolat, G.; Beltran-Gastelum, M.; de Avila, B. E.-F.; Wang, J.; Califano, J. A. Acoustic Nanomotors for Detection of Human Papillomavirus-Associated Head and Neck Cancer. *Otolaryngol.-Head Neck Surg.* **2019**, *161*, 814–822.
- (155) Kiristi, M.; Singh, V. V.; Esteban-Fernández De Ávila, B.; Uygun, M.; Soto, F.; AktaşUygun, D.; Wang, J. Lysozyme-Based Antibacterial Nanomotors. *ACS Nano* **2015**, *9*, 9252–9259.
- (156) Garcia-Gradilla, V.; Sattayasamitsathit, S.; Soto, F.; Kuralay, F.; Yardimci, C.; Wiitala, D.; Galarnyk, M.; Wang, J. Ultrasound-Propelled Nanoporous Gold Wire for Efficient Drug Loading and Release. *Small* **2014**, *10*, 4154–4159.
- (157) Ahmed, S.; Wang, W.; Bai, L.; Gentekos, D. T.; Hoyos, M.; Mallouk, T. E. Density and Shape Effects in the Acoustic Propulsion of Bimetallic Nanorod Motors. *ACS Nano* **2016**, *10*, 4763–4769.
- (158) Soto, F.; Wagner, G. L.; Garcia-Gradilla, V.; Gillespie, K. T.; Lakshmi, D. R.; Karshalev, E.; Angell, C.; Chen, Y.; Wang, J. Acoustically Propelled Nanoshells. *Nanoscale* **2016**, *8*, 17788–17793.
- (159) Zhou, C.; Zhao, L.; Wei, M.; Wang, W. Twists and Turns of Orbiting and Spinning Metallic Microparticles Powered by Megahertz Ultrasound. *ACS Nano* **2017**, *11*, 12668–12676.
- (160) Nadal, F.; Lauga, E. Asymmetric Steady Streaming as a Mechanism for Acoustic Propulsion of Rigid Bodies. *Phys. Fluids* **2014**, *26*, 082001.
- (161) Nadal, F.; Michelin, S. Acoustic Propulsion of a Small, Bottom-Heavy Sphere. *J. Fluid Mech.* **2020**, *898*, A10.
- (162) Nourhani, A.; Lammert, P. E. Geometrical Performance of Self-Phoretic Colloids and Microswimmers. *Phys. Rev. Lett.* **2016**, *116*, 178302.
- (163) Hoyos, M.; Castro, A. Controlling the Acoustic Streaming by Pulsed Ultrasounds. *Ultrasonics* **2013**, *53*, 70–76.
- (164) Ahmed, D.; Baasch, T.; Jang, B.; Pane, S.; Dual, J.; Nelson, B. J. Artificial Swimmers Propelled by Acoustically Activated Flagella. *Nano Lett.* **2016**, *16*, 4968–4974.
- (165) Kaynak, M.; Ozcelik, A.; Nourhani, A.; Lammert, P. E.; Crespi, V. H.; Huang, T. J. Acoustic Actuation of Bioinspired Microswimmers. *Lab Chip* **2017**, *17*, 395–400.
- (166) Zhou, Y.; Wang, H.; Ma, Z.; Yang, J. K. W.; Ai, Y. Acoustic Vibration-Induced Actuation of Multiple Microrotors in Microfluidics. *Adv. Mater. Technol.* **2020**, *9*, 2000323.
- (167) Kaynak, M.; Ozcelik, A.; Nama, N.; Nourhani, A.; Lammert, P. E.; Crespi, V. H.; Huang, T. J. Acoustofluidic Actuation of in Situ Fabricated Microrotors. *Lab Chip* **2016**, *16*, 3532–3537.
- (168) Ahmed, D.; Lu, M.; Nourhani, A.; Lammert, P. E.; Stratton, Z.; Muddana, H. S.; Crespi, V. H.; Huang, T. J. Selectively Manipulable Acoustic-Powered Microswimmers. *Sci. Rep.* **2015**, *5*, 9744–9744.
- (169) Ren, L.; Nama, N.; McNeill, J. M.; Soto, F.; Yan, Z.; Liu, W.; Wang, W.; Wang, J.; Mallouk, T. E. 3D Steerable, Acoustically Powered Microswimmers for Single-Particle Manipulation. *Sci. Adv.* **2019**, *5*, No. eaax3084.
- (170) Aghakhani, A.; Yasa, O.; Wrede, P.; Sitti, M. Acoustically Powered Surface-Slipping Mobile Microrobots. *Proc. Natl. Acad. Sci. U. S. A.* **2020**, *117*, 3469–3477.
- (171) Feng, J.; Yuan, J.; Cho, S. K. 2-D Steering and Propelling of Acoustic Bubble-Powered Microswimmers. *Lab Chip* **2016**, *16*, 2317–2325.
- (172) Kagan, D.; Benchimol, M. J.; Claussen, J. C.; Chuluun-Erdene, E.; Esener, S.; Wang, J. Acoustic Droplet Vaporization and Propulsion of Perfluorocarbon-Loaded Microbubbles for Targeted Tissue Penetration and Deformation. *Angew. Chem., Int. Ed.* **2012**, *51*, 7519–7522.
- (173) Soto, F.; Martin, A.; Ibsen, S.; Vaidyanathan, M.; Garcia-Gradilla, V.; Levin, Y.; Escarpa, A.; Esener, S. C.; Wang, J. Acoustic Microcannons: Toward Advanced Microballistics. *ACS Nano* **2016**, *10*, 1522–1528.
- (174) Soto, F.; Jeerapan, I.; Silva-López, C.; Lopez-Ramirez, M. A.; Chai, I.; Xiaolong, L.; Lv, J.; Kurniawan, J. F.; Martin, L.; Chakravarthy, K.; Wang, J. Noninvasive Transdermal Delivery System of Lidocaine Using an Acoustic Droplet-Vaporization Based Wearable Patch. *Small* **2018**, *14*, 1803266.
- (175) Kwan, J. J.; Myers, R.; Coviello, C. M.; Graham, S. M.; Shah, A. R.; Stride, E.; Carlisle, R. C.; Coussios, C. C. Ultrasound-Propelled Nanocups for Drug Delivery. *Small* **2015**, *11*, 5305–5314.
- (176) Myers, R.; Coviello, C.; Erbs, P.; Foloppe, J.; Rowe, C.; Kwan, J.; Crake, C.; Finn, S.; Jackson, E.; Balloul, J. M.; Story, C.; Coussios, C.; Carlisle, R. Polymeric Cups for Cavitation-Mediated Delivery of Oncolytic Vaccinia Virus. *Mol. Ther.* **2016**, *24*, 1627–1633.
- (177) Zhang, Y.; Zhang, Y.; Li, S. The Secondary Bjerknes Force between Two Gas Bubbles under Dual-Frequency Acoustic Excitation. *Ultrason. Sonochem.* **2016**, *29*, 129–145.
- (178) Mettin, R.; Akhatov, I.; Parltz, U.; Ohl, C. D.; Lauterborn, W. Bjerknes Forces between Small Cavitation Bubbles in a Strong Acoustic Field. *Phys. Rev. E: Stat. Phys., Plasmas, Fluids, Relat. Interdiscip. Top.* **1997**, *56*, 2924–2931.
- (179) Mitri, F. G. Frequency Dependence of the Acoustic Radiation Force Acting on Absorbing Cylindrical Shells. *Ultrasonics* **2005**, *43*, 271–277.
- (180) Ran, W.; Saylor, J. R. The Directional Sensitivity of the Acoustic Radiation Force to Particle Diameter. *J. Acoust. Soc. Am.* **2015**, *137*, 3288–3298.
- (181) Dong, R.; Cai, Y.; Yang, Y.; Gao, W.; Ren, B. Photocatalytic Micro/Nanomotors: From Construction to Applications. *Acc. Chem. Res.* **2018**, *51*, 1940–1947.
- (182) Wang, L.; Li, Q. Photochromism into Nanosystems: Towards Lighting up the Future Nanoworld. *Chem. Soc. Rev.* **2018**, *47*, 1044–1097.
- (183) Xu, L.; Mou, F.; Gong, H.; Luo, M.; Guan, J. Light-Driven Micro/Nanomotors: From Fundamentals to Applications. *Chem. Soc. Rev.* **2017**, *46*, 6905–6926.
- (184) Wang, J.; Xiong, Z.; Zheng, J.; Zhan, X.; Tang, J. Light-Driven Micro/Nanomotor for Promising Biomedical Tools: Principle, Challenge, and Prospect. *Acc. Chem. Res.* **2018**, *51*, 1957–1965.
- (185) Huang, Y.; Liang, Z.; Alsayora, M.; Guo, J.; Fan, D. Light-Gated Manipulation of Micro/Nanoparticles in Electric Fields. *Adv. Intell. Syst.* **2020**, *2*, 1900127.
- (186) Dong, R.; Hu, Y.; Wu, Y.; Gao, W.; Ren, B.; Wang, Q.; Cai, Y. Visible-Light-Driven BiOI-Based Janus Micromotor in Pure Water. *J. Am. Chem. Soc.* **2017**, *139*, 1722–1725.
- (187) Wang, X.; Sridhar, V.; Guo, S.; Talebi, N.; Miguel-López, A.; Hahn, K.; van Aken, P. A.; Sánchez, S. Fuel-Free Nanocap-Like Motors Actuated Under Visible Light. *Adv. Funct. Mater.* **2018**, *28*, 1705862.
- (188) Yu, C.; Yang, K.; Xie, Y.; Fan, Q.; Yu, J. C.; Shu, Q.; Wang, C. Novel Hollow Pt-ZnO Nanocomposite Microspheres with Hierarchical Structure and Enhanced Photocatalytic Activity and Stability. *Nanoscale* **2013**, *5*, 2142–2151.
- (189) Chiu, H. M.; Yang, T. H.; Hsueh, Y. C.; Perng, T. P.; Wu, J. M. Fabrication and Characterization of Well-Dispersed Plasmonic Pt Nanoparticles on Ga-Doped ZnO Nanopagodas Array with Enhanced Photocatalytic Activity. *Appl. Catal., B* **2015**, *163*, 156–166.
- (190) Dong, R.; Zhang, Q.; Gao, W.; Pei, A.; Ren, B. Highly Efficient Light-Driven TiO<sub>2</sub>-Au Janus Micromotors. *ACS Nano* **2016**, *10*, 839–844.
- (191) Singh, D. P.; Choudhury, U.; Fischer, P.; Mark, A. G. Non-Equilibrium Assembly of Light-Activated Colloidal Mixtures. *Adv. Mater.* **2017**, *29*, 1701328.

- (192) Wang, Y.; Zhou, C.; Wang, W.; Xu, D.; Zeng, F.; Zhan, C.; Gu, J.; Li, M.; Zhao, W.; Zhang, J.; Guo, J.; Feng, H.; Ma, X. Photocatalytically Powered Matchlike Nanomotor for Light-Guided Active SERS Sensing. *Angew. Chem., Int. Ed.* **2018**, *57*, 13110–13113.
- (193) Villa, K.; Pumera, M. Fuel-Free Light-Driven Micro/Nanomachines: Artificial Active Matter Mimicking Nature. *Chem. Soc. Rev.* **2019**, *48*, 4966–4978.
- (194) Li, Y.; Mou, F.; Chen, C.; You, M.; Yin, Y.; Xu, L.; Guan, J. Light-Controlled Bubble Propulsion of Amorphous TiO<sub>2</sub>/Au Janus Micromotors. *RSC Adv.* **2016**, *6*, 10697–10703.
- (195) Yan, X.; Xu, J.; Meng, Z.; Xie, J.; Wang, H. A New Mechanism of Light-Induced Bubble Growth to Propel Microbubble Piston Engine. *Small* **2020**, *16*, 2001548.
- (196) Mallick, A.; Roy, S. Visible Light Driven Catalytic Gold Decorated Soft-Oxometalate (SOM) Based Nanomotors for Organic Pollutant Remediation. *Nanoscale* **2018**, *10*, 12713–12722.
- (197) Eskandarloo, H.; Kierulf, A.; Abbaspourrad, A. Light-Harvesting Synthetic Nano- and Micromotors: A Review. *Nanoscale* **2017**, *9*, 12218–12230.
- (198) Wu, Z.; Si, T.; Gao, W.; Lin, X.; Wang, J.; He, Q. Superfast Near-Infrared Light-Driven Polymer Multilayer Rockets. *Small* **2016**, *12*, 577–582.
- (199) Xuan, M.; Shao, J.; Lin, X.; Dai, L.; He, Q. Light-Activated Janus Self-Assembled Capsule Micromotors. *Colloids Surf., A* **2015**, *482*, 92–97.
- (200) Qian, B.; Montiel, D.; Bregulla, A.; Cichos, F.; Yang, H. Harnessing Thermal Fluctuations for Purposeful Activities: The Manipulation of Single Micro-Swimmers by Adaptive Photon Nudging. *Chem. Sci.* **2013**, *4*, 1420–1429.
- (201) Jiang, H. R.; Yoshinaga, N.; Sano, M. Active Motion of a Janus Particle by Self-Thermophoresis in a Defocused Laser Beam. *Phys. Rev. Lett.* **2010**, *105*, 105.
- (202) Wu, Y.; Si, T.; Lin, X.; He, Q. Near Infrared-Modulated Propulsion of Catalytic Janus Polymer Multilayer Capsule Motors. *Chem. Commun.* **2015**, *51*, 511–514.
- (203) Xuan, M.; Wu, Z.; Shao, J.; Dai, L.; Si, T.; He, Q. Near Infrared Light-Powered Janus Mesoporous Silica Nanoparticle Motors. *J. Am. Chem. Soc.* **2016**, *138*, 6492–6497.
- (204) Wu, Z.; Lin, X.; Wu, Y.; Si, T.; Sun, J.; He, Q. Near-Infrared Light-Triggered on/off Motion of Polymer Multilayer Rockets. *ACS Nano* **2014**, *8*, 6097–6105.
- (205) Okawa, D.; Pastine, S. J.; Zettl, A.; Fréchet, J. M. J. Surface Tension Mediated Conversion of Light to Work. *J. Am. Chem. Soc.* **2009**, *131*, 5396–5398.
- (206) Palagi, S.; Mark, A. G.; Reigh, S. Y.; Melde, K.; Qiu, T.; Zeng, H.; Parmeggiani, C.; Martella, D.; Sanchez-Castillo, A.; Kapernaum, N.; Giesselmann, F.; Wiersma, D. S.; Lauga, E.; Fischer, P. Structured Light Enables Biomimetic Swimming and Versatile Locomotion of Photoresponsive Soft Microrobots. *Nat. Mater.* **2016**, *15*, 647–653.
- (207) Chen, H.; Zhao, Q.; Du, X. Light-Powered Micro/Nanomotors. *Micromachines* **2018**, *9*, 41.
- (208) Chang, S. T.; Paunov, V. N.; Petsev, D. N.; Velev, O. D. Remotely Powered Self-Propelling Particles and Micropumps Based on Miniature Diodes. *Nat. Mater.* **2007**, *6*, 235–240.
- (209) Calvo-Marzal, P.; Sattayasamitsathit, S.; Balasubramanian, S.; Windmiller, J. R.; Dao, C.; Wang, J. Propulsion of Nanowire Diodes. *Chem. Commun.* **2010**, *46*, 1623–1624.
- (210) Yan, J.; Han, M.; Zhang, J.; Xu, C.; Luijten, E.; Granick, S. Reconfiguring Active Particles by Electrostatic Imbalance. *Nat. Mater.* **2016**, *15*, 1095–1099.
- (211) Han, M.; Yan, J.; Granick, S.; Luijten, E. Effective Temperature Concept Evaluated in an Active Colloid Mixture. *Proc. Natl. Acad. Sci. U. S. A.* **2017**, *114*, 7513–7518.
- (212) Nishiguchi, D.; Sano, M. Mesoscopic Turbulence and Local Order in Janus Particles Self-Propelling under an Ac Electric Field. *Phys. Rev. E - Stat. Nonlinear, Soft Matter Phys.* **2015**, *92*, 052309.
- (213) Mano, T.; Delfau, J. B.; Iwasawa, J.; Sano, M. Optimal Run-And-Tumble-Based Transportation of a Janus Particle with Active Steering. *Proc. Natl. Acad. Sci. U. S. A.* **2017**, *114*, E2580–E2589.
- (214) Gangwal, S.; Cayre, O. J.; Bazant, M. Z.; Velev, O. D. Induced-Charge Electrophoresis of Metallodielectric Particles. *Phys. Rev. Lett.* **2008**, *100*, 058302.
- (215) Roche, J.; Carrara, S.; Sanchez, J.; Lannelongue, J.; Loget, G.; Bouffier, L.; Fischer, P.; Kuhn, A. Wireless Powering of E-Swimmers. *Sci. Rep.* **2015**, *4*, 1–6.
- (216) Sentic, M.; Loget, G.; Manojlovic, D.; Kuhn, A.; Sojic, N. Light-Emitting Electrochemical “Swimmers”. *Angew. Chem., Int. Ed.* **2012**, *51*, 11284–11288.
- (217) Loget, G.; Zigah, D.; Bouffier, L.; Sojic, N.; Kuhn, A. Bipolar Electrochemistry: From Materials Science to Motion and Beyond. *Acc. Chem. Res.* **2013**, *46*, 2513–2523.
- (218) Loget, G.; Kuhn, A. Propulsion of Microobjects by Dynamic Bipolar Self-Regeneration. *J. Am. Chem. Soc.* **2010**, *132*, 15918–15919.
- (219) Loget, G.; Kuhn, A. Electric Field-Induced Chemical Locomotion of Conducting Objects. *Nat. Commun.* **2011**, *2*, 1–6.
- (220) Chen, C.; Soto, F.; Karshalev, E.; Li, J.; Wang, J. Hybrid Nanovehicles: One Machine, Two Engines. *Adv. Funct. Mater.* **2019**, *29*, 1806290.
- (221) Ren, L.; Wang, W.; Mallouk, T. E. Two Forces Are Better than One: Combining Chemical and Acoustic Propulsion for Enhanced Micromotor Functionality. *Acc. Chem. Res.* **2018**, *51*, 1948–1956.
- (222) Fernández-Barcia, M.; Jang, B.; Alcántara, C. C. J.; Wolff, U.; Gebert, A.; Uhlemann, M.; Chen, X.; Puigmartí-Luis, J.; Sort, J.; Pellicer, E.; Pané, S. Exploiting Electrolyte Confinement Effects for the Electrosynthesis of Two-Engine Micromachines. *Appl. Mater. Today* **2020**, *19*, 100629.
- (223) Yang, R. L.; Zhu, Y. J.; Qin, D. D.; Xiong, Z. C. Light-Operated Dual-Mode Propulsion at the Liquid/Air Interface Using Flexible, Superhydrophobic, and Thermally Stable Photothermal Paper. *ACS Appl. Mater. Interfaces* **2020**, *12*, 1339–1347.
- (224) Yuan, K.; De La Asunción-Nadal, V.; Jurado-Sánchez, B.; Escarpa, A. 2D Nanomaterials Wrapped Janus Micromotors with Built-in Multiengines for Bubble, Magnetic, and Light Driven Propulsion. *Chem. Mater.* **2020**, *32*, 1983–1992.
- (225) Gao, W.; Manesh, K. M.; Hua, J.; Sattayasamitsathit, S.; Wang, J. Hybrid Nanomotor: A Catalytically/Magnetically Powered Adaptive Nanowire Swimmer. *Small* **2011**, *7*, 2047–2051.
- (226) Ren, L.; Zhou, D.; Mao, Z.; Xu, P.; Huang, T. J.; Mallouk, T. E. Rheotaxis of Bimetallic Micromotors Driven by Chemical-Acoustic Hybrid Power. *ACS Nano* **2017**, *11*, 10591–10598.
- (227) Wang, W.; Duan, W.; Zhang, Z.; Sun, M.; Sen, A.; Mallouk, T. E. A Tale of Two Forces: Simultaneous Chemical and Acoustic Propulsion of Bimetallic Micromotors. *Chem. Commun.* **2015**, *51*, 1020–1023.
- (228) Chen, C.; Tang, S.; Teymourian, H.; Karshalev, E.; Zhang, F.; Li, J.; Mou, F.; Liang, Y.; Guan, J.; Wang, J. Chemical/Light-Powered Hybrid Micromotors with “On-the-Fly” Optical Brakes. *Angew. Chem., Int. Ed.* **2018**, *57*, 8110–8114.
- (229) Li, J.; Li, T.; Xu, T.; Kiristi, M.; Liu, W.; Wu, Z.; Wang, J. Magneto-Acoustic Hybrid Nanomotor. *Nano Lett.* **2015**, *15*, 4814–4821.
- (230) Tu, Y.; Peng, F.; Wilson, D. A. Motion Manipulation of Micro- and Nanomotors. *Adv. Mater.* **2017**, *29*, 1701970.
- (231) Wang, J.; Manesh, K. M. Motion Control at the Nanoscale. *Small* **2010**, *6*, 338–345.
- (232) Teo, W. Z.; Pumera, M. Motion Control of Micro-/Nanomotors. *Chem. - Eur. J.* **2016**, *22*, 14796–14804.
- (233) Balasubramanian, S.; Kagan, D.; Manesh, K. M.; Calvo-Marzal, P.; Flechsig, G.; Wang, J. Thermal Modulation of Nanomotor Movement. *Small* **2009**, *5*, 1569–1574.
- (234) Sanchez, S.; Ananth, A. N.; Fomin, V. M.; Viehrig, M.; Schmidt, O. G. Superfast Motion of Catalytic Microjet Engines at Physiological Temperature. *J. Am. Chem. Soc.* **2011**, *133*, 14860–14863.
- (235) Tu, Y.; Peng, F.; Sui, X.; Men, Y.; White, P. B.; Van Hest, J. C. M.; Wilson, D. A. Self-Propelled Supramolecular Nanomotors with Temperature-Responsive Speed Regulation. *Nat. Chem.* **2017**, *9*, 480–486.

- (236) Ji, Y.; Lin, X.; Zhang, H.; Wu, Y.; Li, J.; He, Q. Thermoresponsive Polymer Brush Modulation on the Direction of Motion of Phoretically Driven Janus Micromotors. *Angew. Chem., Int. Ed.* **2019**, *58*, 4184–4188.
- (237) Magdanz, V.; Stoychev, G.; Ionov, L.; Sanchez, S.; Schmidt, O. G. Stimuli-Responsive Microjets with Reconfigurable Shape. *Angew. Chem.* **2014**, *126*, 2711–2715.
- (238) Bandari, V. K.; Nan, Y.; Karnaushenko, D.; Hong, Y.; Sun, B.; Striggow, F.; Karnaushenko, D. D.; Becker, C.; Faghih, M.; Medina-Sánchez, M.; Zhu, F.; Schmidt, O. G. A Flexible Microsystem Capable of Controlled Motion and Actuation by Wireless Power Transfer. *Nat. Electron.* **2020**, *3*, 172–180.
- (239) Orozco, J.; García-Gradilla, V.; D'Agostino, M.; Gao, W.; Cortés, A.; Wang, J. Artificial Enzyme-Powered Microfish for Water-Quality Testing. *ACS Nano* **2013**, *7*, 818–824.
- (240) Gao, S.; Hou, J.; Zeng, J.; Richardson, J. J.; Gu, Z.; Gao, X.; Li, D.; Gao, M.; Wang, D.; Chen, P.; Chen, V.; Liang, K.; Zhao, D.; Kong, B. Superassembled Biocatalytic Porous Framework Micromotors with Reversible and Sensitive PH-Speed Regulation at Ultralow Physiological  $H_2O_2$  Concentration. *Adv. Funct. Mater.* **2019**, *29*, 1808900.
- (241) Ma, X.; Wang, X.; Hahn, K.; Sánchez, S. Motion Control of Urea-Powered Biocompatible Hollow Microcapsules. *ACS Nano* **2016**, *10*, 3597–3605.
- (242) Li, J.; Yu, X.; Xu, M.; Liu, W.; Sandraz, E.; Lan, H.; Wang, J.; Cohen, S. M. Metal-Organic Frameworks as Micromotors with Tunable Engines and Brakes. *J. Am. Chem. Soc.* **2017**, *139*, 611–614.
- (243) Wang, X.; Chen, X.; Alcántara, C. C. J.; Sevim, S.; Hoop, M.; Terzopoulou, A.; de Marco, C.; Hu, C.; de Mello, A. J.; Falcuro, P.; Furukawa, S.; Nelson, B. J.; Puigmartí-Luis, J.; Pané, S. MOFBOTS: Metal-Organic-Framework-Based Biomedical Microrobots. *Adv. Mater.* **2019**, *31*, 1901592.
- (244) Li, J.; Thamphiwatana, S.; Liu, W.; Esteban-Fernández De Ávila, B.; Angsantikul, P.; Sandraz, E.; Wang, J.; Xu, T.; Soto, F.; Ramez, V.; Wang, X.; Gao, W.; Zhang, L.; Wang, J. Enteric Micromotor Can Selectively Position and Spontaneously Propel in the Gastrointestinal Tract. *ACS Nano* **2016**, *10*, 9536–9542.
- (245) Chang, X.; Li, L.; Li, T.; Zhou, D.; Zhang, G. Accelerated Microrockets with a Biomimetic Hydrophobic Surface. *RSC Adv.* **2016**, *6*, 87213–87220.
- (246) Huang, G.; Wang, J.; Liu, Z.; Zhou, D.; Tian, Z.; Xu, B.; Li, L.; Mei, Y. Rocket-Inspired Tubular Catalytic Microjets with Grating-Structured Walls as Guiding Empennages. *Nanoscale* **2017**, *9*, 18590–18596.
- (247) Xu, T.; Soto, F.; Gao, W.; Garcia-Gradilla, V.; Li, J.; Zhang, X.; Wang, J. Ultrasound-Modulated Bubble Propulsion of Chemically Powered Microengines. *J. Am. Chem. Soc.* **2014**, *136*, 8552–8555.
- (248) Moo, J. G. S.; Mayorga-Martinez, C. C.; Wang, H.; Teo, W. Z.; Tan, B. H.; Luong, T. D.; Gonzalez-Avila, S. R.; Ohl, C.-D.; Pumera, M. Bjercknes Forces in Motion: Long-Range Translational Motion and Chiral Directionality Switching in Bubble-Propelled Micromotors via an Ultrasonic Pathway. *Adv. Funct. Mater.* **2018**, *28*, 1702618.
- (249) Lu, X.; Shen, H.; Wei, Y.; Ge, H.; Wang, J.; Peng, H.; Liu, W. Ultrafast Growth and Locomotion of Dandelion-Like Microswarms with Tubular Micromotors. *Small* **2020**, *16*, 2003678.
- (250) Tu, Y.; Peng, F.; Heuvelmans, J. M.; Liu, S.; Nolte, R. J. M.; Wilson, D. A. Motion Control of Polymeric Nanomotors Based on Host-Guest Interactions. *Angew. Chem., Int. Ed.* **2019**, *58*, 8687–8691.
- (251) Solovev, A. A.; Smith, E. J.; Bufon, C. C.; Sanchez, S.; Schmidt, O. G. Light-Controlled Propulsion of Catalytic Microengines. *Angew. Chem., Int. Ed.* **2011**, *50*, 10875.
- (252) Dong, R.; Wang, C.; Wang, Q.; Pei, A.; She, X.; Zhang, Y.; Cai, Y. ZnO-Based Microrockets with Light-Enhanced Propulsion. *Nanoscale* **2017**, *9*, 15027–15032.
- (253) Moo, J. G. S.; Presolski, S.; Pumera, M. Photochromic Spatiotemporal Control of Bubble-Propelled Micromotors by a Spiropyran Molecular Switch. *ACS Nano* **2016**, *10*, 3543–3552.
- (254) Yoshizumi, Y.; Honegger, T.; Berton, K.; Suzuki, H.; Peyrade, D. Trajectory Control of Self-Propelled Micromotors Using AC Electrokinetics. *Small* **2015**, *11*, 5630–5635.
- (255) Guo, J.; Gallegos, J. J.; Tom, A. R.; Fan, D. Electric-Field-Guided Precision Manipulation of Catalytic Nanomotors for Cargo Delivery and Powering Nanoelectromechanical Devices. *ACS Nano* **2018**, *12*, 1179–1187.
- (256) Wang, S.; Liu, X.; Wang, Y.; Xu, D.; Liang, C.; Guo, J.; Ma, X. Biocompatibility of Artificial Micro/Nanomotors for Use in Biomedicine. *Nanoscale* **2019**, *11*, 14099–14112.
- (257) Li, C.; Guo, C.; Fitzpatrick, V.; Ibrahim, A.; Zwierstra, M. J.; Hanna, P.; Lechtig, A.; Nazarian, A.; Lin, S. J.; Kaplan, D. L. Design of Biodegradable, Implantable Devices towards Clinical Translation. *Nat. Rev. Mater.* **2020**, *5*, 61–81.
- (258) Yin, L.; Cheng, H.; Mao, S.; Haasch, R.; Liu, Y.; Xie, X.; Hwang, S. W.; Jain, H.; Kang, S. K.; Su, Y.; Li, R.; Huang, Y.; Rogers, J. A. Dissolvable Metals for Transient Electronics. *Adv. Funct. Mater.* **2014**, *24*, 645–658.
- (259) Wu, Z.; Chen, Y.; Mukasa, D.; Pak, O. S.; Gao, W. Medical Micro/Nanorobots in Complex Media. *Chem. Soc. Rev.* **2020**, *49*, 2869–2885.
- (260) Wu, Z.; Chen, Y.; Mukasa, D.; Pak, O. S.; Gao, W. Medical Micro/Nanorobots in Complex Media. *Chem. Soc. Rev.* **2020**, *49*, 8088.
- (261) Venugopalan, P. L.; Sai, R.; Chandorkar, Y.; Basu, B.; Shivashankar, S.; Ghosh, A. Conformal Cytocompatible Ferrite Coatings Facilitate the Realization of a Nanovoyager in Human Blood. *Nano Lett.* **2014**, *14*, 1968–1975.
- (262) Wu, Z.; Troll, J.; Jeong, H. H.; Wei, Q.; Stang, M.; Ziemssen, F.; Wang, Z.; Dong, M.; Schnichels, S.; Qiu, T.; Fischer, P. A Swarm of Slippery Micropropellers Penetrates the Vitreous Body of the Eye. *Sci. Adv.* **2018**, *4*, No. eaat4388.
- (263) Walker, D.; Käschorf, B. T.; Jeong, H. H.; Lieleg, O.; Fischer, P. Biomolecules: Enzymatically Active Biomimetic Micropropellers for the Penetration of Mucin Gels. *Sci. Adv.* **2015**, *1*, No. e1500501.
- (264) Díez, P.; Esteban-Fernández De Ávila, B.; Ramírez-Herrera, D. E.; Villalonga, R.; Wang, J. Biomedical Nanomotors: Efficient Glucose-Mediated Insulin Release. *Nanoscale* **2017**, *9*, 14307–14311.
- (265) Esteban-Fernández de Ávila, B.; Lopez-Ramirez, M. A.; Mundaca-Urbe, R.; Wei, X.; Ramírez-Herrera, D. E.; Karshalev, E.; Nguyen, B.; Fang, R. H.; Zhang, L.; Wang, J. Multicompartment Tubular Micromotors Toward Enhanced Localized Active Delivery. *Adv. Mater.* **2020**, *32*, 2000091.
- (266) Wei, X.; Beltrán-Gastélum, M.; Karshalev, E.; Esteban-Fernández De Ávila, B.; Zhou, J.; Ran, D.; Angsantikul, P.; Fang, R. H.; Wang, J.; Zhang, L. Biomimetic Micromotor Enables Active Delivery of Antigens for Oral Vaccination. *Nano Lett.* **2019**, *19*, 1914–1921.
- (267) Li, J.; Angsantikul, P.; Liu, W.; Esteban-Fernández de Ávila, B.; Thamphiwatana, S.; Xu, M.; Sandraz, E.; Wang, X.; Delezuk, J.; Gao, W.; Zhang, L.; Wang, J. Micromotors Spontaneously Neutralize Gastric Acid for PH-Responsive Payload Release. *Angew. Chem., Int. Ed.* **2017**, *56*, 2156–2161.
- (268) de Ávila, B. E.-F.; Angsantikul, P.; Li, J.; Angel Lopez-Ramirez, M.; Ramirez-Herrera, D. E.; Thamphiwatana, S.; Chen, C.; Delezuk, J.; Samakapiruk, R.; Ramez, V.; Obonyo, M.; Zhang, L.; Wang, J. Micromotor-Enabled Active Drug Delivery for in Vivo Treatment of Stomach Infection. *Nat. Commun.* **2017**, *8*, 1–9.
- (269) Wu, Z.; Li, L.; Yang, Y.; Hu, P.; Li, Y.; Yang, S. Y.; Wang, L. V.; Gao, W. A Microbotic System Guided by Photoacoustic Computed Tomography for Targeted Navigation in Intestines in Vivo. *Sci. Robot.* **2019**, *4*, No. eaax0613.
- (270) Stanton, M. M.; Park, B. W.; Vilela, D.; Bente, K.; Faivre, D.; Sitti, M.; Sánchez, S. Magnetotactic Bacteria Powered Biohybrids Target E. Coli Biofilms. *ACS Nano* **2017**, *11*, 9968–9978.
- (271) Llopis-Lorente, A.; García-Fernández, A.; Murillo-Cremaes, N.; Hortelaõ, A. C.; Patinõ, T.; Villalonga, R.; Sancenón, F.; Martínez-Mañez, R.; Sánchez, S. Enzyme-Powered Gated Mesoporous Silica Nanomotors for on-Command Intracellular Payload Delivery. *ACS Nano* **2019**, *13*, 12171–12183.
- (272) Zhang, F.; Mundaca-Urbe, R.; Gong, H.; Esteban-Fernández de Ávila, B.; Beltrán-Gastélum, M.; Karshalev, E.; Nourhani, A.; Tong, Y.; Nguyen, B.; Gallot, M.; Zhang, Y.; Zhang, L.; Wang, J. A

- Macrophage-Magnesium Hybrid Biomotor: Fabrication and Characterization. *Adv. Mater.* **2019**, *31*, 1901828.
- (273) Magdanz, V.; Sanchez, S.; Schmidt, O. G. Development of a Sperm-Flagella Driven Micro-Bio-Robot. *Adv. Mater.* **2013**, *25*, 6581–6588.
- (274) Medina-Sánchez, M.; Schwarz, L.; Meyer, A. K.; Hebenstreit, F.; Schmidt, O. G. Cellular Cargo Delivery: Toward Assisted Fertilization by Sperm-Carrying Micromotors. *Nano Lett.* **2016**, *16*, 555–561.
- (275) Felfoul, O.; Mohammadi, M.; Taherkhani, S.; De Lanauze, D.; Zhong Xu, Y.; Loghin, D.; Essa, S.; Jancik, S.; Houle, D.; Lafleur, M.; Gaboury, L.; Tabrizian, M.; Kaou, N.; Atkin, M.; Vuong, T.; Batist, G.; Beauchemin, N.; Radzioch, D.; Martel, S. Magneto-Aerotactic Bacteria Deliver Drug-Containing Nanoliposomes to Tumour Hypoxic Regions. *Nat. Nanotechnol.* **2016**, *11*, 941–947.
- (276) Wu, Z.; Li, J.; de Ávila, B. E.-F.; Li, T.; Gao, W.; He, Q.; Zhang, L.; Wang, J. Water-Powered Cell-Mimicking Janus Micromotor. *Adv. Funct. Mater.* **2015**, *25*, 7497–7501.
- (277) Li, J.; Angsantikul, P.; Liu, W.; Esteban-Fernández de Ávila, B.; Chang, X.; Sandraz, E.; Liang, Y.; Zhu, S.; Zhang, Y.; Chen, C.; Gao, W.; Zhang, L.; Wang, J. Biomimetic Platelet-Camouflaged Nanorobots for Binding and Isolation of Biological Threats. *Adv. Mater.* **2018**, *30*, 1704800.
- (278) Wang, D.; Gao, C.; Zhou, C.; Lin, Z.; He, Q. Leukocyte Membrane-Coated Liquid Metal Nanoswimmers for Actively Targeted Delivery and Synergistic Chemophotothermal Therapy. *Research* **2020**, *2020*, 3676954.
- (279) Esteban-Fernandez de Avila, B.; Angsantikul, P.; Ramirez-Herrera, D. E.; Soto, F.; Teymourian, H.; Dehaini, D.; Chen, Y.; Zhang, L.; Wang, J. Hybrid Biomembrane-Functionalized Nanorobots for Concurrent Removal of Pathogenic Bacteria and Toxins. *Sci. Robot.* **2018**, *3*, No. eaat0485.
- (280) Kadiri, V. M.; Bussi, C.; Holle, A. W.; Son, K.; Kwon, H.; Schütz, G.; Gutierrez, M. G.; Fischer, P. Biocompatible Magnetic Micro- and Nanodevices: Fabrication of FePt Nanopropellers and Cell Transfection. *Adv. Mater.* **2020**, *32*, 2001114.
- (281) Yasa, I. C.; Ceylan, H.; Bozuyuk, U.; Wild, A.-M.; Sitti, M. Elucidating the Interaction Dynamics between Microswimmer Body and Immune System for Medical Microrobots. *Sci. Robot.* **2020**, *5*, No. eaaz3867.
- (282) Pijpers, I. A. B.; Cao, S.; Llopis-Lorente, A.; Zhu, J.; Song, S.; Joosten, R. R. M.; Meng, F.; Friedrich, H.; Williams, D. S.; Sánchez, S.; van Hest, J. C. M.; Abdelmohsen, L. K. E. A. Hybrid Biodegradable Nanomotors through Compartmentalized Synthesis. *Nano Lett.* **2020**, *20*, 4472–4480.
- (283) Park, S. J.; Lee, Y. K.; Cho, S.; Uthaman, S.; Park, I.-K.; Min, J.-J.; Ko, S. Y.; Park, J.-O.; Park, S. Effect of Chitosan Coating on a Bacteria-Based Alginate Microrobot. *Biotechnol. Bioeng.* **2015**, *112*, 769–776.
- (284) Chen, C.; Karshalev, E.; Li, J.; Soto, F.; Castillo, R.; Campos, I.; Mou, F.; Guan, J.; Wang, J. Transient Micromotors That Disappear When No Longer Needed. *ACS Nano* **2016**, *10*, 10389–10396.
- (285) Chen, C.; Karshalev, E.; Guan, J.; Wang, J. Magnesium-Based Micromotors: Water-Powered Propulsion, Multifunctionality, and Biomedical and Environmental Applications. *Small* **2018**, *14*, 1704252.
- (286) Gao, W.; Dong, R.; Thamphiwatana, S.; Li, J.; Gao, W.; Zhang, L.; Wang, J. Artificial Micromotors in the Mouse's Stomach: A Step toward in Vivo Use of Synthetic Motors. *ACS Nano* **2015**, *9*, 117–123.
- (287) Lin, X.; Wu, Z.; Wu, Y.; Xuan, M.; He, Q. Self-Propelled Micro-/Nanomotors Based on Controlled Assembled Architectures. *Adv. Mater.* **2016**, *28*, 1060–1072.
- (288) Lin, X.; Xu, B.; Zhu, H.; Liu, J.; Solovev, A.; Mei, Y. Requirement and Development of Hydrogel Micromotors towards Biomedical Applications. *Research* **2020**, *2020*, 7659749.
- (289) Wu, Z.; Lin, X.; Zou, X.; Sun, J.; He, Q. Biodegradable Protein-Based Rockets for Drug Transportation and Light-Triggered Release. *ACS Appl. Mater. Interfaces* **2015**, *7*, 250–255.
- (290) Fernández-Medina, M.; Qian, X.; Hovorka, O.; Städler, B. Disintegrating Polymer Multilayers to Jump-Start Colloidal Micromotors. *Nanoscale* **2019**, *11*, 733–741.
- (291) Sugai, N.; Morita, Y.; Komatsu, T. Nonbubble-Propelled Biodegradable Microtube Motors Consisting Only of Protein. *Chem. - Asian J.* **2019**, *14*, 2953–2957.
- (292) Pena-Francesch, A.; Giltinan, J.; Sitti, M. Multifunctional and Biodegradable Self-Propelled Protein Motors. *Nat. Commun.* **2019**, *10*, 1–10.
- (293) Yan, X.; Zhou, Q.; Vincent, M.; Deng, Y.; Yu, J.; Xu, J.; Xu, T.; Tang, T.; Bian, L.; Wang, Y. X. J.; Kostarelos, K.; Zhang, L. Multifunctional Biohybrid Magnetite Microrobots for Imaging-Guided Therapy. *Sci. Robot.* **2017**, *2*, No. eaaq1155.
- (294) Yan, X.; Xu, J.; Zhou, Q.; Jin, D.; Vong, C. I.; Feng, Q.; Ng, D. H. L.; Bian, L.; Zhang, L. Molecular Cargo Delivery Using Multicellular Magnetic Microswimmers. *Appl. Mater. Today* **2019**, *15*, 242–251.
- (295) Wang, X.; Qin, X.-H.; Hu, C.; Terzopoulou, A.; Chen, X.-Z.; Huang, T.-Y.; Maniura-Weber, K.; Pané, S.; Nelson, B. J. 3D Printed Enzymatically Biodegradable Soft Helical Microswimmers. *Adv. Funct. Mater.* **2018**, *28*, 1804107.
- (296) Bozuyuk, U.; Yasa, O.; Yasa, I. C.; Ceylan, H.; Kizile, S.; Sitti, M. Light-Triggered Drug Release from 3D-Printed Magnetic Chitosan Microswimmers. *ACS Nano* **2018**, *12*, 9617–9625.
- (297) Peters, C.; Hoop, M.; Pané, S.; Nelson, B. J.; Hierold, C. Degradable Magnetic Composites for Minimally Invasive Interventions: Device Fabrication, Targeted Drug Delivery, and Cytotoxicity Tests. *Adv. Mater.* **2016**, *28*, 533–538.
- (298) Ceylan, H.; Yasa, I. C.; Yasa, O.; Tabak, A. F.; Giltinan, J.; Sitti, M. 3D-Printed Biodegradable Microswimmer for Theranostic Cargo Delivery and Release. *ACS Nano* **2019**, *13*, 3353–3362.
- (299) Tu, Y.; Peng, F.; André, A. A. M.; Men, Y.; Srinivas, M.; Wilson, D. A. Biodegradable Hybrid Stomatocyte Nanomotors for Drug Delivery. *ACS Nano* **2017**, *11*, 1957–1963.
- (300) Tang, S.; Zhang, F.; Gong, H.; Wei, F.; Zhuang, J.; Karshalev, E.; Esteban-Fernandez de Avila, B.; Huang, C.; Zhou, Z.; Li, Z.; Yin, L.; Dong, H.; Fang, R. H.; Zhang, X.; Zhang, L.; Wang, J. Enzyme-Powered Janus Platelet Cell Robots for Active and Targeted Drug Delivery. *Sci. Robot.* **2020**, *5*, No. eaba6137.
- (301) Vutukuri, H. R.; Hoore, M.; Abaurrea-Velasco, C.; van Buren, L.; Dutto, A.; Auth, T.; Fedosov, D. A.; Gompper, G.; Vermant, J. Active Particles Induce Large Shape Deformations in Giant Lipid Vesicles. *Nature* **2020**, *586*, 52–56.
- (302) Wehner, M.; Truby, R. L.; Fitzgerald, D. J.; Mosadegh, B.; Whitesides, G. M.; Lewis, J. A.; Wood, R. J. An Integrated Design and Fabrication Strategy for Entirely Soft, Autonomous Robots. *Nature* **2016**, *536*, 451–455.
- (303) Rus, D.; Tolley, M. T. Design, Fabrication and Control of Soft Robots. *Nature* **2015**, *521*, 467–475.
- (304) Dasgupta, D.; Pally, D.; Saini, D. K.; Bhat, R.; Ghosh, A. Nanomotors Sense Local Physicochemical Heterogeneities in Tumor Microenvironments. *Angew. Chem.* **2020**, *132*, 23898.
- (305) Alapan, Y.; Yasa, O.; Schauer, O.; Giltinan, J.; Tabak, A. F.; Sourjik, V.; Sitti, M. Soft Erythrocyte-Based Bacterial Microswimmers for Cargo Delivery. *Sci. Robot.* **2018**, *3*, No. eaar4423.
- (306) Lum, G. Z.; Ye, Z.; Dong, X.; Marvi, H.; Erin, O.; Hu, W.; Sitti, M. Shape-Programmable Magnetic Soft Matter. *Proc. Natl. Acad. Sci. U. S. A.* **2016**, *113*, E6007–E6015.
- (307) Medina-Sánchez, M.; Magdanz, V.; Guix, M.; Fomin, V. M.; Schmidt, O. G. Swimming Microrobots: Soft, Reconfigurable, and Smart. *Adv. Funct. Mater.* **2018**, *28*, 1707228.
- (308) Malachowski, K.; Jamal, M.; Jin, Q.; Polat, B.; Morris, C. J.; Gracias, D. H. Self-Folding Single Cell Grippers. *Nano Lett.* **2014**, *14*, 4164–4170.
- (309) Jin, Q.; Yang, Y.; Jackson, J.; Yoon, C.; Gracias, D. H. *Nano Lett.* **2020**, *20*, 5383–5390.
- (310) Cui, J.; Huang, T. Y.; Luo, Z.; Testa, P.; Gu, H.; Chen, X. Z.; Nelson, B. J.; Heyderman, L. J. Nanomagnetic Encoding of Shape-Morphing Micromachines. *Nature* **2019**, *575*, 164–168.
- (311) Huang, H. W.; Uslu, F. E.; Katsamba, P.; Lauga, E.; Sakar, M. S.; Nelson, B. J. Adaptive Locomotion of Artificial Microswimmers. *Sci. Adv.* **2019**, *5*, No. eaau1532.

- (312) Huang, H. W.; Huang, T. Y.; Charilaou, M.; Lyttle, S.; Zhang, Q.; Pané, S.; Nelson, B. J. Investigation of Magnetotaxis of Reconfigurable Micro-Origami Swimmers with Competitive and Cooperative Anisotropy. *Adv. Funct. Mater.* **2018**, *28*, 1802110.
- (313) Tasoglu, S.; Diller, E.; Guven, S.; Sitti, M.; Demirci, U. Untethered Micro-Robotic Coding of Three-Dimensional Material Composition. *Nat. Commun.* **2014**, *5*, 1–9.
- (314) Magdanz, V.; Guix, M.; Hebenstreit, F.; Schmidt, O. G. Dynamic Polymeric Microtubes for the Remote-Controlled Capture, Guidance, and Release of Sperm Cells. *Adv. Mater.* **2016**, *28*, 4084–4089.
- (315) Qiu, T.; Lee, T. C.; Mark, A. G.; Morozov, K. I.; Münster, R.; Mierka, O.; Turek, S.; Leshansky, A. M.; Fischer, P. Swimming by Reciprocal Motion at Low Reynolds Number. *Nat. Commun.* **2014**, *5*, 1–8.
- (316) Wang, W.; Zhou, C. A Journey of Nanomotors for Targeted Cancer Therapy: Principles, Challenges, and a Critical Review of the State-of-the-Art. *Adv. Healthcare Mater.* **2020**, 2001236.
- (317) Wei, T.; Liu, J.; Li, D.; Chen, S.; Zhang, Y.; Li, J.; Fan, L.; Guan, Z.; Lo, C.; Wang, L.; Man, K.; Sun, D. Development of Magnet-Driven and Image-Guided Degradable Microrobots for the Precise Delivery of Engineered Stem Cells for Cancer Therapy. *Small* **2020**, *16*, 1906908.
- (318) Cheng, M.; Zhang, L.; Shi, F. Design of Functionally Cooperating Systems and Application towards Self-Propulsive Mini-Generators. *Mater. Chem. Front.* **2021**, *5*, 129.
- (319) Slavkov, I.; Carrillo-Zapata, D.; Carranza, N.; Diego, X.; Jansson, F.; Kaandorp, J.; Hauert, S.; Sharpe, J. Morphogenesis in Robot Swarms. *Sci. Robot.* **2018**, *3*, No. eaau9178.
- (320) McGuire, K. N.; de Wagter, C.; Tuyls, K.; Kappen, H. J.; de Croon, G. C. H. E. Minimal Navigation Solution for a Swarm of Tiny Flying Robots to Explore an Unknown Environment. *Sci. Robot.* **2019**, *4*, No. eaaw9710.
- (321) Luan, J.; Wang, D.; Wilson, D. A. Leveraging Synthetic Particles for Communication: From Passive to Active Systems. *Nanoscale* **2020**, *12*, 21015.
- (322) Lei, L.; Wang, S.; Zhang, X.; Lai, W.; Wu, J.; Gao, Y. Phoretic Self-Assembly of Active Colloidal Molecules. *Chin. Phys. B* **2020** DOI: 10.1088/1674-1056/abc2bd.
- (323) Guo, Z.; Liu, J.; Wang, D.-W.; Xu, J.; Liang, K. Biofriendly Micro/Nanomotors Operating on Biocatalysis: From Natural to Biological Environments. *Biophys. Reports* **2020**, *6*, 179–192.
- (324) Sridhar, V.; Podjaski, F.; Kröger, J.; Jiménez-Solano, A.; Park, B. W.; Lotsch, B. V.; Sitti, M. Carbon Nitride-Based Light-Driven Microswimmers with Intrinsic Photocharging Ability. *Proc. Natl. Acad. Sci. U. S. A.* **2020**, *117*, 24748–24756.
- (325) Li, Q.; Hu, E.; Yu, K.; Xie, R.; Lu, F.; Lu, B.; Bao, R.; Zhao, T.; Dai, F.; Lan, G. Self-Propelling Janus Particles for Hemostasis in Perforating and Irregular Wounds with Massive Hemorrhage. *Adv. Funct. Mater.* **2020**, *30*, 2004153.
- (326) Li, Z.; Zhang, H.; Wang, D.; Gao, C.; Sun, M.; Wu, Z.; He, Q. Reconfigurable Assembly of Active Liquid Metal Colloidal Cluster. *Angew. Chem., Int. Ed.* **2020**, *59*, 19884–19888.
- (327) Soto, F.; Wang, J.; Deshmukh, S.; Demirci, U. Reversible Design of Dynamic Assemblies at Small Scales. *Adv. Intell. Syst.* **2020**, 2000193.
- (328) Kong, L.; Mayorga-Martinez, C. C.; Guan, J.; Pumera, M. Smart Microdevices Laying “Breadcrumbs” to Find the Way Home: Chemotactic Homing TiO<sub>2</sub>/Pt Janus Microrobots. *Chem. - Asian J.* **2019**, *14*, 2456–2459.
- (329) Dong, R.; Li, J.; Rozen, I.; Ezhilan, B.; Xu, T.; Christianson, C.; Gao, W.; Saintillan, D.; Ren, B.; Wang, J. Vapor-Driven Propulsion of Catalytic Micromotors. *Sci. Rep.* **2015**, *5*, 1–7.
- (330) Ezhilan, B.; Gao, W.; Pei, A.; Rozen, I.; Dong, R.; Jurado-Sanchez, B.; Wang, J.; Saintillan, D. Motion-Based Threat Detection Using Microrods: Experiments and Numerical Simulations. *Nanoscale* **2015**, *7*, 7833–7840.
- (331) Li, M.; Brinkmann, M.; Pagonabarraga, I.; Seemann, R.; Fleury, J. B. Spatiotemporal Control of Cargo Delivery Performed by Programmable Self-Propelled Janus Droplets. *Commun. Phys.* **2018**, *1*, 1–8.
- (332) Zhao, G.; Pumera, M. Marangoni Self-Propelled Capsules in a Maze: Pollutants “sense and Act” in Complex Channel Environments. *Lab Chip* **2014**, *14*, 2818–2823.
- (333) Uspal, W. E.; Popescu, M. N.; Dietrich, S.; Tasinkevych, M. Guiding Catalytically Active Particles with Chemically Patterned Surfaces. *Phys. Rev. Lett.* **2016**, *117*, 048002.
- (334) Wang, Z.; Wang, Z.; Li, J.; Cheung, S. T. H.; Tian, C.; Kim, S. H.; Yi, G. R.; Ducrot, E.; Wang, Y. Active Patchy Colloids with Shape-Tunable Dynamics. *J. Am. Chem. Soc.* **2019**, *141*, 14853–14863.
- (335) Chen, C.; Chang, X.; Teymourian, H.; Ramírez-Herrera, D. E.; Esteban-Fernández de Ávila, B.; Lu, X.; Li, J.; He, S.; Fang, C.; Liang, Y.; Mou, F.; Guan, J.; Wang, J. Bioinspired Chemical Communication between Synthetic Nanomotors. *Angew. Chem., Int. Ed.* **2018**, *57*, 241–245.
- (336) Ibele, M. E.; Lammert, P. E.; Crespi, V. H.; Sen, A. Emergent, Collective Oscillations of Self-Mobile Particles and Patterned Surfaces under Redox Conditions. *ACS Nano* **2010**, *4*, 4845–4851.
- (337) Yu, T.; Chuphal, P.; Thakur, S.; Reigh, S. Y.; Singh, D. P.; Fischer, P. Chemical Micromotors Self-Assemble and Self-Propel by Spontaneous Symmetry Breaking. *Chem. Commun.* **2018**, *54*, 11933–11936.
- (338) Kim, H.; Kang, J.; Zhou, Y.; Kuentler, A. S.; Kim, Y.; Chen, C.; Emrick, T.; Hayward, R. C. Light-Driven Shape Morphing, Assembly, and Motion of Nanocomposite Gel Surfers. *Adv. Mater.* **2019**, *31*, 1900932.
- (339) Nourhani, A.; Brown, D.; Pletzer, N.; Gibbs, J. G. Engineering Contactless Particle-Particle Interactions in Active Microswimmers. *Adv. Mater.* **2017**, *29*, 1703910.
- (340) Solovev, A. A.; Mei, Y.; Schmidt, O. G. Catalytic Microstrider at the Air-Liquid Interface. *Adv. Mater.* **2010**, *22*, 4340–4344.
- (341) Karshalev, E.; Kumar, R.; Jeerapan, I.; Castillo, R.; Campos, I.; Wang, J. Multistimuli-Responsive Camouflage Swimmers. *Chem. Mater.* **2018**, *30*, 1593–1601.
- (342) Koepele, C. A.; Guix, M.; Bi, C.; Adam, G.; Cappelleri, D. J. 3D-Printed Microrobots with Integrated Structural Color for Identification and Tracking. *Adv. Intell. Syst.* **2020**, *2*, 1900147.
- (343) Li, J.; Shklyaev, O. E.; Li, T.; Liu, W.; Shum, H.; Rozen, I.; Balazs, A. C.; Wang, J. Self-Propelled Nanomotors Autonomously Seek and Repair Cracks. *Nano Lett.* **2015**, *15*, 7077–7085.
- (344) Mayorga-Martinez, C. C.; Moo, J. G. S.; Khezri, B.; Song, P.; Fisher, A. C.; Sofer, Z.; Pumera, M. Self-Propelled Supercapacitors for On-Demand Circuit Configuration Based on WS<sub>2</sub> Nanoparticles Micromachines. *Adv. Funct. Mater.* **2016**, *26*, 6662–6667.
- (345) Wang, Y.; Duan, W.; Zhou, C.; Liu, Q.; Gu, J.; Ye, H.; Li, M.; Wang, W.; Ma, X. Phoretic Liquid Metal Micro/Nanomotors as Intelligent Filler for Targeted Microwelding. *Adv. Mater.* **2019**, *31*, 1905067.
- (346) Gao, C.; Wang, Y.; Ye, Z.; Lin, Z.; Ma, X.; He, Q. Biomedical Micro-/Nanomotors: From Overcoming Biological Barriers to In Vivo Imaging. *Adv. Mater.* **2020**, 2000512.
- (347) van Moolenbroek, G. T.; Patiño, T.; Llop, J.; Sánchez, S. Engineering Intelligent Nanosystems for Enhanced Medical Imaging. *Adv. Intell. Syst.* **2020**, *2*, 2000087.
- (348) Vilela, D.; Cossío, U.; Parmar, J.; Martínez-Villacorta, A. M.; Gómez-Vallejo, V.; Llop, J.; Sánchez, S. Medical Imaging for the Tracking of Micromotors. *ACS Nano* **2018**, *12*, 1220–1227.
- (349) Hortelao, A. C.; Simó, C.; Guix, M.; Guallar-Garrido, S.; Julián, E.; Vilela, D.; Rejc, L.; Ramos-Cabrer, P.; Cossío, U.; Gómez-Vallejo, V.; Patiño, T.; Llop, J.; Sánchez, S. Monitoring the Collective Behavior of Enzymatic Nanomotors in Vitro and in Vivo by PET-CT; *bioRxiv* 2020.06.22.146282; DOI: 10.1101/2020.06.22.146282.
- (350) Iacovacci, V.; Blanc, A.; Huang, H.; Ricotti, L.; Schibli, R.; Mencias, A.; Behe, M.; Pané, S.; Nelson, B. J. High-Resolution SPECT Imaging of Stimuli-Responsive Soft Microrobots. *Small* **2019**, *15*, 1900709.
- (351) Fan, X.; Sun, M.; Sun, L.; Xie, H. Ferrofluid Droplets as Liquid Microrobots with Multiple Deformabilities. *Adv. Funct. Mater.* **2020**, *30*, 2000138.

- (352) Ghosh, S.; Ghosh, A. Mobile Nanotweezers for Active Colloidal Manipulation. *Sci. Robot.* **2018**, *3*, 76.
- (353) Ghosh, S.; Ghosh, A. All Optical Dynamic Nanomanipulation with Active Colloidal Tweezers. *Nat. Commun.* **2019**, *10*, 1–8.
- (354) Aubret, A.; Youssef, M.; Sacanna, S.; Palacci, J. Targeted Assembly and Synchronization of Self-Spinning Microgears. *Nat. Phys.* **2018**, *14*, 1114–1118.
- (355) Zhang, Q.; Dong, R.; Chang, X.; Ren, B.; Tong, Z. Spiropyran-Decorated SiO<sub>2</sub>-Pt Janus Micromotor: Preparation and Light-Induced Dynamic Self-Assembly and Disassembly. *ACS Appl. Mater. Interfaces* **2015**, *7*, 24585–24591.
- (356) Sentürk, O. I.; Schauer, O.; Chen, F.; Sourjik, V.; Wegner, S. V. Red/Far-Red Light Switchable Cargo Attachment and Release in Bacteria-Driven Microswimmers. *Adv. Healthcare Mater.* **2020**, *9*, 1900956.
- (357) Gao, W.; Pei, A.; Feng, X.; Hennessy, C.; Wang, J. Organized Self-Assembly of Janus Micromotors with Hydrophobic Hemispheres. *J. Am. Chem. Soc.* **2013**, *135*, 998–1001.
- (358) Maggi, C.; Simmchen, J.; Saglimbeni, F.; Katuri, J.; Dipalo, M.; De Angelis, F.; Sanchez, S.; Di Leonardo, R. Self-Assembly of Micromachining Systems Powered by Janus Micromotors. *Small* **2016**, *12*, 446–451.
- (359) Han, K.; Shields, C. W.; Diwakar, N. M.; Bharti, B.; López, G. P.; Velev, O. D. Sequence-Encoded Colloidal Origami and Microbot Assemblies from Patchy Magnetic Cubes. *Sci. Adv.* **2017**, *3*, No. e1701108.
- (360) Alapan, Y.; Yigit, B.; Beker, O.; Demirörs, A. F.; Sitti, M. Shape-Encoded Dynamic Assembly of Mobile Micromachines. *Nat. Mater.* **2019**, *18*, 1244–1251.
- (361) Ahmed, S.; Gentekos, D. T.; Fink, C. A.; Mallouk, T. E. Self-Assembly of Nanorod Motors into Geometrically Regular Multimers and Their Propulsion by Ultrasound. *ACS Nano* **2014**, *8*, 11053–11060.
- (362) Ahmed, D.; Baasch, T.; Blondel, N.; Läubli, N.; Dual, J.; Nelson, B. J. Neutrophil-Inspired Propulsion in a Combined Acoustic and Magnetic Field. *Nat. Commun.* **2017**, *8*, 1–8.
- (363) Solovev, A. A.; Sanchez, S.; Pumbera, M.; Mei, Y. F.; Schmidt, O. C. Magnetic Control of Tubular Catalytic Microbots for the Transport, Assembly, and Delivery of Micro-Objects. *Adv. Funct. Mater.* **2010**, *20*, 2430–2435.
- (364) Villa, K.; Krejčová, L.; Novotný, F.; Heger, Z.; Sofer, Z.; Pumbera, M. Cooperative Multifunctional Self-Propelled Paramagnetic Microrobots with Chemical Handles for Cell Manipulation and Drug Delivery. *Adv. Funct. Mater.* **2018**, *28*, 1804343.
- (365) Boymelgreen, A. M.; Balli, T.; Miloh, T.; Yossifon, G. Active Colloids as Mobile Microelectrodes for Unified Label-Free Selective Cargo Transport. *Nat. Commun.* **2018**, *9*, 1–8.
- (366) Nourhani, A.; Lammert, P. E.; Borhan, A.; Crespi, V. H. Kinematic Matrix Theory and Universalities in Self-Propellers and Active Swimmers. *Phys. Rev. E - Stat. Nonlinear, Soft Matter Phys.* **2014**, *89*, 062304.
- (367) Nourhani, A.; Crespi, V. H.; Lammert, P. E. Gaussian Memory in Kinematic Matrix Theory for Self-Propellers. *Phys. Rev. E - Stat. Nonlinear, Soft Matter Phys.* **2014**, *90*, 062304.
- (368) Nourhani, A.; Lammert, P. E.; Borhan, A.; Crespi, V. H. Chiral Diffusion of Rotary Nanomotors. *Phys. Rev. E - Stat. Nonlinear, Soft Matter Phys.* **2013**, *87*, 050301.
- (369) Nourhani, A.; Ebbens, S. J.; Gibbs, J. G.; Lammert, P. E. Spiral Diffusion of Rotating Self-Propellers with Stochastic Perturbation. *Phys. Rev. E: Stat. Phys., Plasmas, Fluids, Relat. Interdiscip. Top.* **2016**, *94*, 030601.
- (370) Zhou, D.; Gao, Y.; Yang, J.; Li, Y. C.; Shao, G.; Zhang, G.; Li, T.; Li, L. Light-Ultrasound Driven Collective “Firework” Behavior of Nanomotors. *Adv. Sci.* **2018**, *5*, 1800122.
- (371) Zhang, J.; Yan, J.; Granick, S. Directed Self-Assembly Pathways of Active Colloidal Clusters. *Angew. Chem., Int. Ed.* **2016**, *55*, S166–S169.
- (372) Wang, X.; Baraban, L.; Misko, V. R.; Nori, F.; Huang, T.; Cuniberti, G.; Fassbender, J.; Makarov, D. Visible Light Actuated Efficient Exclusion Between Plasmonic Ag/AgCl Micromotors and Passive Beads. *Small* **2018**, *14*, 1802537.
- (373) Yan, J.; Bae, S. C.; Granick, S. Rotating Crystals of Magnetic Janus Colloids. *Soft Matter* **2015**, *11*, 147–153.
- (374) Mou, F.; Zhang, J.; Wu, Z.; Du, S.; Zhang, Z.; Xu, L.; Guan, J. Phototactic Flocking of Photochemical Micromotors. *iScience* **2019**, *19*, 415–424.
- (375) Palacci, J.; Sacanna, S.; Steinberg, A. P.; Pine, D. J.; Chaikin, P. M. Living Crystals of Light-Activated Colloidal Surfers. *Science* **2013**, *339*, 936–940.
- (376) Kochergin, Y. S.; Villa, K.; Novotný, F.; Plutnar, J.; Bojdy, M. J.; Pumbera, M. Multifunctional Visible-Light Powered Micromotors Based on Semiconducting Sulfur- and Nitrogen-Containing Donor-Acceptor Polymer. *Adv. Funct. Mater.* **2020**, *30*, 2002701.
- (377) Wu, X.; Xue, X.; Wang, J.; Liu, H. Phototropic Aggregation and Light-Guided Long-Distance Collective Transport of Colloidal Particles. *Langmuir* **2020**, *36*, 6819–6827.
- (378) Kagan, D.; Balasubramanian, S.; Wang, J. Chemically Triggered Swarming of Gold Microparticles. *Angew. Chem., Int. Ed.* **2011**, *50*, 503–506.
- (379) Hong, Y.; Diaz, M.; Cordova-Figueroa, U. M.; Sen, A. Light-Driven Titanium-Dioxide-Based Reversible Microfireworks and Micromotor/Micropump Systems. *Adv. Funct. Mater.* **2010**, *20*, 1568–1576.
- (380) Xu, T.; Soto, F.; Gao, W.; Dong, R.; Garcia-Gradilla, V.; Magaña, E.; Zhang, X.; Wang, J. Reversible Swarming and Separation of Self-Propelled Chemically Powered Nanomotors under Acoustic Fields. *J. Am. Chem. Soc.* **2015**, *137*, 2163–2166.
- (381) Xie, H.; Sun, M.; Fan, X.; Lin, Z.; Chen, W.; Wang, L.; Dong, L.; He, Q. Reconfigurable Magnetic Microrobot Swarm: Multimode Transformation, Locomotion, and Manipulation. *Sci. Robot.* **2019**, *4*, No. eaav8006.
- (382) Kaiser, A.; Snezhko, A.; Aranson, I. S. Flocking Ferromagnetic Colloids. *Sci. Adv.* **2017**, *3*, No. e1601469.
- (383) Demirörs, A. F.; Pillai, P. P.; Kowalczyk, B.; Grzybowski, B. A. Colloidal Assembly Directed by Virtual Magnetic Moulds. *Nature* **2013**, *503*, 99–103.
- (384) Yigit, B.; Alapan, Y.; Sitti, M. Programmable Collective Behavior in Dynamically Self-Assembled Mobile Microbotic Swarms. *Adv. Sci.* **2019**, *6*, 1801837.
- (385) Dong, X.; Sitti, M. Controlling Two-Dimensional Collective Formation and Cooperative Behavior of Magnetic Microrobot Swarms. *Int. J. Rob. Res.* **2020**, *39*, 617–638.
- (386) Sadati, M.; Nourhani, A.; Fredberg, J. J.; Taheri Qazvini, N. Glass-like Dynamics in the Cell and in Cellular Collectives. *Wiley Interdiscip. Rev. Syst. Biol. Med.* **2014**, *6*, 137–149.
- (387) Schneider, L.; Cammer, M.; Lehman, J.; Nielsen, S.; Guerra, C.; Veland, I.; Stock, C.; Hoffmann, E.; Yoder, B.; Schwab, A.; Satir, P.; Christensen, S. Directional Cell Migration and Chemotaxis in Wound Healing Response to PDGF-AA Are Coordinated by the Primary Cilium in Fibroblasts. *Cell. Physiol. Biochem.* **2010**, *25*, 279–292.
- (388) Snyderman, R.; Shin, H. S.; Hausman, M. H. A Chemotactic Factor for Mononuclear Leukocytes. *Exp. Biol. Med.* **1971**, *138*, 387–390.
- (389) Eisenbach, M.; Giojalas, L. C. Sperm Guidance in Mammals - An Unpaved Road to the Egg. *Nat. Rev. Mol. Cell Biol.* **2006**, *7*, 276–285.
- (390) Zhuang, J.; Sitti, M. Chemotaxis of Bio-Hybrid Multiple Bacteria-Driven Microswimmers. *Sci. Rep.* **2016**, *6*, 1–10.
- (391) Chen, C.; Chang, X.; Angsantikul, P.; Li, J.; Esteban-Fernández de Ávila, B.; Karshalev, E.; Liu, W.; Mou, F.; He, S.; Castillo, R.; Liang, Y.; Guan, J.; Zhang, L.; Wang, J. Chemotactic Guidance of Synthetic Organic/Inorganic Payloads Functionalized Sperm Micromotors. *Adv. Biosyst.* **2018**, *2*, 1700160.
- (392) Shao, J.; Xuan, M.; Zhang, H.; Lin, X.; Wu, Z.; He, Q. Chemotaxis-Guided Hybrid Neutrophil Micromotors for Targeted Drug Transport. *Angew. Chem.* **2017**, *129*, 13115–13119.
- (393) Somasundar, A.; Ghosh, S.; Mohajerani, F.; Massenbur, L. N.; Yang, T.; Cremer, P. S.; Velegol, D.; Sen, A. Positive and Negative

- Chemotaxis of Enzyme-Coated Liposome Motors. *Nat. Nanotechnol.* **2019**, *14*, 1129–1134.
- (394) Chen, C.; Mou, F.; Xu, L.; Wang, S.; Guan, J.; Feng, Z.; Wang, Q.; Kong, L.; Li, W.; Wang, J.; Zhang, Q. Light-Steered Isotropic Semiconductor Micromotors. *Adv. Mater.* **2017**, *29*, 1603374.
- (395) Zheng, J.; Dai, B.; Wang, J.; Xiong, Z.; Yang, Y.; Liu, J.; Zhan, X.; Wan, Z.; Tang, J. Orthogonal Navigation of Multiple Visible-Light-Driven Artificial Microswimmers. *Nat. Commun.* **2017**, *8*, 1–7.
- (396) Ye, Z.; Sun, Y.; Zhang, H.; Song, B.; Dong, B. A Phototactic Micromotor Based on Platinum Nanoparticle Decorated Carbon Nitride. *Nanoscale* **2017**, *9*, 18516–18522.
- (397) Singh, D. P.; Uspal, W. E.; Popescu, M. N.; Wilson, L. G.; Fischer, P. Photogravitactic Microswimmers. *Adv. Funct. Mater.* **2018**, *28*, 1706660.
- (398) Soto, F.; Kupor, D.; Lopez-Ramirez, M. A.; Wei, F.; Karshalev, E.; Tang, S.; Tehrani, F.; Wang, J. Onion-like Multifunctional Microtrap Vehicles for Attraction-Trapping-Destruction of Biological Threats. *Angew. Chem., Int. Ed.* **2020**, *59*, 3480–3485.
- (399) Wu, J.; Balasubramanian, S.; Kagan, D.; Manesh, K. M.; Campuzano, S.; Wang, J. Motion-Based DNA Detection Using Catalytic Nanomotors. *Nat. Commun.* **2010**, *1*, 1–6.
- (400) Zhang, X.; Chen, C.; Wu, J.; Ju, H. Bubble-Propelled Jellyfish-like Micromotors for DNA Sensing. *ACS Appl. Mater. Interfaces* **2019**, *11*, 13581–13588.
- (401) Xie, Y.; Fu, S.; Wu, J.; Lei, J.; Ju, H. Motor-Based Microprobe Powered by Bio-Assembled Catalase for Motion Detection of DNA. *Biosens. Bioelectron.* **2017**, *87*, 31–37.
- (402) Van Nguyen, K.; Minter, S. D. DNA-Functionalized Pt Nanoparticles as Catalysts for Chemically Powered Micromotors: Toward Signal-on Motion-Based DNA Biosensor. *Chem. Commun.* **2015**, *51*, 4782–4784.
- (403) Kagan, D.; Campuzano, S.; Balasubramanian, S.; Kuralay, F.; Flechsig, G. U.; Wang, J. Functionalized Micromachines for Selective and Rapid Isolation of Nucleic Acid Targets from Complex Samples. *Nano Lett.* **2011**, *11*, 2083–2087.
- (404) Orozco, J.; Campuzano, S.; Kagan, D.; Zhou, M.; Gao, W.; Wang, J. Dynamic Isolation and Unloading of Target Proteins by Aptamer-Modified Microtransporters. *Anal. Chem.* **2011**, *83*, 7962–7969.
- (405) Kuralay, F.; Sattayasamitsathit, S.; Gao, W.; Uygun, A.; Katzenberg, A.; Wang, J. Self-Propelled Carbohydrate-Sensitive Microtransporters with Built-in Boronic Acid Recognition for Isolating Sugars and Cells. *J. Am. Chem. Soc.* **2012**, *134*, 15217–15220.
- (406) Balasubramanian, S.; Kagan, D.; Jack Hu, C. M.; Campuzano, S.; Lobo-Castañón, M. J.; Lim, N.; Kang, D. Y.; Zimmerman, M.; Zhang, L.; Wang, J. Micromachine-Enabled Capture and Isolation of Cancer Cells in Complex Media. *Angew. Chem., Int. Ed.* **2011**, *50*, 4161–4164.
- (407) Campuzano, S.; Orozco, J.; Kagan, D.; Guix, M.; Gao, W.; Sattayasamitsathit, S.; Claussen, J. C.; Merkoci, A.; Wang, J. Bacterial Isolation by Lectin-Modified Microengines. *Nano Lett.* **2012**, *12*, 396–401.
- (408) Draz, M. S.; Kochehyoky, K. M.; Vasan, A.; Battalapalli, D.; Sreeram, A.; Kanakasabapathy, M. K.; Kallakuri, S.; Tsibris, A.; Kuritzkes, D. R.; Shafiee, H. DNA Engineered Micromotors Powered by Metal Nanoparticles for Motion Based Cellphone Diagnostics. *Nat. Commun.* **2018**, *9*, 1–13.
- (409) Draz, M. S.; Lakshminarasimulu, N. K.; Krishnakumar, S.; Battalapalli, D.; Vasan, A.; Kanakasabapathy, M. K.; Sreeram, A.; Kallakuri, S.; Thirumalaraju, P.; Li, Y.; Hua, S.; Yu, X. G.; Kuritzkes, D. R.; Shafiee, H. Motion-Based Immunological Detection of Zika Virus Using Pt-Nanomotors and a Cellphone. *ACS Nano* **2018**, *12*, 5709–5718.
- (410) Moo, J. G. S.; Wang, H.; Zhao, G.; Pumera, M. Biomimetic Artificial Inorganic Enzyme-Free Self-Propelled Microfish Robot for Selective Detection of Pb<sup>2+</sup> in Water. *Chem. - Eur. J.* **2014**, *20*, 4292–4296.
- (411) Singh, V. V.; Kaufmann, K.; Esteban-Fernández De Ávila, B.; Uygun, M.; Wang, J. Nanomotors Responsive to Nerve-Agent Vapor Plumes. *Chem. Commun.* **2016**, *52*, 3360–3363.
- (412) Su, Y.; Ge, Y.; Liu, L.; Zhang, L.; Liu, M.; Sun, Y.; Zhang, H.; Dong, B. Motion-Based pH Sensing Based on the Cartridge-Case-like Micromotor. *ACS Appl. Mater. Interfaces* **2016**, *8*, 4250–4257.
- (413) de la Asunción-Nadal, V.; Pacheco, M.; Jurado Sánchez, B.; Escarpa, A. Chalcogenides-Based Tubular Micromotors in Fluorescent Assays. *Anal. Chem.* **2020**, *92*, 9188–9193.
- (414) Molinero-Fernández, Á.; Moreno-Guzmán, M.; Arruza, L.; López, M. A.; Escarpa, A. Polymer-Based Micromotor Fluorescence Immunoassay for On-the-Move Sensitive Procalcitonin Determination in Very Low Birth Weight Infants' Plasma. *ACS Sensors* **2020**, *5*, 1336–1344.
- (415) Jurado-Sánchez, B.; Pacheco, M.; Rojo, J.; Escarpa, A. Magnetocatalytic Graphene Quantum Dots Janus Micromotors for Bacterial Endotoxin Detection. *Angew. Chem., Int. Ed.* **2017**, *56*, 6957–6961.
- (416) Esteban-Fernández De Ávila, B.; Lopez-Ramirez, M. A.; Báez, D. F.; Jodra, A.; Singh, V. V.; Kaufmann, K.; Wang, J. Aptamer-Modified Graphene-Based Catalytic Micromotors: Off-On Fluorescent Detection of Ricin. *ACS Sensors* **2016**, *1*, 217–221.
- (417) Pacheco, M.; Jurado-Sánchez, B.; Escarpa, A. Sensitive Monitoring of Enterobacterial Contamination of Food Using Self-Propelled Janus Microsensors. *Anal. Chem.* **2018**, *90*, 2912–2917.
- (418) Singh, V. V.; Kaufmann, K.; Orozco, J.; Li, J.; Galarnyk, M.; Arya, G.; Wang, J. Micromotor-Based on-off Fluorescence Detection of Sarin and Soman Simulants. *Chem. Commun.* **2015**, *51*, 11190–11193.
- (419) Zhang, Y.; Zhang, L.; Yang, L.; Vong, C. L.; Chan, K. F.; Wu, W. K. K.; Kwong, T. N. Y.; Lo, N. W. S.; Ip, M.; Wong, S. H.; Sung, J. J. Y.; Chiu, P. W. Y.; Zhang, L. Real-Time Tracking of Fluorescent Magnetic Spore-Based Microrobots for Remote Detection of *C. Diff* Toxins. *Sci. Adv.* **2019**, *5*, No. eaau9650.
- (420) Esteban-Fernández De Ávila, B.; Angell, C.; Soto, F.; Lopez-Ramirez, M. A.; Báez, D. F.; Xie, S.; Wang, J.; Chen, Y. Acoustically Propelled Nanomotors for Intracellular siRNA Delivery. *ACS Nano* **2016**, *10*, 4997–5005.
- (421) Esteban-Fernández De Ávila, B.; Ramírez-Herrera, D. E.; Campuzano, S.; Angsantikul, P.; Zhang, L.; Wang, J. Nanomotor-Enabled pH-Responsive Intracellular Delivery of Caspase-3: Toward Rapid Cell Apoptosis. *ACS Nano* **2017**, *11*, 5367–5374.
- (422) Hansen-Bruhn, M.; de Ávila, B. E.-F.; Beltrán-Gastélum, M.; Zhao, J.; Ramírez-Herrera, D. E.; Angsantikul, P.; Vesterager Gothelf, K.; Zhang, L.; Wang, J. Active Intracellular Delivery of a Cas9/SgRNA Complex Using Ultrasound-Propelled Nanomotors. *Angew. Chem.* **2018**, *130*, 2687–2691.
- (423) Zhang, F.; Zhuang, J.; Esteban Fernández De Ávila, B.; Tang, S.; Zhang, Q.; Fang, R. H.; Zhang, L.; Wang, J. A Nanomotor-Based Active Delivery System for Intracellular Oxygen Transport. *ACS Nano* **2019**, *13*, 11996–12005.
- (424) Esteban-Fernández De Ávila, B.; Martín, A.; Soto, F.; Lopez-Ramirez, M. A.; Campuzano, S.; Vázquez-Machado, G. M.; Gao, W.; Zhang, L.; Wang, J. Single Cell Real-Time miRNAs Sensing Based on Nanomotors. *ACS Nano* **2015**, *9*, 6756–6764.
- (425) Simmchen, J.; Baeza, A.; Ruiz, D.; Esplandiú, M. J.; Vallet-Regí, M. Asymmetric Hybrid Silica Nanomotors for Capture and Cargo Transport: Towards a Novel Motion-Based DNA Sensor. *Small* **2012**, *8*, 2053–2059.
- (426) Patino, T.; Porchetta, A.; Jannasch, A.; Lladó, A.; Stumpp, T.; Schäffer, E.; Ricci, F.; Sánchez, S. Self-Sensing Enzyme-Powered Micromotors Equipped with pH-Responsive DNA Nanoswitches. *Nano Lett.* **2019**, *19*, 3440–3447.
- (427) Fan, X.; Hao, Q.; Li, M.; Zhang, X.; Yang, X.; Mei, Y.; Qiu, T. Hotspots on the Move: Active Molecular Enrichment by Hierarchically Structured Micromotors for Ultrasensitive SERS Sensing. *ACS Appl. Mater. Interfaces* **2020**, *12*, 28783–28791.
- (428) Han, D.; Fang, Y.; Du, D.; Huang, G.; Qiu, T.; Mei, Y. Automatic Molecular Collection and Detection by Using Fuel-Powered Microengines. *Nanoscale* **2016**, *8*, 9141–9145.

- (429) Ghosh, A.; Dasgupta, D.; Pal, M.; Morozov, K. I.; Leshansky, A. M.; Ghosh, A. Helical Nanomachines as Mobile Viscometers. *Adv. Funct. Mater.* **2018**, *28*, 1705687.
- (430) Wang, L.; Li, T.; Li, L.; Wang, J.; Song, W.; Zhang, G. Microrocket Based Viscometer. *ACS Appl. Mater. Sci. Technol.* **2015**, *4*, S3020–S3023.
- (431) Jeong, H. H.; Mark, A. G.; Lee, T. C.; Alarcón-Correa, M.; Eslami, S.; Qiu, T.; Gibbs, J. G.; Fischer, P. Active Nanorheology with Plasmonics. *Nano Lett.* **2016**, *16*, 4887–4894.
- (432) Muiños-Landin, S.; Ghazi-Zahedi, K.; Cichos, F. Reinforcement Learning of Artificial Microswimmers. **2018**. *arXiv preprint:1803.06425*.
- (433) Shang, W.; Lu, H.; Wan, W.; Fukuda, T.; Shen, Y. Vision-Based Nano Robotic System for High-Throughput Non-Embedded Cell Cutting. *Sci. Rep.* **2016**, *6*, 1–14.
- (434) Li, T.; Chang, X.; Wu, Z.; Li, J.; Shao, G.; Deng, X.; Qiu, J.; Guo, B.; Zhang, G.; He, Q.; Li, L.; Wang, J. Autonomous Collision-Free Navigation of Microvehicles in Complex and Dynamically Changing Environments. *ACS Nano* **2017**, *11*, 9268–9275.
- (435) Pal, M.; Somalwar, N.; Singh, A.; Bhat, R.; Eswarappa, S. M.; Saini, D. K.; Ghosh, A. Maneuverability of Magnetic Nanomotors Inside Living Cells. *Adv. Mater.* **2018**, *30*, 1800429.
- (436) Pal, M.; Dasgupta, D.; Somalwar, N.; Vr, R.; Tiwari, M.; Teja, D.; Narayana, S. M.; Katke, A.; Rs, J.; Bhat, R.; Saini, D. K.; Ghosh, A. Helical Nanobots as Mechanical Probes of Intra- and Extracellular Environments. *J. Phys.: Condens. Matter* **2020**, *32*, 224001.
- (437) Sun, M.; Liu, Q.; Fan, X.; Wang, Y.; Chen, W.; Tian, C.; Sun, L.; Xie, H. Autonomous Biohybrid Urchin-Like Microperforator for Intracellular Payload Delivery. *Small* **2020**, *16*, 1906701.
- (438) Lin, Z.; Fan, X.; Sun, M.; Gao, C.; He, Q.; Xie, H. Magnetically Actuated Peanut Colloid Motors for Cell Manipulation and Patterning. *ACS Nano* **2018**, *12*, 2539–2545.
- (439) Schuerle, S.; Vizcarra, I. A.; Moeller, J.; Sakar, M. S.; Özkale, B.; Lindo, A. M. H.; Mushtaq, F.; Schoen, I.; Pané, S.; Vogel, V.; Nelson, B. J. Robotically Controlled Microprey to Resolve Initial Attack Modes Preceding Phagocytosis. *Sci. Robot.* **2017**, *2*, No. eaah6094.
- (440) Liang, Z.; Fan, D. Visible Light-Gated Reconfigurable Rotary Actuation of Electric Nanomotors. *Sci. Adv.* **2018**, *4*, No. eaau0981.
- (441) Liang, Z.; Teal, D.; Fan, D. Light Programmable Micro/Nanomotors with Optically Tunable in-Phase Electric Polarization. *Nat. Commun.* **2019**, *10*, 1–10.
- (442) Sharma, R.; Velev, O. D. Remote Steering of Self-Propelling Microcircuits by Modulated Electric Field. *Adv. Funct. Mater.* **2015**, *25*, 5512–5519.
- (443) Ohiri, U.; Shields, C. W.; Han, K.; Tyler, T.; Velev, O. D.; Jokerst, N. Reconfigurable Engineered Motile Semiconductor Microparticles. *Nat. Commun.* **2018**, *9*, 1–9.
- (444) Lu, X.; Zhao, K.; Liu, W.; Yang, D.; Shen, H.; Peng, H.; Guo, X.; Li, J.; Wang, J. A Human Microrobot Interface Based on Acoustic Manipulation. *ACS Nano* **2019**, *13*, 11443–11452.
- (445) Lu, X.; Martin, A.; Soto, F.; Angsantikul, P.; Li, J.; Chen, C.; Liang, Y.; Hu, J.; Zhang, L.; Wang, J. Parallel Label-Free Isolation of Cancer Cells Using Arrays of Acoustic Microstreaming Traps. *Adv. Mater. Technol.* **2018**, *4*, 1800374.
- (446) Lu, X.; Soto, F.; Li, J.; Li, T.; Liang, Y.; Wang, J. Topographical Manipulation of Microparticles and Cells with Acoustic Microstreaming. *ACS Appl. Mater. Interfaces* **2017**, *9*, 38870–38876.
- (447) Elizabeth Hulme, S.; DiLuzio, W. R.; Shevkoplyas, S. S.; Turner, L.; Mayer, M.; Berg, H. C.; Whitesides, G. M. Using Ratchets and Sorters to Fractionate Motile Cells of Escherichia Coli by Length. *Lab Chip* **2008**, *8*, 1888–1895.
- (448) Melde, K.; Mark, A. G.; Qiu, T.; Fischer, P. Holograms for Acoustics. *Nature* **2016**, *537*, 518–522.
- (449) Heidari, M.; Bregulla, A.; Landin, S. M.; Cichos, F.; von Klitzing, R. Self-Propulsion of Janus Particles near a Brush-Functionalized Substrate. *Langmuir* **2020**, *36*, 7775–7780.
- (450) Xiao, Z.; Wei, M.; Wang, W. A Review of Micromotors in Confinements: Pores, Channels, Grooves, Steps, Interfaces, Chains, and Swimming in the Bulk. *ACS Appl. Mater. Interfaces* **2019**, *11*, 6667–6684.
- (451) Vizsnyiczai, G.; Frangipane, G.; Bianchi, S.; Saglimbeni, F.; Dell'Arciprete, D.; Di Leonardo, R. A Transition to Stable One-Dimensional Swimming Enhances E. Coli Motility through Narrow Channels. *Nat. Commun.* **2020**, *11*, 1–7.
- (452) Katuri, J.; Uspal, W. E.; Simmchen, J.; Miguel-López, A.; Sánchez, S. Cross-Stream Migration of Active Particles. *Sci. Adv.* **2018**, *4*, No. eaao1755.
- (453) Restrepo-Pérez, L.; Soler, L.; Martínez-Cisneros, C. S.; Sánchez, S.; Schmidt, O. G. Trapping Self-Propelled Micromotors with Microfabricated Chevron and Heart-Shaped Chips. *Lab Chip* **2014**, *14*, 1515–1518.
- (454) Davies Wykes, M. S.; Zhong, X.; Tong, J.; Adachi, T.; Liu, Y.; Ristroph, L.; Ward, M. D.; Shelley, M. J.; Zhang, J. Guiding Microscale Swimmers Using Teardrop-Shaped Posts. *Soft Matter* **2017**, *13*, 4681–4688.
- (455) Simmchen, J.; Katuri, J.; Uspal, W. E.; Popescu, M. N.; Tasinkevych, M.; Sánchez, S. Topographical Pathways Guide Chemical Microswimmers. *Nat. Commun.* **2016**, *7*, 1–9.
- (456) Nourhani, A.; Crespi, V. H.; Lammert, P. E. Guiding Chiral Self-Propellers in a Periodic Potential. *Phys. Rev. Lett.* **2015**, *115*, 118101.
- (457) Katuri, J.; Caballero, D.; Voituriez, R.; Samitier, J.; Sanchez, S. Directed Flow of Micromotors through Aligned Interactions with Micropatterned Ratchets. *ACS Nano* **2018**, *12*, 7282–7291.
- (458) Jordan, J. M. *Robots*; The MIT Press, 2016.
- (459) Harari, Y. N. *Homo Deus: A Brief History of Tomorrow*; Harper, 2017.
- (460) Soto, F.; Wang, J.; Ahmed, R.; Demirci, U. Medical Micro/Nanorobots in Precision Medicine. *Adv. Sci.* **2020**, *7*, 2002203.
- (461) Hall, D.; Williams, C. *Big Hero 6*; Walt Disney Studios Motion Pictures: United States, 2014.
- (462) Crichton, M. *Prey*; HarperCollins, 2002.
- (463) Doherty, R. P.; Varkevissar, T.; Teunisse, M.; Hoecht, J.; Ketsetzi, S.; Ouhajji, S.; Kraft, D. J. Catalytically Propelled 3D Printed Colloidal Microswimmers. *Soft Matter* **2020**, *16*, 10463.
- (464) Guimarães, C. F.; Gasperini, L.; Marques, A. P.; Reis, R. L. The Stiffness of Living Tissues and Its Implications for Tissue Engineering. *Nat. Rev. Mater.* **2020**, *5*, 351–370.
- (465) Dong, R. Y.; Zhang, Y.; Lou, K.; Granick, S. Micromotor That Carries Its Own Fuel Internally. *Langmuir* **2020**, *36*, 7701–7705.
- (466) Katsamba, P.; Lauga, E. Micro-Tug-of-War: A Selective Control Mechanism for Magnetic Swimmers. *Phys. Rev. Appl.* **2016**, *5*, 064019.
- (467) Mandal, P.; Chopra, V.; Ghosh, A. Independent Positioning of Magnetic Nanomotors. *ACS Nano* **2015**, *9*, 4717–4725.
- (468) Huo, X.; Wu, Y.; Boymelgreen, A.; Yossifon, G. Analysis of Cargo Loading Modes and Capacity of an Electrically-Powered Active Carrier. *Langmuir* **2020**, *36* DOI: 10.1021/acs.langmuir.9b03036.
- (469) Guimarães, C. F.; Gasperini, L.; Ribeiro, R. S.; Carvalho, A. F.; Marques, A. P.; Reis, R. L. High-Throughput Fabrication of Cell-Laden 3D Biomaterial Gradients. *Mater. Horiz.* **2020**, *7*, 2414–2421.
- (470) Karshalev, E.; Yan, J.; Campos, I.; Sandraz, E.; Li, J.; Wang, J. Small-Scale Propellers Deliver Miniature Versions of Themselves. *Small* **2020**, *16*, 2000453.
- (471) Faria, M.; Björnalm, M.; Thurecht, K. J.; Kent, S. J.; Parton, R. G.; Kavallaris, M.; Johnston, A. P. R.; Gooding, J. J.; Corrie, S. R.; Boyd, B. J.; Thordarson, P.; Whittaker, A. K.; Stevens, M. M.; Prestidge, C. A.; Porter, C. J. H.; Parak, W. J.; Davis, T. P.; Crampin, E. J.; Caruso, F. Minimum Information Reporting in Bio-Nano Experimental Literature. *Nat. Nanotechnol.* **2018**, *13*, 777–785.
- (472) Hobson, D. W. Commercialization of Nanotechnology. *Wiley Interdiscip. Rev.: Nanomed. Nanobiotechnol.* **2009**, *1*, 189–202.
- (473) Thuruthel, T. G.; Shih, B.; Laschi, C.; Tolley, M. T. Soft Robot Perception Using Embedded Soft Sensors and Recurrent Neural Networks. *Sci. Robot.* **2019**, *4*, 1488.

